On the efficiency of decentralized epidemic management and competitive viral marketing

Olivier Lindamulage de Silva

UNIVERSITÉ DE LORRAINE

École doctorale IAEM Lorraine

On the Efficiency of Decentralized Epidemic Management and Competitive Viral Marketing

THÈSE

présentée et soutenue publiquement le Jeudi 28 Septembre 2023

pour l'obtention du

Doctorat de l'Université de Lorraine

(Spécialité Automatique, Traitement du signal et des Images, Génie informatique)

par

Olivier Lindamulage De Silva

Composition du jury

Président :	J. DAAFOUZ	Professeur des Universités - Université de Lorraine, CRAN
Rapporteurs :	E. PANTELEY	Directeur de Recherche CNRS, L2S
	Y.HAYEL	Professeur des Universités - Avignon Université, LIA
Examinateurs :	V. BELMEGA	Professeure de l'Université Gustave Eiffel, LIGM
	P. FRASCA	Chargé de Recherche CNRS, GIPSA-Lab
Encadrants :	I.-C. MORĂRESCU	Professeur des Universités - Université de Lorraine, CRAN
	S. LASAULCE	Directeur de Recherche CNRS, CRAN

Centre de Recherche en Automatique de Nancy CNRS - UMR 7039

Université de Lorraine

2 avenue de la Forêt de Haye, 54516 Vandoeuvre-lès-Nancy

Tél. + 33 (0)3.83.59.59.59

Mis en page avec la classe thesul.

À ma maman
À ma bien-aimée Lucille
À Mathieu, Angélique, Natasha et Kévin

Je dédie le fruit de ce travail accompli en vous exprimant toute ma gratitude infinie.

“La vie est comme une bicyclette, il faut avancer pour ne pas perdre l’équilibre.”
Albert Einstein

Remerciements

Je souhaite exprimer ma sincère reconnaissance envers les membres du jury pour avoir accepté d'examiner attentivement mon travail de thèse. Un remerciement spécial à monsieur Jamal DAAFOUZ pour avoir présidé mon jury, ainsi qu'à Elena Panteley et Yezekael Hayel pour leur contribution en tant que rapporteurs.

Je suis infiniment reconnaissant envers mes mentors, Constantin et Samson, pour leur confiance en moi dans la réalisation de ce projet de recherche. Leur accompagnement m'a permis d'apprendre énormément et grâce à leurs conseils, j'ai pu constater ma propre évolution et être fier de la personne que je suis devenue en seulement 3 ans. Je tiens à exprimer ma profonde gratitude envers Constantin pour sa patience et ses précieux conseils, qui m'ont été d'une grande aide tant sur le plan professionnel que personnel. Quant à Samson, je souhaite lui adresser mes sincères remerciements pour sa confiance, son soutien inébranlable, son expertise et son humanisme.

Je tiens à témoigner toute ma gratitude envers M. Vineeth Satheeskumar Varma, Chargé de Recherche CNRS – CRAN, et M. Ming Cao, Professeur des Universités à la faculté des sciences et de l'ingénierie de l'Université de Groningue, pour leur collaboration et leur expertise. Leurs contributions ont joué un rôle clé dans la réussite de ce projet de recherche. Je suis reconnaissant envers M. Ming Cao pour mon séjour à la faculté des sciences et de l'ingénierie de l'université de Groningue, qui a élargi mes horizons et enrichi mon expérience de recherche. Je voudrais également remercier M. Romain Postoyan, Chargé de Recherche CNRS – CRAN, et M. Mathieu Granzotto, Chargé de recherche à l'Université de Melbourne, pour m'avoir initié au monde de la recherche lors de mon stage de fin d'études. Leur encadrement et leur soutien ont été déterminants pour mon développement en tant que chercheur. Je suis également reconnaissant qu'ils aient poursuivi nos travaux jusqu'à leur publication. Leur collaboration a été une expérience enrichissante et je les remercie chaleureusement pour leur contribution.

Mes remerciements vont également au Commandant Rémy Sachez, Chef BRH de la base aérienne 133 Nancy-Ochey, pour sa confiance, ses conseils et son soutien dans mes responsabilités, que ce soit dans ma recherche académique ou dans mes tâches en gestion de projet en tant que réserviste dans l'armée de l'air et de l'espace.

Je suis pleinement conscient que ces simples mots ne peuvent véritablement exprimer toute ma gratitude envers mes proches. Notamment à ma petite amie Lucille pour son amour indéfectible qui fut source constante de force et de motivation. Je souhaite également exprimer ma profonde gratitude envers ma famille. Leur soutien et leur amour inconditionnel ont été des piliers essentiels dans ma vie et m'ont permis de persévérer et de réaliser mes objectifs.

Je suis profondément reconnaissant envers toutes les personnes qui, de près ou de loin, ont contribué à mon développement personnel et ont apporté leur soutien à la réalisation de ce projet. Leurs encouragements et leur appui ont été inestimables tout au long de ce parcours de thèse.

Résumé

Cette thèse explore la prise de décision décentralisée dans les dynamiques épidémiques et de marketing viral en utilisant la théorie des jeux afin d'évaluer son efficacité. La thèse commence par une revue des outils mathématiques, mettant l'accent sur la théorie des graphes/jeux. Dans la suite de ce manuscrit, l'analyse de jeu épidémiologique et de compétition en marketing viral est établie. Notamment, dans le chapitre 2 où il est présenté un jeu épidémique en réseau dans lequel chaque joueur (région ou pays) cherche à trouver un compromis entre les pertes socio-économiques et sanitaires, tout en prenant en compte des contraintes telles que la disponibilité des unités de soins intensifs (USI). L'équilibre de Nash et l'équilibre de Nash généralisé sont analysés, et l'impact de la décentralisation sur l'efficacité est mesuré à l'aide de paramètres tels que le prix de l'anarchie (PoA) et le prix de la connectivité (PoC). Une application pratique du jeu à un scénario de Covid-19 est également illustrée. Le chapitre 3 étend l'analyse du chapitre 2 en incorporant la dynamique des opinions dans le contrôle décentralisé d'une épidémie en réseau. L'analyse se concentre sur l'existence et l'unicité de l'équilibre de Nash généralisé (GNE), et un algorithme pour atteindre le GNE est proposé. Les simulations identifient les scénarios où la décentralisation est acceptable en termes d'efficacité globale et soulignent l'importance de la dynamique des opinions dans les processus de prise de décision. Finalement, le chapitre 4 explore un modèle de duopole de Stackelberg dans le contexte des campagnes de marketing viral. L'objectif est de caractériser la stratégie d'allocation optimale des budgets publicitaires entre les régions pour maximiser la part de marché. Des stratégies d'équilibre sont déduites et des conditions pour un résultat de type "le gagnant rafle tout" sont établies. Les résultats théoriques sont complétés par des simulations numériques et un exemple illustrant la caractérisation de l'équilibre.

Cette thèse offre des perspectives précieuses sur l'efficacité de la prise de décision décentralisée dans les dynamiques épidémiques et de marketing viral. Les résultats ont des implications pour la gestion des soins de santé, la concurrence commerciale et d'autres domaines connexes.

Mots-clés: Théorie des jeux, Théorie des graphes, Modèle épidémique en réseau, Modèle Susceptible-Infected-Recovered (SIR), Modèle Susceptible-Infected-Susceptible (SIS), marketing viral, équilibre de Nash, équilibre de Stackelberg.

Abstract

This thesis investigates decentralized decision-making in epidemic and viral marketing dynamics. The mathematical framework of game theory is exploited to design and assess the effectiveness of decentralized strategies. The thesis begins with a review of mathematical tools, emphasizing graph theory and game theory. Chapter 2 presents a networked epidemic game where each player (region or country) seeks to implement a tradeoff between socio-economic and health looses, incorporating constraints such as intensive care unit (ICU) availability. Nash equilibrium and Generalized Nash equilibrium are analyzed, and the influence of decentralization on global efficiency is measured using metrics like the Price of Anarchy (PoA) and the Price of Connectedness (PoC). The practical application of the game to a Covid-19 scenario is illustrated. Chapter 3 extends the analysis of Chapter 2 by incorporating opinion dynamics into the decentralized control of a networked epidemic. A new game model is introduced, where players represent geographical aera balancing socio-economic and health losses ; the game is built to implement features of practical interests and to possess some mathematical properties (e.g., posynomiality) which makes its analysis tractable. The analysis focuses on the existence and uniqueness of the Generalized Nash Equilibrium (GNE), and an algorithm for computing the GNE is proposed. Numerical simulations quantify the efficiency loss induced by decentralization in the presence and absence of opinion dynamics. The results identify scenarios where decentralization is acceptable in terms of global efficiency measures and highlight the importance of opinion dynamics in decision-making processes. Chapter 4 explores a Stackelberg duopoly model in the context of viral marketing campaigns. The objective is to characterize the optimal allocation strategy of advertising budgets across regions to maximize market share. A relatively simple Equilibrium strategies are derived, and conditions for a "winner takes all" outcome are established. Theoretical findings are complemented by numerical simulations and an example illustrating equilibrium characterization.

This thesis offers valuable insights into the effectiveness of decentralized decision-making in the context of epidemic and viral marketing dynamics. The findings have implications for healthcare management, business competition, and related fields.

Keywords: Game Theory, Graph Theory, Networked Epidemic Model, Susceptible-Infected-Recovered (SIR) model, Susceptible-Infected-Susceptible (SIS) model, Viral Marketing, Nash equilibrium, Stackelberg equilibrium

Résumé étendu en français

En réponse à l'épidémie de Covid-19 en 2020, de nombreux pays ont adopté des politiques centralisées uniformes de distanciation sociale, comme la Chine, la France, l'Italie et l'Espagne, dans le but de contenir la propagation du virus. Cependant, cette approche a entraîné des incohérences entre le niveau de gravité des mesures et la situation locale. Parmi les conséquences de ce décalage, on trouve : des pertes économiques locales évitables, des dommages psychologiques potentiellement évitables, un manque d'acceptation de la part des citoyens, de la frustration, et donc une dégradation en termes d'efficacité des mesures [1, 2, 3]. La décentralisation de la prise de décision dans un système fédéral présente plusieurs avantages potentiels [4] :
La flexibilité et l'adaptabilité : Les décideurs locaux, qui connaissent bien les besoins et les défis spécifiques de leur juridiction, peuvent personnaliser les interventions et les stratégies pour les aligner sur les caractéristiques uniques de leur population, de leur infrastructure et de leurs ressources.
L'expertise et la connaissance locales : Les décideurs politiques au niveau régional ou organisationnel possèdent une profonde compréhension de leurs domaines spécifiques, y compris des facteurs culturels, sociaux et économiques qui peuvent influencer la dynamique de transmission des maladies.
Un temps de réponse plus rapide : Les autorités locales ont l'autonomie de prendre des décisions rapidement et de mettre en œuvre rapidement des mesures de contrôle, éliminant ainsi le besoin d'approbations longues d'une autorité centralisée.
Une responsabilité et une transparence accrues : Les décideurs locaux sont directement responsables de leurs actions et de leurs résultats, ce qui renforce leur engagement en faveur d'une prise de décision efficace et d'une allocation des ressources. De plus, les systèmes décentralisés encouragent souvent une plus grande participation et un plus grand engagement de la communauté, favorisant la transparence et renforçant la confiance du public dans le processus de prise de décision.

Dans l'ensemble, la valeur ajoutée de la gestion décentralisée des épidémies réside dans

l'amélioration de la logistique et de la distribution des ressources. Dans un système décentralisé, la prise de décision est répartie entre les entités locales et les parties prenantes, permettant des opérations logistiques efficaces. En effet, les entités locales peuvent évaluer les besoins spécifiques de leur région et allouer les ressources en conséquence, réduisant ainsi les goulets d'étranglement et les retards. De plus, la gestion décentralisée réduit la dépendance à une entité centrale, permettant aux entités locales de mobiliser leurs propres efforts et de répondre efficacement aux épidémies. Par exemple, en 2021, l'expérience acquise sur la pandémie montre que permettre aux régions (par exemple, les provinces en Chine, les États aux États-Unis, les Länder en Allemagne ou les régions en France) d'ajuster localement les décisions peut être plus approprié. Cela est également vrai en ce qui concerne la vaccination. Par conséquent, différents pays ont adopté différentes stratégies de contrôle, privilégiant des aspects tels que l'éducation, la protection sociale, l'économie ou la santé. Même au sein d'un même pays, les mesures mises en œuvre étaient différentes pour les régions en fonction de la situation locale. Ces mesures visent à établir un équilibre entre les aspects socio-économiques et les aspects sanitaires. Un autre facteur important dans la propagation de l'épidémie est le comportement des individus dans les régions. En réponse à l'épidémie de Covid-19, les gens ont spontanément réduit les contacts sociaux, sont restés chez eux autant que possible, ont adopté des mesures d'hygiène ou de distanciation sociale plus strictes, ou ont porté des masques, indépendamment de la politique gouvernementale mais suivant une mode. Les actions gouvernementales ont été sujettes à un glissement comportemental contrôlable via les réseaux sociaux [5, 6].

Ce contexte motive la formalisation et l'étude du problème de la gestion décentralisée des épidémies, qui implique plusieurs régions géographiques interconnectées, telles que les pays, les métropoles, les provinces, les régions et les États. Chaque région n'a qu'un contrôle local sur les épidémies et un objectif individuel, et une question centrale est de savoir si la décentralisation entraîne une perte de performance significative en termes de mesure d'efficacité globale. Ce problème est pertinent non seulement dans la gestion des épidémies, mais aussi dans l'économie, comme lorsqu'une entreprise cherche à maximiser la diffusion de biens ou de services tout en déléguant les politiques de diffusion à des entités locales [7] ou, plus généralement, pour le marketing viral [8]. Tout en s'abstenant d'une explication complexe de la signification du marketing viral, il est essentiel de garder à l'esprit que le marketing viral exploite l'influence sociale et le bouche-à-oreille pour maximiser l'impact des campagnes marketing, créant une sensibilisation et un engagement significatifs avec les offres de l'entreprise, conduisant à l'expansion de la part de marché [9].

Cette thèse vise à étudier de manière approfondie le processus de prise de décision décentralisée dans le contexte des phénomènes de propagation dans les réseaux. Elle se concentre spécifiquement sur l'application de la prise de décision décentralisée à la gestion des épidé-

mies, en considérant des scénarios avec et sans dynamique d'opinion, ainsi que dans le paysage concurrentiel des campagnes de marketing viral entre entreprises [10, 9, 11]. En exploitant la puissance de la théorie des jeux, l'objectif principal de cette étude est de découvrir les subtilités de la prise de décision décentralisée dans les phénomènes de propagation en réseau, et leur impact sur la dynamique globale et l'efficacité par rapport aux stratégies centralisées.

Dans la suite, une déclaration complète et détaillée des objectifs de la thèse est présentée.

Objectifs

La théorie des jeux, un cadre mathématique largement utilisé dans l'analyse des processus de prise de décision, a connu une adoption croissante dans le domaine des phénomènes de propagation. En considérant les différentes parties prenantes impliquées dans les phénomènes de propagation, comme les prestataires de soins de santé, les gouvernements, les individus ou les entreprises, la théorie des jeux apparaît comme un outil précieux pour identifier les stratégies qui atteignent un équilibre et évaluer leur impact sur le résultat global. En particulier, l'examen de l'équilibre de Nash dans ce contexte de jeu conduit à un scénario dans lequel aucune partie prenante n'a intérêt à s'écarter unilatéralement de sa stratégie choisie. Comprendre l'impact de ces stratégies d'équilibre sur le résultat global est crucial pour les décideurs et les chercheurs. En étudiant les conséquences et les implications des différentes stratégies, la théorie des jeux nous permet d'évaluer l'efficacité, l'efficience et l'équité des résultats obtenus.

Les jeux examinés dans cette thèse sont analysés en utilisant une méthodologie couramment employée en théorie des jeux. Plus précisément, la méthodologie implique l'analyse de l'existence d'un équilibre dans un jeu, de l'unicité de cet équilibre, et de sa déterminance. Une fois ces questions abordées, une analyse numérique est utilisée pour évaluer l'efficacité des solutions identifiées. Dans l'ensemble, cette méthodologie sert d'outil puissant pour comprendre la dynamique stratégique des jeux et identifier les stratégies optimales pour les joueurs. Elle est largement utilisée dans des disciplines telles que l'économie, la science politique et les affaires, permettant l'analyse d'une large gamme de scénarios, allant de jeux simples à deux joueurs à des jeux complexes à plusieurs joueurs.

Structure de la thèse

Ce manuscrit est structuré en quatre chapitres principaux. Dans la suite, nous en donnons un bref résumé. Une conclusion générale et des perspectives sont présentées à la fin du manuscrit.

Chapitre 1 : Revue des outils mathématiques

Ce chapitre donne un aperçu des concepts fondamentaux et des outils théoriques utilisés dans cette thèse. La première section de cette thèse, connue sous le nom d'état de l'art, se concentre sur la présentation des connaissances existantes et des contributions relatives à la prise de dé-

cision en épidémiologie, en opinion ou en phénomènes de propagation du marketing viral. Elle vise à donner un aperçu de l'état actuel de la recherche et des avancées dans le domaine, en mettant en évidence les principales découvertes, méthodologies et cadres théoriques qui ont façonné notre compréhension du domaine. La section suivante de ce chapitre sert à revisiter et à renforcer les concepts fondamentaux de la théorie des graphes et de la théorie des jeux, qui forment la pierre angulaire de l'analyse menée dans cette thèse. La théorie des graphes fournit les outils nécessaires pour modéliser et analyser la nature interconnectée des réseaux, tandis que la théorie des jeux offre un cadre pour étudier la prise de décision stratégique dans les systèmes complexes. Ensemble, ces fondements théoriques permettent une analyse complète du processus de prise de décision décentralisée dans le contexte des phénomènes de propagation en réseau.

Chapitre 2 : Sur l'efficacité de la gestion décentralisée des épidémies et application à la Covid-19

Dans ce chapitre, nous tentons d'examiner la possible perte d'efficacité due à la décentralisation de la prise de décision épidémique. À cette fin, nous proposons un modèle mathématique relativement simple mais complet. Plus précisément, nous introduisons un jeu sous forme stratégique fondé sur un modèle Susceptible-Infected-Recovered (SIR) en réseau [12, 13]. Dans ce jeu, chaque joueur correspond à une région géographique, et son objectif est d'établir des règles de distanciation sociale pour minimiser un coût particulier, qui est un compromis entre les pertes socio-économiques et sanitaires. De plus, le coût attribué à chaque région est influencé non seulement par ses propres actions, mais aussi par les actions entreprises par les régions voisines. En effet, les interactions entre les joueurs sont représentées par une matrice d'adjacence pondérée. La décision de chaque joueur est supposée rester constante pendant un temps fini (défini comme la "phase de travail").

La principale contribution théorique de ce chapitre est l'analyse détaillée de l'existence et de l'unicité de la stratégie de Nash. Ce faisant, nous introduisons un cadre appelé "Régime d'interconnexion faible" (RIF), qui permet l'existence d'un équilibre de Nash (EN) dans le jeu proposé. De plus, cette analyse garantit la bien-posée des deux mesures d'efficacité utilisées pour évaluer l'efficacité de la stratégie décentralisée, le Prix de l'Anarchie (PoA) et le Prix de la Connectivité (PoC). Dans une partie étendue de notre travail, nous intégrons également un facteur essentiel dans la gestion des épidémies - la disponibilité et l'adéquation des ressources de soins de santé, avec une attention particulière portée aux unités de soins intensifs (USI). Ces éléments sont intégrés dans le processus de prise de décision, ce qui nous conduit à explorer une forme généralisée du jeu. En conséquence, nous étendons notre analyse à l'étude de l'équilibre de Nash généralisé de ce nouveau jeu, où des conditions spécifiques concernant l'existence d'un

tel équilibre sont explorées et établies.

Chapitre 3 : Sur l'efficacité de la gestion décentralisée des épidémies en présence de dynamiques d'opinion

Ce chapitre propose un modèle mathématique pour évaluer les effets de la décentralisation sur la gestion des épidémies, en tenant compte de dynamiques perturbatrices telles que le comportement social ou la vaccination. Nous considérons un modèle mathématique relativement simple qui capture les principales caractéristiques d'intérêt, composé d'un jeu sous forme stratégique (généralisé) construit à partir d'un modèle compartimental Susceptible-Infected-Recovered (SIR) en réseau [12, 13] couplé à un modèle de dynamique d'opinion variant dans le temps [14, 15, 11, 16, 17, 18]. Comme au chapitre 2, chaque joueur représente une zone géographique qui minimise un coût individuel, en mettant en œuvre un compromis donné entre les pertes socio-économiques, les pertes globales/locales en termes de nombre de reproduction du virus [19, 20, 21, 22], les coûts de sensibilisation et un coût d'opinion moyen. Nous notons que le modèle de jeu proposé est un jeu sous forme stratégique généralisée joué en un coup, c'est-à-dire que les actions sanitaires sont fixées sur un horizon temporel fini, et que chaque région applique N+1 campagnes de sensibilisation pour influencer les croyances des individus antagonistes dans les réseaux sociaux. En supposant que le graphique épidémique soit fortement connecté : les propriétés d'existence et d'unicité du GNE sont garanties ; un algorithme qui converge vers le GNE est proposé ; il est montré que le problème de gestion centralisée peut être transformé en un problème d'optimisation convexe. Ces résultats nous permettent d'évaluer, grâce à des résultats numériques, la perte (mesurée en termes de Prix de l'Anarchie (PoA)) induite soit par la décentralisation, avec ou sans prise en compte de la dynamique d'opinion.

Chapitre 4 : Un design de marketing viral Stackelberg pour deux joueurs concurrents

Le terme "phénomène viral" est dérivé du concept "d'épidémie". Le chapitre 4 de cette thèse aborde le problème du marketing viral où deux entreprises sont en concurrence pour gagner une plus grande part de marché en proposant un service ou un produit à des clients dispersés dans plusieurs régions géographiques. À cette fin, le marketing viral est modélisé comme un équilibre, en utilisant spécifiquement le concept de "le gagnant prend tout" [23], pour lequel un cas particulier de ce modèle est l'état stable d'un système SIS multi-virus [24]. Il est important de noter que des instances de tels équilibres ont été enregistrées dans des scénarios réels, un exemple classique étant la concurrence entre Facebook et Myspace, comme détaillé dans [24]. L'un des principaux objectifs de ce travail est de caractériser la stratégie d'allocation du budget publicitaire pour chaque entreprise à travers les régions afin de maximiser sa part de marché lors

de la concurrence. Pour atteindre cet objectif, nous introduisons un modèle de jeu Stackelberg relativement simple qui capture les principaux effets de la concurrence pour la part de marché. En analysant les équilibres du jeu Stackelberg à deux niveaux dans des contextes pessimistes et optimistes, nous fournissons la stratégie d'allocation budgétaire associée. Notre analyse établit les conditions dans lesquelles la solution du jeu conduit à l'issue "le gagnant prend tout". Nous complétons nos résultats théoriques par des simulations numériques et fournissons un exemple pour illustrer davantage notre caractérisation de l'équilibre.

Chapitre 5 : Remarques conclusives et perspectives

Dans ce dernier chapitre, nous donnons un aperçu des contributions apportées à la littérature par notre travail de recherche. Nous réfléchissons aux principales conclusions et idées obtenues à partir des chapitres précédents, en soulignant leur importance pour répondre aux objectifs de recherche. De plus, nous discutons des perspectives potentielles pour des travaux futurs qui peuvent encore améliorer et élargir l'analyse menée dans cette thèse.

Contents

Glossary

CRAN	CRAN
UL	Université de Lorraine
UMR	Unité Mixte de Recherche

List of Figures

List of Tables

Introduction

In response to the outbreak of the Covid-19 epidemic in 2020, many countries adopted uniform centralized social distancing policies, such as China, France, Italy and Spain, in an effort to contain the spread of the virus. However, this approach resulted in inconsistencies between the severity level of the measures and the local situation. Among the consequences of this mismatch we find : avoidable local economic losses, potentially avoidable psychological damages, lack of acceptance from citizens, frustration, and thus a degradation in terms of measures effectiveness [1, 2, 3]. Decentralizing decision-making in a federal system presents several potential advantages [4] :

Flexibility and Adaptability : Local decision-makers, who have in-depth knowledge of their jurisdiction's specific needs and challenges, can customize interventions and strategies to align with the unique characteristics of their population, infrastructure, and resources.

Local Expertise and Knowledge : Policy makers at the regional or organizational level possess a deep understanding of their specific areas, including cultural, social, and economic factors that can influence disease transmission dynamics.

Faster Response Time : Local authorities have the autonomy to make prompt decisions and swiftly implement control measures, eliminating the need for lengthy approvals from a centralized authority.

Increased Accountability and Transparency : Local decision-makers are directly accountable for their actions and outcomes, which strengthens their commitment to effective decision-making and resource allocation. Additionally, decentralized systems often encourage greater community participation and engagement, promoting transparency and building public trust in the decision-making process. Overall, the added value of decentralized epidemic management is improved logistics and resource distribution. In a decentralized system, decision-making is distributed among local entities and stakeholders, allowing for efficient logistical operations. Indeed, local entities can assess the specific needs of their region and allocate resources accordingly, reducing bottlenecks and delays. Furthermore, decentralized management reduces

dependency on a central entity, empowering local entities to mobilize their own efforts and respond effectively to epidemics. For instance, in 2021, the experience acquired on the pandemic shows that allowing regions (e.g., provinces in China, states in the USA, Länder in Germany, or regions in France) to locally adjust the decisions may be more suited. This is also true when it comes to vaccination. Consequently, different countries adopted different control strategies prioritizing aspects such as education, social welfare, economy, or health. Also within a given country the measures implemented were different for regions depending on the local situation. These measures have been aiming at achieving a certain tradeoff between socio-economic aspects and health aspects. Another important factor in epidemic propagation is the behavior of individuals in the regions. In response to the Covid-19 outbreak, people have spontaneously reduced social contact, stayed home whenever possible, adopted stricter hygiene or social distancing measures, or worn masks, regardless the government policy but following a fad. Government actions have been subject to controllable behavioral drift via social networks [5, 6].

This context motivates the formalization and study of the problem of decentralized epidemic management, which involves several interconnected geographical regions, such as countries, metropoles, provinces, regions, and states. Each region has only local control over the epidemics and an individual objective, and a central question is whether decentralization results in a significant performance loss in terms of a global efficiency measure. This problem is relevant not only in epidemic management but also in economics, such as when a company aims to maximize the dissemination of goods or services while delegating dissemination policies to local entities [7] or more generally for viral marketing [8]. While refraining from a complex explanation of the meaning of viral marketing, it is essential to bear in mind that viral marketing leverages social influence and word-of-mouth to maximize the impact of marketing campaigns, creating significant awareness and engagement with the company's offerings, leading to market share expansion [9].

This thesis aims to comprehensively investigate the decentralized decision-making process in the context of propagation phenomena in networks. It specifically focuses on the application of decentralized decision-making in epidemic management, considering scenarios with and without opinion dynamics, as well as in the competitive landscape of viral marketing campaigns between firms [10, 9, 11]. By leveraging the power of game theory, the main objective of this study is to uncover the subtleties of decentralized decision-making in network propagation phenomena, and their impact on overall dynamics and effectiveness compared to centralized strategies.

In the following, a complete and detailed statement of the thesis objectives is presented.

Objectives

Game theory, a mathematical framework widely employed in the analysis of decision-making processes, has witnessed a growing adoption within the field of spreading phenomena. Through the consideration of various stakeholders involved in spreading phenomena, such as healthcare providers, governments, individuals, or firms, game theory emerges as a valuable tool for identifying strategies that reach an equilibrium and evaluating their impact on the overall outcome. In particular, examining Nash equilibrium in this game setting leads to a scenario in which no stakeholder has an incentive to unilaterally deviate from their chosen strategy. Understanding the impact of these equilibrium strategies on the overall outcome is crucial for decision-makers and researchers alike. By studying the consequences and implications of different strategies, game theory enables us to assess the effectiveness, efficiency and fairness of the results obtained.

The games examined in this thesis are analyzed using a commonly employed methodology in game theory. Specifically, the methodology involves the analysis of whether a game possesses an equilibrium, the uniqueness of said equilibrium, and its determinacy. Once these questions have been addressed, numerical analysis is employed to evaluate the effectiveness of the identified solutions. Overall, this methodology serves as a powerful tool for comprehending the strategic dynamics of games and identifying optimal strategies for players. It is extensively used in disciplines including economics, political science, and business, enabling the analysis of a wide range of scenarios, ranging from simple two-player games to complex multi-players games.

Structure of the thesis

This manuscript is structured in four main chapters. In the following, we give a brief summary of each of them. A general conclusion and perspectives are presented at the end of the manuscript.

Chapter 1 : Review of mathematical tools

This chapter provides an overview of the fundamental concepts and theoretical tools used in this thesis. The first section of this thesis, known as the state of the art, focuses on presenting the existing body of knowledge and contributions relating to decision-making in epidemiological, opinion or viral marketing propagation phenomena. It serves to provide an overview of the current state of research and advances in the field, highlighting the key findings, methodologies and theoretical frameworks that have shaped our understanding of the field. The subsequent section of this chapter serves to revisit and reinforce fundamental concepts in graph theory and game theory, which form the cornerstone of the analysis in this thesis. Graph theory provides

the necessary tools to model and analyze the interconnected nature of networks, while game theory offers a framework to study strategic decision-making in complex systems. Together, these theoretical foundations enable a comprehensive analysis of the decentralized decision-making process within the context of networked spreading phenomena.

Chapter 2 : On the Efficiency of Decentralized Epidemic Management and Application to Covid-19

In this chapter, we attempt to examine the possible loss of efficiency due to the decentralization of epidemic decision-making. To this end, we propose a relatively simple but complete mathematical model. Specifically, we introduce a strategic-form game that is founded on a networked Susceptible-Infected-Recovered (SIR) model [12, 13]. In this game, every player corresponds to a geographic region, and their objective is to establish social distancing rules to minimize a particular cost, which is a trade-off between socio-economic and health losses. Furthermore, the cost assigned to each region is influenced not only by its own actions but also by the actions undertaken by neighboring regions. Indeed, the interactions between players are represented by a weighted adjacency matrix. The decision of each player is assumed to remain constant throughout a finite time (defined as the "working phase").

The primary theoretical contribution of this chapter is the detailed analysis of the existence and uniqueness of the Nash strategy. In doing so, we introduce a framework known as the "Weak Interconnection Regime" (**WIR**), which allows the existence of a Nash equilibrium (NE) in the proposed game. Moreover, this analysis ensures the well-posedness of the two efficiency measures used to evaluate the effectiveness of the decentralized strategy, the Price of Anarchy (PoA) and the Price of Connectedness (PoC). In an extended part of our work, we also incorporate a critical factor in the management of epidemics - the availability and adequacy of healthcare resources, with a particular emphasis on intensive care units (ICUs). These elements are integrated into the decision-making process, leading us to explore a generalized form of the game. As a result, we extend our analysis to the study of the generalized Nash equilibrium of this new game, wherein specific conditions pertaining to the existence of such an equilibrium are explored and established.

Chapter 3 : On the Efficiency of Decentralized Epidemic Management in the Presence of Opinion Dynamics

This chapter considers a mathematical model to evaluate the effects of decentralization on epidemic management, taking into account perturbing dynamics such as social behavior or vaccination. We consider a relatively simple mathematical model that captures the main features of interest, consisting of a (generalized) strategic form game built from a networked Susceptible-

Infected-Recovered (SIR) compartmental model [12, 13] coupled with a time varying opinion dynamics model [14, 15, 11, 16, 17, 18]. Like in Chapter 2, each player represents a geographical area which minimizes individual cost, by implementing a given trade-off between socio-economic losses, global/local losses in terms of the reproduction number of the virus [19, 20, 21, 22], awareness costs, and an average opinion cost. We note that the proposed game model is a generalized strategic form game played in one-shot i.e., the sanitary actions are fixed over a finite time horizon, and $N + 1$ awareness campaigns are applied by each region to influence the beliefs of antagonistic individuals in the social networks. By assuming the epidemic graph to be strongly connected : the existence and uniqueness properties of the GNE are shown to be guaranteed ; an algorithm that converges to the GNE is proposed ; it is shown that the centralized management problem can be transformed into a convex optimization problem. These results allow us to assess through numerical results the loss (measured in terms of Price of Anarchy (PoA)) induced either by decentralization with or without taking into account the opinion dynamic.

Chapter 4 : A Stackelberg Viral Marketing Design for Two Competing Players

The term "viral phenomenon" is derived from the concept of "epidemic.". In Chapter 4 of this thesis tackles the problem of viral marketing where two firms compete to gain a greater market share by offering a service or product to customers dispersed over multiple geographical regions. To this end, viral marketing is modeled as an equilibrium, specifically using the concept of “winner takes all" [23], for which a particular case of such model is the steady-state of a multi-virus SIS system [24]. It’s significant to note that instances of such equilibria have been recorded in actual scenarios, a classic example being the competition between Facebook and Myspace, as detailed in [24]. One of the main objectives of this work is to characterize the advertising budget allocation strategy for each firm across regions to maximize its market share when competing. To achieve this goal, we introduce a relatively straightforward Stackelberg game model that captures the principal effects of market share competition. By analyzing the equilibria of the two-level Stackelberg game in both pessimistic and optimistic settings, we provide the associated budget allocation strategy. Our analysis establishes the conditions under which the solution of the game leads to the “winner takes all” outcome. We complement our theoretical results with numerical simulations and provide an example to further illustrate our equilibrium characterization.

Chapter 5 : Concluding remarks and perspectives

In this final chapter, we provide an overview of the contributions made in the literature through our research work. We reflect on the key findings and insights obtained from the previous chapters, highlighting their significance in addressing the research objectives. Additionally, we discuss potential perspectives for future works that can further enhance and expand upon the analysis conducted in this thesis.

Publications

- O. Lindamulage De Silva, S. Lasaulce, I-C. Morărescu, "On the Efficiency of Decentralized Epidemic Management and Application to Covid-19", IEEE Control. Syst. Lett. 6 : 884-889 (2022) and presented at the 60th IEEE Control and Decision Conference (CDC), 2021.
- O. Lindamulage De Silva, I-C. Morărescu, S. Lasaulce, "Etude de l'efficacité de la gestion dé ecentralisée d'une épidémie et application au Covid-19", 28th Gretsi conference, Nancy, France, Sep. 2022.
- O. Lindamulage De Silva, V. S. Varma, M. Cao, I-C. Morărescu, S. Lasaulce, "A Stackelberg viral marketing design for two competing players", IEEE Control. Syst. Lett. (accepted) and will be presented at the 62th IEEE Control and Decision Conference (CDC), 2023.
- O. Lindamulage De Silva, S. Lasaulce, I-C. Morărescu, V. S. Varma, "On the Efficiency of Decentralized Epidemic Management in the Presence of Opinion Dynamics", IEEE Trans. Control. Netw. Syst. (under review).
- M. Granzotto, O. Lindamulage de Silva, R. Postoyan, D. Nešić, Z-P. Jiang, "Regularizing policy iteration for recursive feasibility and stability", 61th IEEE Control and Decision Conference (CDC), 2021.
- M. Granzotto, O. Lindamulage de Silva, R. Postoyan, D. Nešić, Z-P. Jiang, "Policy iteration : for want of recursive feasibility, all is not lost", IEEE Trans. Automat. Contr. (under review).

Chapter 1

Review of Mathematical Tools

The present chapter aims to offer a comprehensive introduction to the basic concepts and theoretical tools that are used in this thesis. The first section of this chapter, known as the state of the art, is devoted to showcasing the currently available body of knowledge and contributions relating to decision-making process within the realms of epidemiology, opinion dynamics, and viral marketing propagation phenomena. The goal is to outline the current trajectory of research and advances in the field, highlighting the key findings, methodologies and theoretical frameworks that have shaped our understanding of the field. The subsequent part of this chapter aims to review the basics notions of graph theory and game theory, which both form the cornerstone of the analytical framework utilized in this thesis. Graph theory supplies the required tools to construct models of and analyze the interconnected nature of networks. While, game theory presents a framework for examining strategic decision-making in complex systems. Together, these theoretical foundations enable a comprehensive analysis of the decentralized decision-making process within the context of networked spreading phenomena.

1.1 State-of-the-art

In 2020, many governments around the world had to take drastic measures to mitigate the propagation of the SARS-Cov2 virus. Especially over the first half of 2020, similar measures were taken over large geographical areas such as countries. One major drawback from implementing such a (uniform) policy was that there has been a mismatch between the measures severity level and the local situation. Among the consequences of this mismatch we find : avoi-

dable local economic losses, potentially avoidable psychological damages, frustration, and thus a degradation in terms of measures effectiveness [1, 2, 3]. On the other hand, epidemic models have played a significant role in understanding and managing infectious diseases for several decades. These models provide valuable insights into the dynamics of disease transmission and aid in formulating effective public health interventions.

The early mathematical models of epidemics emerged in the late 19th and early 20th centuries. Among them we highlight the Daniel Bernoulli's model in 1766 [26], which focuses on smallpox and demonstrates the potential of vaccination in reducing infection rates. Another influential contribution was the work of Kermack and McKendrick in 1927 [27], who introduced the Susceptible-Infectious-Recovered (SIR) model and established the foundation for subsequent developments in epidemic modeling. In the mid-20th century, basic compartmental models expanded upon the SIR framework. Anderson and May's model in [28] introduced additional compartments, such as the exposed and immune classes, allowing for a more realistic representation of disease progression. During the same era, the concept of the basic reproduction number, denoted as $\mathcal{R}_0$, gained prominence. This metric was originally introduced in the field of demography [29] and subsequently adopted by epidemiologists to quantify the potential spread of infectious diseases within a population [30]. A value of $\mathcal{R}_0$ greater than 1 indicates that the disease has the potential to spread throughout the population, while a value less than 1 suggests that the disease is unlikely to cause a large-scale epidemic. Estimating $\mathcal{R}_0$ involves the use of mathematical models that incorporate various assumptions and factors, such as the infectiousness of the disease, the contact rate between infected and susceptible individuals, and the duration of infectiousness.

Building on the historical development of epidemic models, the experience gained from the pandemic in 2021 has highlighted the benefits of allowing regions (e.g., provinces in China, states in the USA, Länder in Germany, or regions in France) to locally adjust decisions in managing the spread of the disease. This is also true when it comes to vaccination. Consequently, different countries adopted different control strategies prioritizing aspects such as education, social welfare, economy, or health. Also within a given country the measures implemented were different for regions depending on the local situation. These measures have been aiming at achieving a certain tradeoff between socio-economic aspects and health aspects. Motivated by this observation and in order to assess the potential efficiency loss induced by decentralizing the epidemic management, we consider mathematical models that is relatively simple while capturing the main effects of interest. In Chapter 2 and Chapter 3, we propose mathematical models to analyze the effects of decentralization on the epidemics management based on existing epidemic network models [31, 32, 33], [34, Chapter 9.3].

In Chapter 2, it is considered a strategic-form game which is built from a networked Susceptible-

Infected-Recovered (SIR) compartmental model [12, 13]. Precisely, a game where each player represents a geographical region which decides social-distancing rules which aim at minimizing a cost. Each individual cost implements a given trade-off between socio-economic losses and health losses.

To the best of our knowledge, the game introduced in Chapter 2 differs from existing works for several reasons. In [35], the players are the individuals but their decision consist in controlling social distancing with others to find a balance between social interactions and the chances of being infected by the virus that spreads through a single region SIR model. The main differences between the work in Chapter 2 and the existing results on networked epidemic games (e.g., [36, 37, 38, 39]) can be summarized as follows : we consider an SIR model while the existing game models are applied to the networked SIS model (Susceptible-Infected-Susceptible) ; we control the inter-regions transmission rates while the existing works that are considering networks described by a binary adjacency matrix ; we propose a one-shot game over a finite time horizon unlike the existing works consider infinite time games with constant actions ; we exploit the ICUs constraint in the game analysis.

Another important factor in epidemic propagation is the compliance to sanitary rules by the population. Specifically, in response to the Covid-19 outbreak, people have spontaneously reduced social contact, stayed home whenever possible, adopted stricter hygiene or social distancing measures, or worn masks, regardless of government policy but following a fad. Government actions have been subject to controllable behavioral drift via social networks [5, 6]. In light of these observations, in Chapter 3, we propose a mathematical model to evaluate the effects of decentralization on epidemic management, taking into account perturbing dynamics such as social behavior or vaccination. A relatively simple mathematical model is considered, that captures the main features of interest, consisting of a (generalized) strategic form game built from a networked Susceptible-Infected-Recovered (SIR) compartmental model [12, 13] coupled with an opinion dynamics model [14, 15, 11, 16, 17, 18]. Such as in Chapter 2, the game considers each player as a geographical area aiming to minimize individual cost, which implements a given trade-off between socio-economic losses, global/local losses in terms of the reproduction number of the virus [19, 20, 21, 22], awareness costs, and an average opinion cost.

To the best of our knowledge, the game introduced in Chapter 3 exhibits several distinctive features when compared to existing works. The main differences between the present research work and prior research on networked epidemic games (e.g., [36, 37, 38, 39, 40, 41]) can be summarized as follow. Firstly, the game is over a networked SIR model coupled with a time-varying opinion dynamics model. Secondly, it proposes a one-shot game based on an epidemic model that includes a behavioral drift. Thirdly, the research work sets a static and generalized strategic form game that allows a tradeoff between key socio-economic and health aspects to be

found and enables a complete analysis of the generalized Nash equilibrium.

On the other hand, the problem of decentralizing the decision making in order to mitigate an outbreak is relevant not only in epidemic management but also in economics, such as when a company aims to maximize the dissemination of goods or services while delegating dissemination policies to local entities [7] or more generally for viral marketing [8]. Viral marketing (VM) is a strategy to promote different products/services using social networks. The information spreads as a virus from one person to their family, friends and colleagues. To model the spread of information or services within a population, various mathematical frameworks have been developed. In the context of viral marketing, two prominent modeling approaches are opinion dynamics models (see [42, 7] for instance) and epidemic models (see [43, 44] for instance). Opinion dynamics models focus on capturing how opinions and preferences evolve among individuals in a social network, considering factors such as interaction patterns, biased influences, and coupled decision-making processes. On the other hand, epidemic models capture the transmission of diseases or information within a population, incorporating parameters such as infection rates, recovery rates, and population connectivity, which play a crucial role in understanding the dynamics of service propagation and devising effective marketing strategies to maximize the spread and adoption of the service. It is noteworthy that the equilibriua of viral marketing dynamics can take specific forms such as the “winner takes all" [23]. A game considering multi virus SIS dynamics leading to a "winner takes all" steady state has been presented in [24]. It is noteworthy that such an equilibrium has been observed in real life, see for instance the classical example of Facebook and Myspace [24]. In the context of viral marketing duopoly, the concept of “winner takes all" refers to a scenario where two competing firms engage in viral marketing campaigns to gain a larger market share. In this situation, the firm that effectively leverages viral marketing techniques and achieves widespread adoption of its product or service tends to capture the majority of the market, leaving the competitor with a significantly smaller share. It has been proven that targeted marketing combined with social network spreading has advantages over conventional mass campaigns, including cost-effectiveness and the ability to reach specific customer groups [7]. Basically, the authors formulated the problem as an optimal budget allocation and they shown that most individuals have to be targeted by the marketing campaign in order to get a maximum profit. The problem of competition to get a larger market share has been addressed in [45], where the authors introduced a duopoly model which accounts for the knowledge of opinion dynamics through a social network and characterized the Nash strategies of the players.

Unlike these works that take advantage of node centrality (network topology) but rely on linear opinion dynamic models for the service spreading, we assume in Chapter 4 “a winner takes all” model based on [24, 43, 44]. This setup is more suitable for certain types of pro-

ducts/services, such as video streaming and activities in social networking platforms. The main goal of Chapter 4 is to formulate a two-level Stackelberg game, where two players compete over several regions to get a higher market share subject to overall fixed budget constraints.

The budget allocated by a firm to a certain region modifies the spreading rate of the associated service in that region, and the model of “winner takes all" behavior allows us to decouple the analysis of the investment strategy for each region. The main contribution of this chapter lies in the characterization of its solutions where each player has to solve a budget allocation problem which is different from the ones that can be found in the literature. In [46], a dynamic optimization problem under budget constraints is formulated to control a single-virus SIS model. In [47], optimal control of joint multi-virus infection and information dissemination is considered for the sensitive-warned-infected-recovered-susceptible (SWIRS) model, without budget constraints. The differences between the present work and the existing results on epidemic control (e.g., [40, 48, 49, 50, 51]) are mainly related to the fact that our model can handle a multi-virus SIS epidemic model by considering budget constraints. Two existing works are relatively close to the present one. The first is [52] in which the authors formulate a static and strategic form game to deal with a bi-virus SIS epidemic model over a single region without a budget constraint. The second one is [8] in which only one player solves the optimal budget allocation problem over several regions.

1.2 Preliminaries and definitions

1.2.1 Graph theory

Graph theory is a branch of mathematics that deals with the study of networks and their properties. The origins of graph theory can be traced back to the 18th century, when mathematicians such as Euler and Bernoulli began to study the properties of the Königsberg bridge problem [53], which involved finding a path through the city of Königsberg that crossed each of its seven bridges only once. This problem led to the development of many important concepts in graph theory, such as Eulerian and Hamiltonian paths, and the famous Euler’s formula, which relates the number of vertices, edges, and faces of a planar graph. Graphs are a powerful tool for modeling complex systems and analyzing their properties that can be applied to many different problems and fields. One of the most significant applications of graph theory is in social networks, where nodes represent the entities, and edges represent the connections/influences between them. Graph theory is also well established in the optimization community [54, 55]. For example, Dijkstra’s algorithm in [56], which is used to find the shortest path between two nodes in a graph, is widely used in network routing protocols. Lastly, graph theory is used to study complex biological systems [57].

In what follows, we present the basic notions of graph theory based on [34, 58].

Definitions and concepts

Definition 1. *A graph G can be represented as a pair $\mathscr{G} = (\mathscr{V}, \mathscr{E})$, where $\mathscr{V}$ is a collection of $K > 1$ vertices or nodes, defined as $\mathscr{V} = \{1, ..., K\}$, and $\mathscr{E} \subset \mathscr{V} \times \mathscr{V}$ is a set of edges or pairs of distinct vertices (i, j) such that i and j represent the start and end nodes of an information flow. It is assumed that there are no self-loops in G, meaning that for all $i \in \mathscr{V}$, $(i, i) \notin \mathscr{E}$.*

The concept of proximity between agents in agent-based modeling is frequently conveyed through the concept of neighborhood.

Definition 2. *A set of agents that are in close proximity to a particular agent i, can be expressed mathematically as*

$$\mathscr{N}_i = \{j \in \mathscr{V} : (i, j) \in \mathscr{E}\}.$$

When the connection between two agents represents an information flow, one may wonder if the flow is bidirectional or unidirectional. Following that, the concepts of directed and undirected graphs naturally address the question. In graph theory, an undirected graph is a set of vertices (also known as nodes) connected by edges, where the edges do not have a specific direction or orientation. In other words, an undirected graph is a collection of points, some of which are connected by lines, without any arrowheads indicating the direction of the connections. Formally, we state the following definition.

Definition 3. *An undirected graph is defined as a pair $\mathscr{G} = (\mathscr{V}, \mathscr{E})$, where $\mathscr{V}$ is a set of vertices and $\mathscr{E}$ is a set of edges, where each edge is an unordered pair of distinct vertices from $\mathscr{V}$ i.e., the edge $(i, j) \in \mathscr{E}$ is the same as $(j, i) \in \mathscr{E}$ for any vertices i and j in $\mathscr{V}$.*

Definition 4. *The degree of a vertex in an undirected graph is the number of edges incident to it.*

The specificity of directed graphs (digraphs) is that the edges are directed i.e. the order in which the indices i and j appear is significant. One may have the edge (i, j) but not the edge (j, i).

Definition 5. *A directed graph is defined as a pair $\mathscr{G} = (\mathscr{V}, \mathscr{E})$, where $\mathscr{V}$ is a set of vertices and $\mathscr{E}$ is a set of directed edges, where each directed edge is an ordered pair of distinct vertices from $\mathscr{V}$, called directed edges or arcs. Each directed edge (i, j) is a pair of vertices i and j, where i is the source vertex and j the destination vertex. Direction of the edge is indicated by an arrowhead and points from the source vertex to the destination vertex. The set of directed edges $\mathscr{E}$ may contain self-loops (i.e., an edge that connects a vertex to itself).*

Definition 6. *For digraphs, the definition of degree is related to outdegree and indegree.*

(i) The outdegree of a vertex in a directed graph is the number of edges that originate from it, i.e., the number of directed edges that have that vertex as their source.

(ii) The indegree of a vertex is the number of edges that terminate at it, i.e., the number of directed edges that have that vertex as their destination.

A weighted directed graph, also known as a directed weighted graph, is a mathematical structure that consists of a set of vertices or nodes, and a set of edges, where each edge is a directed connection between two vertices, and has an associated weight.

Definition 7. *A weighted directed graph $\mathscr{G}$ is defined as a tuple $(\mathscr{V}, \mathscr{E}, w)$ where :*

$\mathscr{V}$ is a finite set of vertices or nodes, represented by $\mathscr{V} = \{1, \ldots, K\}$.

$\mathscr{E}$ is a set of directed edges or arcs, represented by $\mathscr{E} \subseteq \mathscr{V} \times \mathscr{V}$.

$w : \mathscr{E} \to \mathbb{R}$ is a weight function that assigns a real-valued weight or cost to each edge in $\mathscr{E}$.

In a weighted directed graph, the direction of the edges is significant, meaning that an edge (i, j) is not equivalent to the edge (j, i) unless they have the same weight. This is in contrast to an undirected graph, where the edges are bidirectional and have the same weight in both directions.

Definition 8. *A path from vertex i to vertex j in $\mathscr{G}$ is a finite sequence of vertices $(v_0, v_1, v_2, \ldots, v_n)$, where $v_0 = i$ and $v_n = j$, and each consecutive pair of vertices (v_k, v_{k+1}) is a directed edge in $\mathscr{E}$. The length of a path is the number of edges in the path, i.e., n.*

Definition 9. *A path is said to be simple if it does not repeat any vertex, except possibly the first and last vertices. That is, a simple path from i to j is a path $(v_0, v_1, v_2, \ldots, v_n)$ such that $v_0 = i$, $v_n = j$, and no vertex appears more than once in the sequence $(v_1, v_2, \ldots, v_{n-1})$.*

Despite their mathematical nature, graphs can be visually depicted through the use of a graphical schema, where each element from the set $\mathscr{V}$ is represented as a circle, and edges are indicated by lines. When graphs are used to model multi-agent systems (MAS), each vertex is considered an agent, and edges between vertices signify communication between the agents.

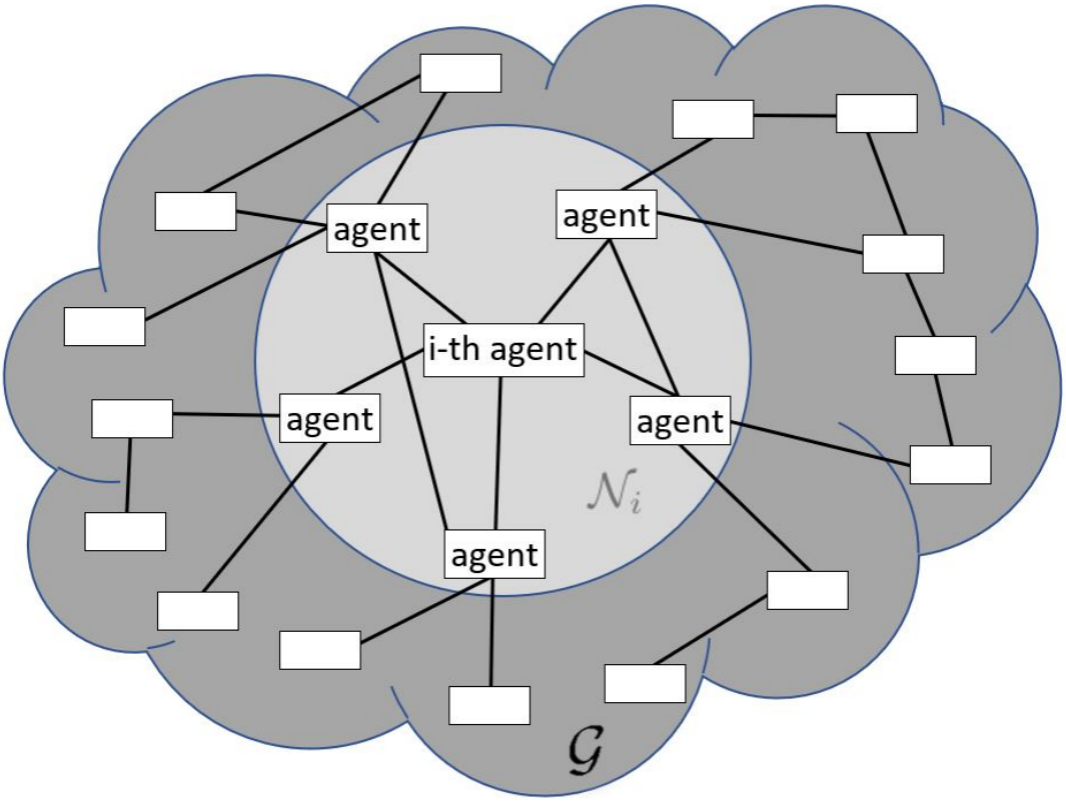

FIGURE 1.1 – "Network from the agent i point of view. The cloud $\mathcal{G}$ represents the whole network whereas the light grey circle $\mathcal{N}_i$ corresponds to the agent i and its neighbors. Black lines are connections between agents." [25]

Definition 10. *An undirected graph $\mathcal{G} = (\mathcal{V}, \mathcal{E})$ is said to be connected if for every pair of vertices i, j in $\mathcal{V}$, there exists a path from i to j. A path is defined as a sequence of vertices, where each pair of adjacent vertices is connected by an edge in $\mathcal{E}$.*

Definition 11. *A digraph $\mathcal{G} = (\mathcal{V}, \mathcal{E})$ is connected if $\forall i \in \mathcal{V}$, there exists a path from node i to every other node $j \in \mathcal{V} \setminus \{i\}$.*

Definition 12. *A digraph $\mathcal{G} = (\mathcal{V}, \mathcal{E})$ is strongly connected if for every edge $(i, j) \in \mathcal{V}^2$, a path extending from node i to node j can be established.*

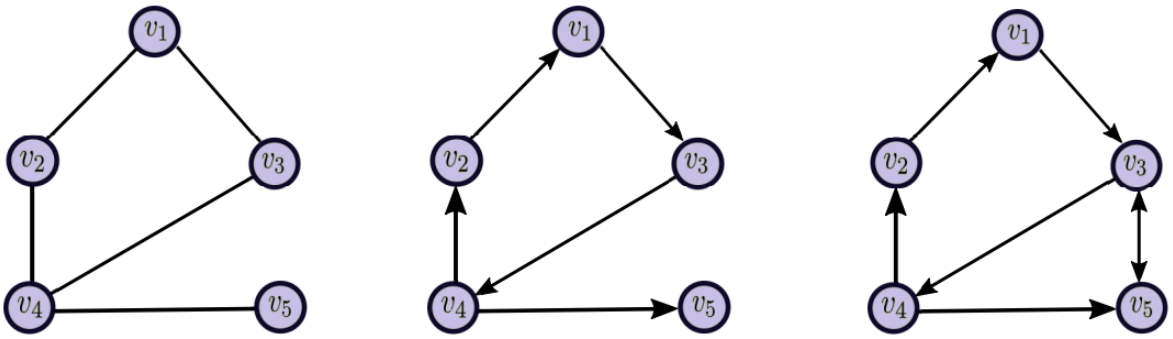

(a) Connected undirected graph

(b) Connected digraph

(c) Strongly connected diraph

FIGURE 1.2 – The figure provided in the given context visually demonstrates various types of graphs, which are commonly used in mathematical and computer science fields. The different categories of graphs presented in the figure include connected graphs, strongly connected graphs, undirected graphs, and directed graphs.

Definition 13. *The adjacency matrix* $\boldsymbol{A} = [a_{ij}] \in \mathbb{R}^{K\times K}$ *of a graph* $\mathscr{G}$ *is defined such that the entry* $a_{ij} = 1$ *if there exists an edge from vertex* i *to vertex* j*, and* $a_{ij} = 0$ *otherwise.*

(i) For an undirected graph, the adjacency matrix is a symmetric matrix.

(ii) For a directed graph, the adjacency matrix is not necessarily symmetric.

The adjacency matrix is a useful tool for analyzing graph properties and relationships. By storing and manipulating graph data in a matrix format, researchers and practitioners can efficiently perform various computations, such as determining the shortest path between two nodes or identifying connected components of the graph.

Definition 14. *The graph Laplacian matrix associated with the graph* $\mathscr{G}$ *is defined as*

$$L_{ij} = \begin{cases} \displaystyle\sum_{k=1,\ k\neq i}^{K} a_{ik} & \text{if } i = j \\ -a_{ij} & \text{otherwise.} \end{cases}$$

The Laplacian matrix $\boldsymbol{L}$ of a graph $\mathscr{G}$ can be constructed by subtracting the adjacency matrix $\boldsymbol{A}$ from the diagonal matrix $\boldsymbol{D}$, which encodes the degrees of the vertices. In the case of an undirected graph, the Laplacian matrix $\boldsymbol{L}$ is a symmetric positive semi-definite matrix. Additionally, the Laplacian matrix $\boldsymbol{L}$ satisfies the row-sum property i.e., the sum of the entries in each row of $\boldsymbol{L}$ is zero. This property holds for all types of graphs, regardless of their orientation.

Spectral graph theory constitutes a mathematical paradigm that examines the eigenvalues of matrices associated with graphs, with particular emphasis on the spectral attributes of the Laplacian matrix associated with the graph. The study of such spectral properties can yield

significant insights into the underlying structural characteristics of the graph. In what follows, we establish a set of matrix features that are related to graph theory.

Definition 15. *A matrix $\boldsymbol{M} = [m_{ij}]_{1\leq i,j\leq K} \in \mathbb{R}^{K\times K}$ is symmetric iff $\boldsymbol{M} = \boldsymbol{M}^\top$ i.e., $\forall\ i, j$ $m_{ij} = m_{ji}$.*

Definition 16. *A matrix $\boldsymbol{M} = [m_{ij}]_{1\leq i,j\leq K} \in \mathbb{R}^{K\times K}$ is positive semi-definite iff for all vector x, $x^\top \boldsymbol{M} x \geq 0$ and $\boldsymbol{M}$ is positive definite iff for all vector $x \neq 0$, $x^\top \boldsymbol{M} x > 0$.*

According to [58], we state the following theorem.

Theorem 1. *Let $\mathscr{G}$ be an undirected graph and $\boldsymbol{L}$ be its Laplacian matrix, then the eigenvalues $\lambda_i \in \mathbb{R}$, for $i \in \mathscr{V}$ of $\boldsymbol{L}$ are ordered as follows : $\lambda_1 \leq \lambda_2 \leq \ldots \leq \lambda_K$, where K is the number of vertices in $\mathscr{G}$. Then,*

(i) $\lambda_1 = 0$ *is a simple eigenvalue associated with the eigenvector* 1_K.

(ii) $\lambda_2 > 0$ *is called the algebraic connectivity of the graph.*

(iii) There exists an orthogonal matrix $\boldsymbol{T} \in \mathbb{R}^{K\times K}$ (i.e., $\boldsymbol{T}\boldsymbol{T}^\top = \boldsymbol{T}^\top\boldsymbol{T}$) such that

$$\boldsymbol{T}^\top \boldsymbol{L}\boldsymbol{T} = \mathrm{diag}(\lambda_1, \ldots, \lambda_K).$$

Corollary 1. *The graph $\mathscr{G}$ is connected iff $\lambda_2 > 0$.*

Corollary 2. *The number of connected components in the graph $\mathscr{G}$ is equal to the dimension of the null space of the Laplacian $\boldsymbol{L}$.*

The spectral radius of a matrix $\boldsymbol{M}$, referred to as $\rho(\boldsymbol{M})$, represents the largest modulus among all eigenvalues of $\boldsymbol{M}$. When examining a directed graph that comprises positively weighted edges, the adjacency matrix of such a graph is inherently nonnegative. Conversely, given a nonnegative matrix, it is feasible to associate a directed graph. Ultimately, a nonnegative matrix is classified as irreducible if and only if the directed graph it is associated with is strongly connected. From [59] the Perron-Frobenius lemma is derived.

Lemma 1. *Let $\boldsymbol{M} \in \mathbb{R}^{K\times K}$ is a nonnegative and irreducible matrix. Then, the following statements hold true for its spectral radius :*

(i) $\rho(\boldsymbol{M}) > 0$ *is a simple eigenvalue of $\boldsymbol{M}$,*

(ii) there exists a vector $u \in \mathbb{R}^K_{>0}$ such that $\boldsymbol{M}u = \rho(\boldsymbol{M})u$,

(iii) $\rho(\boldsymbol{M}) = \inf\{\lambda \in \mathbb{R} :\ \boldsymbol{M}u = \lambda u,\ u \in \mathbb{R}^K_{>0}\}$.

It is worth noting that since a matrix $\boldsymbol{M}$ is irreducible if and only if its associated directed graph $\mathscr{G}$ is strongly connected, the above lemma holds for the spectral radius of the adjacency matrix of any strongly connected, positively weighted directed graph. Therefore, we can draw the following corollary.

Corollary 3. *Let $\boldsymbol{M} \in \mathbb{R}^{K\times K}$ is a nonnegative and irreducible matrix. Then, the largest eigenvalue λ_1 of $\boldsymbol{M}$ is real, simple, and equal to the spectral radius $\rho(\boldsymbol{M})$.*

1.2.2 Game theory

Game theory, as a branch of mathematics, has emerged as a powerful tool for modeling strategic interactions among agents in a wide range of fields. The foundational work by John von Neumann and Oskar Morgenstern in 1944 [60] laid the groundwork for game theory, and subsequent contributions by John Nash in the 1950s, notably his concept of Nash equilibrium [61], have significantly advanced the field. Game theory serves as a framework for analyzing systems comprising interacting agents, where each agent aims to maximize their individual utility, which is typically influenced by their own actions as well as the actions of other agents within the system. This introduces additional complexities compared to classical optimization frameworks, where an agent's utility is independent of others and depends solely on its own choices. However, despite methodological differences, game theory remains closely related to classical optimization theory. For instance, potential games [62] highlight the maximum achievable utility for agents through a function intrinsically linked to the game, known as the potential function. Despite these complexities, game theory provides a powerful framework for analyzing strategic interactions among agents and finds significant applications in diverse fields such as economics, political science, biology, computer science, wireless communications [63], and network security [64]. Game theory aims to construct models that capture the complexities of player interactions, establish various solution concepts, predict potential solutions based on specific information and behavioral assumptions, analyze feasible outcomes, and design effective strategies to achieve specific goals. Before delving into the fundamental concepts of game theory, it is beneficial to explore common scenarios where game theory naturally applies.

The Colonel Blotto game (employed to illustrate the theory of Chapter 4 in Section 4.3)

The Colonel Blotto game is a classic strategic form game often used in game theory and political science [65]. The game assumes two players, each of which is assigned a certain amount of resources. The objective of the game is to distribute these resources across multiple fronts in a way that maximizes the chance of winning. The Colonel Blotto game model has been employed to illustrate the theory discussed in Chapter 4, specifically in Section 4.3.

Let's take a simplified example with a battle with two Colonels. Each Colonel $k \in \{1, 2\}$ has a total of $\mathrm{B_k}$ resources (e.g., number of soldiers) to distribute across $K > 1$ battlefields. Let us denote by $u_k = (u_{k1}, u_{k2}, \ldots, u_{kK})$ where $u_{k\ell}$ for $\ell \in \{1, \ldots, K\}$ is the amount of resources that Colonel k allocates to battlefield ℓ. The utility of each Colonel k, denoted by J_k, is determined by the number of battlefields they win. That is, Colonel k wins a battlefield ℓ if $u_{k\ell} > u_{-k\ell}$ where $u_{-k\ell]}$ is the amount of resources the opposing Colonel allocates to battlefield ℓ. Therefore, we can write the utility function for each Colonel k as :

$$J_k(u_k, u_{-k}) = \sum_{\ell=1}^{K} \mathbb{1}(u_{k\ell} > u_{-k\ell}),$$

where : $\mathbb{1}$ is the indicator function that equals 1 if the condition inside the brackets is true, and 0 otherwise ; $u_{-k} := (u_{-k1}, \ldots, u_{-kK})$. Under this formulation, each player seeks to maximize their utility given their resource constraint, and taking into account the strategy of the other player :

$$\max_{u_k} J_k(u_k, u_{-k})$$

$$\text{s.t.} \quad \begin{array}{l} \forall \ell \in \{1, \ldots, K\}, u_{k\ell} \geq 0, \\ \sum_{\ell=1}^{K} u_{k\ell} \leq \mathrm{B_k}. \end{array}$$

This optimization problem encapsulates the strategic nature of the Colonel Blotto game, where players must strategically allocate their resources across different battlefields to maximize their chances of winning more battlefields than their opponent.

Braess paradox (analysed in the numerical performance of Chapter 2 in Section 2.4)

The following inequality in optimization theory is a widely acknowledged result

$$\max_{x \in \mathcal{A}} f(x) \leq \max_{x \in \mathcal{B}} f(x), \tag{1.1}$$

stating that the maximum value of a function $f(x)$ over a set $\mathcal{A}$ is less than or equal to the maximum value of the same function $f(x)$ over a set $\mathcal{B}$ with $\mathcal{A} \subseteq \mathcal{B}$. This inequality holds true when the variable x is a $K-$dimensional vector, denoted as $x = (x_1, \ldots, x_K)$. It is crucial to emphasize that this inequality holds because the optimization is performed with respect to the entire vector x. When all variables in the vector are simultaneously optimized, the inequality naturally arises. However, if the function were optimized with respect to only one variable while the remaining variables were controlled by an external entity, there is no inherent reason for this inequality to hold. Although this observation may appear trivial and is a well-established

principle in game theory, there are practical situations where this concept has not been fully comprehended or recognized. To illustrate this point, the example introduced by Braess in 1969 [66] can be considered.

The Braess paradox is a well-known concept in game theory and transportation network theory, highlights the counter-intuitive phenomenon wherein the addition of new roads or routes to a network can lead to increased congestion and longer travel times. This paradox challenges the conventional assumption that expanding the road infrastructure will always result in improved traffic flow and reduced travel times. The Braess paradox is graphically represented in the following figure [1].

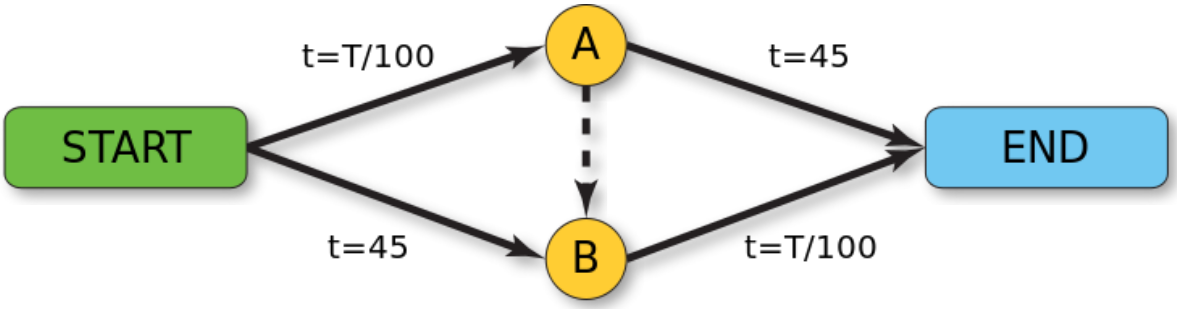

FIGURE 1.3 – The routing scenarios considered by Braess

Consider $N = 4000$ drivers and let us denote the number of drivers choosing the Start-A-End route as "N_a" and the number of drivers choosing the Start-B-End route as "N_b". At equilibrium, we have $N_a = N_b = 2000$, resulting in each route taking 65 minutes. Without the dashed road A-B, the travel time for the Start-A-End route with a drivers is $N_a/100+45$ minutes, and the travel time for the Start-B-End route with N_b drivers is $N_b/100+45$ minutes. Now, let's introduce the dashed road A-B, assuming it has a negligible travel time of approximately 0 minutes. One driver tries the Start-A-B-End route and finds that their time is $N_a/100 + N_b/100$ minutes. As this new route appears advantageous, more drivers start using it. Let's denote the number of drivers choosing the Start-A-B-End route as x. Therefore, the total number of drivers on the Start-A-B-End route becomes $N_a + x$, and the total number of drivers on the Start-B-End route becomes $N_b + x$. The travel time for the Start-A-B-End route with $N_a + x$ drivers becomes $\frac{N_a + x}{100} + \frac{N_b + x}{100}$ minutes. The travel time for the Start-B-End route with $N_b + x$ drivers remains the same as before, $N_b/100 + 45$ minutes. Now, we can analyze the changes in travel times as the number of drivers using the Start-A-B-End route increase and find the critical point at which both routes take the same amount of time, indicating the loss of advantage for

1. Source : `https://en.wikipedia.org/wiki/Braess%27s_paradox`

the Start-A-B-End route. Setting the travel times for both routes equal, we have :

$$\frac{N_a + x}{100} + \frac{N_b + x}{100} = \frac{N_b}{100} + 45.$$

Since $N_a = N_b = 2000$ at equilibrium, we substitute these values it follows that for $x = 1250$, the number of drivers using the Start-A-B-End route, both routes take the same amount of time, which is 65 minutes. Beyond this point, the advantage of the Start-A-B-End route diminishes, and its travel time starts increasing. As more drivers switch to the Start-A-B-End route, congestion builds up, and the travel time on both routes continues to increase. Ultimately, the travel time for both routes settles at 80 minutes when all drivers have switched to the Start-A-B-End route, resulting in a total loss of 15 minutes compared to the original equilibrium travel time of 65 minutes. This mathematical explanation highlights the critical point at which the advantage of the new route diminishes, leading to increased congestion and longer travel times for all drivers. Several real-life examples provide empirical evidence of Braess paradox :

Stuttgart, Germany : In 1969, investments were made in the road network of Stuttgart with the expectation of alleviating traffic congestion. However, the traffic situation did not improve until a section of the newly-built road was closed for traffic. This unexpected observation suggested that the added road was contributing to congestion rather than alleviating it, demonstrating the counterintuitive nature of Braess paradox [67].

42nd Street, New York City, USA : In 1990, the closure of 42nd Street in New York City resulted in a reduction in congestion in the surrounding area. This outcome contradicted the expectation that additional road capacity would lead to improved traffic flow. Instead, the closure of the road demonstrated the counterintuitive nature of Braess paradox and highlighted the importance of considering the intricate interactions within transportation networks [68].

Seoul, South Korea : In Seoul, there were initially three tunnels in the city. However, in 2003, one of the tunnels was closed to restore a river and create a park. Surprisingly, the closure of the tunnel led to an improvement in traffic flow. This observation challenged the conventional belief that more routes always lead to better transportation efficiency. The discovery was made by experts in urban planning who observed the positive impact of the closure on traffic congestion in the area [69].

These real-life examples serve as empirical evidence of the counter intuitive nature of Braess paradox. Moreover, this paradox has been observed to be prevalent within the realm of decentralized epidemic management, as explicitly demonstrated through the numerical performance of Chapter 2 in Section 2.4.

Some useful definitions and theorems

The foundation of the thesis lies in the clear definition of two key concepts : the one-shot game and the Stackelberg game. These definitions are essential for comprehending the subsequent analysis and findings presented in the thesis. In game theory, a one-shot game involves simultaneous decision-making without knowledge of others' choices. Players independently select strategies, and outcomes are based on the combined strategies. No revisions are allowed after decisions are made. The Stackelberg game is a specific type of game in which players make their decisions sequentially, rather than simultaneously as in a one-shot game. A leader moves first and chooses a strategy, while followers observe and respond strategically. The leader's decision considers the followers' strategic responses. It represents hierarchical decision-making, where the leader has an advantage in determining their action before others.

Definition 17. *A game represented in normal form can be described by an ordered vector denoted as* $\mathcal{G} := (\mathcal{K}, (\mathcal{U}_k)_{k\in\mathcal{K}}, (\mathcal{J}_k)_{k\in\mathcal{K}})$*. In this representation :*

- $\mathcal{K} := \{1, \ldots, K\}$ *refers to the finite set of players involved in the game with* $K > 0$ *players.*
- $\mathcal{U} := \mathcal{U}_1 \times \mathcal{U}_2 \times \ldots \times \mathcal{U}_K$ *denotes the Cartesian product of the strategy sets, where* $\mathcal{U}_k$ *is the strategy set of player* $k \in \mathcal{K}$*.*
- $(J_k)_{k\in\mathcal{K}} := (J_1, \ldots, J_K)$ *and* J_k *represents the utility function vector (in the case of maximization convention) or cost function (in the case of minimization convention) for each player* $k \in \mathcal{K}$*, where* $J_k : \mathcal{U} \to \mathbb{R}$*.*

Within this framework, each player $k \in \mathcal{K}$ *selects an action* u_k *from their respective strategy set,* $\mathcal{U}_k$*, and receives a utility,* $J_k(u_1, \ldots, u_K)$*, which is contingent upon the collective action choices made by all players involved in the game.*

In what follows, we will denote by u the control action profile $u := (u_1, \ldots, u_K) \in \mathcal{U}$ and we will also use the notation u_{-k} to refer to the reduced action profile
$u_{-k} := (u_1, \ldots, u_{k-1}, u_{k+1}, \ldots, u_K) \in \mathcal{U}_{-k}$ where $\mathcal{U}_{-k} := \mathcal{U}_1 \times \ldots \times \mathcal{U}_{k-1} \times \mathcal{U}_{k+1} \times \ldots \times \mathcal{U}_K$.

The concept of best response shifts the focus to the individual level, where players strive to maximize their utilities (or minimize their own cost functions) based on the strategies chosen by others.

Definition 18. *The best response (*BR*) of player* $k \in \mathcal{K}$ *to the reduced strategy profile* $u_{-k} \in \mathcal{U}_{-k}$ *is*

$$BR_k(u_{-k}) := \underset{u_k\in\mathcal{U}_k}{\operatorname{argmax}}\ J_k(u_k, u_{-k}),\ \textit{(or argmin for minimization).}$$

The best response map of a player forms the foundation for understanding Nash equilibrium in game theory. A best response is an optimal strategy for a player, given the strategies of the

other players. It represents the choice that maximizes (or minimizes) a player's utility or payoff, taking into account the actions of others. Nash equilibrium, on the other hand, extends the notion of best response to a solution concept where each player's strategy is a best response to the strategies chosen by others. In a Nash equilibrium, no player has an incentive to unilaterally deviate from their chosen strategy, as doing so would result in a lower payoff.

Definition 19. *The action profile u^{NE} is a Nash equilibrium strategy of the game $\mathcal{G}$ if : $\forall k \in \mathcal{K}$ and $u_k \in \mathcal{U}_k$,*

$$J_k(u^{\mathrm{NE}}) \geq J_k(u_k, u_{-k}^{\mathrm{NE}}),\ (\leq \textit{ for minimization}).$$

A Nash equilibrium can be characterized by the concept of best-response.

Definition 20. *A strategy profile u^{NE} is a Nash equilibrium if*

$$u^{\mathrm{NE}} \in \mathrm{BR}(u^{\mathrm{NE}}),$$

where

$$\begin{aligned} \mathrm{BR}: \ \mathcal{U} &\to \mathcal{U} \\ u &\mapsto \mathrm{BR} := (\mathrm{BR}_1, \ldots, \mathrm{BR}_K). \end{aligned}$$

The characterization of Nash equilibria as solutions to a fixed point problem was formalized by Nash in [61]. This perspective reveals why standard existence theorems for Nash equilibria rely on topological and geometrical assumptions. The Debreu-Fan-Glicksberg theorem, as described in [70], provides a valuable existence theorem for Nash equilibria. This theorem builds upon the contributions of [71, 72, 73]. The authors in [70] further elaborate on the specific requirements and conditions that need to be satisfied for the application of the Debreu-Fan-Glicksberg theorem. To refresh our understanding of the terminology, let's recall the definition of quasi-concave and quasi-convex functions before discussing the Debreu-Fan-Glicksberg theorem.

Definition 21. *Let a function $f : \mathcal{X} \to \mathbb{R}$, where $\mathcal{X}$ is a convex set. The function f is said to be :*
Quasi-concave function if, for any points $x, y \in \mathcal{X}$ and $\lambda \in [0, 1]$, the following condition holds :

$$f(\lambda x + (1-\lambda)y) \geq \min\{f(x), f(y)\}.$$

Quasi-convex function if, for any points $x, y \in \mathcal{X}$ and $\lambda \in [0, 1]$, the following condition holds :

$$f(\lambda x + (1-\lambda)y) \leq \max\{f(x), f(y)\}.$$

Building upon this notion, the Debreu-Fan-Glicksberg theorem [70] states the existence theorem of at least one pure Nash equilibrium in the game.

Theorem 2 (Debreu-Fan-Glicksberg theorem (1952))**.** *If for each $k \in \mathcal{K}$, the strategy set $\mathcal{U}_k$ is both compact and convex, and the utility (cost) function J_k is continuous w.r.t. the strategy profile u and quasi-concave (quasi-convex for minimization) w.r.t. u_k, then it can be concluded that the game $\mathcal{G}$ possesses at least one pure Nash equilibrium.*

While the Debreu-Fan-Glicksberg theorem focuses on the existence of equilibria in a broader class of games, the uniqueness theorem derived by Rosen in [74] provides a specific condition, the diagonally strict concavity (DSC), to ensure the uniqueness of the equilibrium.

Theorem 3 (Rosen theorem (1965))**.** *Assume that, $\forall k \in \mathcal{K}$, $\mathcal{U}_k$ is a non-empty, compact and convex set; $J_k(u)$ is a continuous function in $u \in \mathcal{U}$ and concave (convex for minimization) in u_k. Let $\delta = (\delta_1, \ldots, \delta_K)$ be a vector of fixed positive parameters. Let define a weighted non-negative sum of the function J_k given by $\sigma(u, \delta) := \sum_{k=1}^{K} \delta_k J_k(u)$ and $g(u, \delta) := [\delta_1 \nabla_{u_1} J_1(u), \ldots, \delta_K \nabla_{u_K} J_K(u)]$ the pseudogradient of the function σ. If the following holds for some $\delta > 0$: $\forall (u^a, u^b) \in \mathcal{U}^2,\ u^a \neq u^b$*

$$(u^a - u^b)\Big(g(u^b, \delta) - g(u^a, \delta)\Big)^\top > 0 \text{ (for maximization)},$$
$$(u^a - u^b)\Big(g(u^a, \delta) - g(u^b, \delta)\Big)^\top > 0 \text{ (for minimization)},$$

then the game $\mathcal{G}$ has a unique NE.

In the study of game theory, 'dominated action' is a key idea. It helps us understand how players make decisions within a game. It simply means that some actions or plans can consistently give better results than others, no matter what the other players decide. This idea forms the basis of strategic decision-making, encouraging players to avoid dominated actions and choose better ones instead.

Definition 22. *For any player $k \in \mathcal{K}$ and two distinct actions u_k^a and u_k^b belonging to the action set $\mathcal{U}_k$ for player k.*

- *Action u_k^a is said to weakly dominate action u_k^b if the following conditions hold :*
  - *(i) For any $u_{-k} \in \mathcal{U}_{-k}$, $J_k(u_k^a, u{-}k) \geq J_k(u_k^b, u_{-k})$ (in the case of maximization convention) or $J_k(u_k^a, u_{-k}) \leq J_k(u_k^b, u_{-k})$ (in the case of minimization convention).*
  - *(ii) There exists at least one strategy profile $u_{-k} \in \mathcal{U}_{-k}$ for which the inequality is strict, meaning $J_k(u_k^a, u{-}k) > J_k(u_k^b, u_{-k})$ (for maximization convention) or $J_k(u_k^a, u_{-k}) < J_k(u_k^b, u_{-k})$ (for minimization convention).*

- *Action u_k^a is said to strongly dominate action u_k^b if the inequality is always strict for any $u_{-k} \in \mathcal{U}_{-k}$.*

The concept of dominance in game theory extends beyond individual strategies to encompass the comparison of entire action profiles. While dominance focuses on the superiority of one strategy over another for an individual player, Pareto dominance broadens the scope to evaluate the overall effectiveness and efficiency of action profiles in a multi-player setting.

Definition 23. *Action profile u^a is said to Pareto dominate action profile u^b if and only if the following conditions hold simultaneously :*

(i) For every player $k \in \mathcal{K}$, u_k^a weakly dominates u_k^b.

(ii) There exists at least one player $k \in \mathcal{K}$ such that u_k^a strictly dominates u_k^b.

Pareto dominance (or Pareto optimality) captures the notion of improvement for at least one player without worsening the situation for any other player. It represents a powerful criterion for assessing the desirability of action profiles, as it identifies outcomes that are collectively preferable and non-inferior to alternative outcomes. In the literature of non-cooperative games, the term "social welfare" (SW) introduced by Arrow in [75] allows for a comprehensive evaluation of system performance, considering the contributions of each entity in decentralized decision-making environments.

Definition 24. *The social welfare of a game is defined as the sum of the utilities (or cost function) of all players :*

$$SW = \sum_{k=1}^{K} J_k.$$

A social optimum represents the highest level of social welfare (or minimal level, depending on the convention). It is considered Pareto optimal as it ensures that no alternative strategy can improve the welfare of any individual without worsening the welfare of others [76]. However, it should be noted that the converse is not always guaranteed and holds only under certain conditions. Specifically, if the feasible range of utilities forms a convex region, then the converse holds true [77]. In practical scenarios, social welfare can serve as a useful measure when the players experience similar propagation conditions, leading to comparable utilities after averaging, such as over fading gains. However, if the players encounter significantly different propagation conditions, the use of social welfare as a performance measure can be debatable and may even result in unfair outcomes. To address this issue, Papadimitriou [78] introduced the concept of the price of anarchy (PoA). The Price of Anarchy (PoA) is a measure used to quantify the inefficiency of equilibria in game theory. It assesses the degradation in overall system performance caused by the self-interested behavior of individual players.

Definition 25.

$$\mathrm{PoA} := \frac{\max\limits_{u \in \mathcal{U}^{\mathrm{NE}}} \sum\limits_{k=1}^{K} J_k(u)}{\min\limits_{u \in \mathcal{U}} \sum\limits_{k=1}^{K} J_k(u)},$$

where $\mathcal{U}^{\mathrm{NE}}$ is the set of NE of $\mathcal{G}$.

In a game with a finite number of players, the PoA is defined as the ratio between the worst possible social welfare achieved at a Nash equilibrium and the social welfare that could be achieved at a globally optimal solution. A higher PoA value indicates a greater inefficiency in the resulting equilibria, where the achieved social welfare falls significantly short of the optimal level. Conversely, a lower PoA signifies a more desirable outcome with minimal deviation from the optimal social welfare. The PoA provides insights into the impact of decentralized decision-making on overall system performance, highlighting the trade-off between individual rationality and collective efficiency in game-theoretic settings.

A generalized form game extends the conventional framework of game theory by incorporating specific constraint sets that shape strategic interactions. In this expanded model, players must consider not only their utilities but also the constraints they need to satisfy, as well as the strategies chosen by other players. These constraints can include various factors such as resource limitations, capacity restrictions, or regulatory requirements. By accounting for these constraints, a generalized form game provides a more comprehensive analysis of strategic decision-making, encompassing both players' objectives and the interplay between utilities and constraints.

Definition 26. *A game represented in generalized form can be described by an ordered 4-uplet denoted as $\widetilde{\mathcal{G}} := (\mathcal{K}, (\mathcal{U}_k)_{k\in\mathcal{K}}, (\mathcal{C}_k)_{k\in\mathcal{K}}, (J_k)_{k\in\mathcal{K}})$. In this representation :*

- *$\mathcal{K} := \{1, \ldots, K\}$ refers to the finite set of players involved in the game with $K > 0$ players.*
- *$\mathcal{U} := \mathcal{U}_1 \times \mathcal{U}_2 \times \ldots \times \mathcal{U}_K$ denotes the Cartesian product of the strategy sets, where $\mathcal{U}_k$ is the strategy set of player $k \in \mathcal{K}$.*
- *$(J_k)_{k\in\mathcal{K}} := (J_1, \ldots, J_K)$ and J_k represents the utility function vector (in the case of maximization convention) or cost function (in the case of minimization convention) for each player $k \in \mathcal{K}$, where $J_k : \mathcal{U} \to \mathbb{R}$.*
- *For a given $u_{-k} \in \mathcal{U}_{-k}$, $\mathcal{C}_k(u_{-k}) := \{u_k \in \mathcal{U}_k : \ g_k(u_k, u_{-k}) \leq 0\}$, where $g_k : \mathcal{U} \to \mathbb{R}^m$ is a constraint function where $m > 0$ is the number of constraints and "$\leq$" is an element-by-element inequality.*

Within this framework, each player $k \in \mathcal{K}$ selects an action u_k from their respective strategy

set i.e., $u_k \in \mathcal{C}_k(u_{-k})$, and receives a utility, $J_k(u_1, \ldots, u_K)$, which is contingent upon the collective action choices made by all players involved in the game.

Building upon the framework of a generalized form game, the concept of a Generalized Nash Equilibrium (GNE) emerges as a solution concept that captures the interplay between players' strategies and the associated constraints. Unlike traditional Nash equilibria, which focus solely on the optimization of individual utilities, a GNE takes into account the simultaneous satisfaction of the players' constraints.

Definition 27. *The generalized Nash equilibrium for a generalized game $\widetilde{\mathcal{G}}$ is defined as a strategy u^{GNE} that verifies for all $k \in \mathcal{K}$,*

$$u_k^{\mathrm{GNE}} \in \underset{u_k \in \mathcal{C}_k(u_{-k}^{\mathrm{GNE}})}{\operatorname{argmax}} J_k(u_k, u_{-k}^{\mathrm{GNE}}), \text{ (or argmin for minimization).}$$

To ensure clarity on the terminology, let us recall the definitions of upper and lower semi-continuity of a set-valued map before presenting the theorem that guarantees the existence of a Generalized Nash Equilibrium (GNE).

Definition 28. *Let us consider a set-valued map, denoted as $F : \mathcal{X} \to 2^{\mathcal{Y}}$.*

- *F is said to be upper semicontinuous (u.s.c) at a point $x \in \mathcal{X}$ if, for any open set $\mathcal{V} \subseteq \mathcal{Y}$ containing $F(x)$, there exists an open neighborhood $\mathcal{W} \subset \mathcal{X}$ of x such that $F(x') \subseteq \mathcal{V}$ for all $x' \in \mathcal{W}$.*
- *F is said to be lower semicontinuous (l.s.c) at a point $x \in \mathcal{X}$ if, for any open set $\mathcal{V} \subseteq \mathcal{Y}$ containing $F(x)$, there exists an open neighborhood $\mathcal{W} \subset \mathcal{X}$ of x such that $F(x') \cap \mathcal{V} \neq \emptyset$ for all $x' \in \mathcal{W}$.*

According to [79, Theorem 3.1] and based on the concept discussed above, we can establish the existence theorem, which guarantees the presence of at least one Generalized Nash Equilibrium (GNE) in the game. The theorem is presented below.

Theorem 4 (Dutang (2013))**.** *The game $\widetilde{\mathcal{G}} := (\mathcal{K}, (\mathcal{U}_k)_{k\in\mathcal{K}}, (J_k)_{k\in\mathcal{K}}, (\mathcal{C}_k)_{k\in\mathcal{K}})$. Assume for all players, we have :*

(i) $\mathcal{U}_k$ is nonempty, convex and compact subset of a Euclidean space.

(ii) $\mathcal{C}_k$ is both u.s.c. and l.s.c. in u_{-k}.

(iii) $\forall u_{-k} \in \mathcal{U}_{-k}$, $\mathcal{C}_k(u_{-k})$ is nonempty, closed, convex.

(iv) J_k, is continuous on $\mathrm{G_r}(\mathcal{C}_k) := \{(u_k, u_{-k}) \in \mathcal{U}_k \times \mathcal{U}_{-k} : \ u_k \in \mathcal{C}_k(u_{-k})\}$.

(v) $\forall u_{-k} \in \mathcal{U}_{-k}$, $J_k(\cdot, u_{-k})$ is quasi-concave (or quasi-convex for minimization) w.r.t u_k.

Then the game $\widetilde{\mathcal{G}}$ has at least one generalized Nash equilibrium.

The Stackelberg game introduces a distinctive leader-follower dynamic that deviates from the conventional framework of simultaneous decision-making observed in Nash equilibria (Stackelberg analysis holds a particular relevance in Chapter 4 of this thesis). It introduces a distinctive leader-follower dynamic where one player assumes the role of the leader, while the remaining players act as followers. This hierarchical structure enables the leader to strategically select their action, leveraging their advantageous position of moving first, while considering the anticipated responses from the followers. Within the context of a multi-level Stackelberg game, the utility functions are intricately designed to capture the inherent hierarchy and decision-making process. The utility functions in a multi-level Stackelberg game can be defined as follows :

$$\begin{cases} J_K^S(u_1,\dots,u_K) = J_K(u_1,\dots,u_K) \\ J_{K-1}^S(u_1,\dots,u_{K-1}) = J_{K-1}^S(u_1,\dots,u_{K-1},u_K(u_1,\dots,u_{K-1})) \\ \vdots \\ J_1^S(u_1) = J^1(u_1,u_2(u_1),u_3(u_1,u_2(u_1)),\dots,u_K(u_1,u_2(u_1),\dots,u_{K-1}(u_{K-1}(\dots(u_1))))). \end{cases}$$

Here, $u_2(u_1)$, $u_3(u_2(u_1))$, and so on, represent the reactions of player 2 to player 1, player 3 to player 2 and player 1, respectively. The strategic form of the multi-level Stackelberg game $\mathcal{G}^S$ can be defined as :

$$\mathcal{G}^S = \left(\mathcal{K}, (\mathcal{U}_k)_{1\leq k\leq K}, \left(J_k^S\right)_{1\leq k\leq K}\right)$$

where :

- $\mathcal{K} := \{1,\dots,K\}$ represents the set of players.
- $\mathcal{U}_k$ denotes the set of possible actions for player k.
- J_k^S represents the utility function of player k in the multi-level Stackelberg game.

A multi-level Stackelberg solution is defined as a pure Nash equilibrium of the game $\mathcal{G}^S$. In other words, u^S is considered a Stackelberg solution if it satisfies the following definition.

Definition 29. *The strategy profile u^S is a Stackelberg solution of the game $\mathcal{G}^S$ if it verifies the following equations :*

$$\begin{cases} u_K^S(u_1,u_2,\dots,u_{K-1}) \in \underset{u_K\in\mathcal{U}_K}{\operatorname{argmax}}\ J_K^S(u_1,u_2,\dots,u_K) \\ u_{K-1}^S(u_1,u_2,\dots,u_{K-2}) \in \underset{u_{K-1}\in\mathcal{U}_{K-1}}{\operatorname{argmax}}\ J_{K-1}^S(u_1,u_2,\dots,u_{K-1}) \\ \vdots \\ u_1^S \in \underset{u_1\in\mathcal{U}_1}{\operatorname{argmax}}\ J_1^S(u_1). \end{cases}$$

In this definition, a multi-level Stackelberg solution is a pure Nash equilibrium where each player's action is the best response to the actions of the other players. The solution is obtained

by finding the optimal actions that maximize the respective utility functions for each player, considering the hierarchical relationships and reactions between the players.

Chapter 2

On the Efficiency of Decentralized Epidemic Management and Application to Covid-19

In this chapter, we aim to investigate the possible efficiency losses incurred by decentralizing the management of epidemics. To this end, we propose a relatively straightforward but yet comprehensive mathematical model. Specifically, we introduce a strategic-form game that is built on a networked Susceptible-Infected-Recovered (SIR) model [12, 13]. In this game, each player corresponds to a geographic region, and its objective is to implement a tradeoff between socio-economic and health aspects. The cost of a region is not only impacted by its own actions but also by the actions taken by neighboring regions. The interactions between players are represented by a weighted adjacency matrix. The action of each player is assumed to remain constant over periods of time, which correspond to the management phases of the epidemic.

The primary theoretical contribution of this chapter is the detailed analysis of the existence and uniqueness of the Nash equilibrium. To do so, we introduce a framework known as the 'Weak Interconnection Regime' (**WIR**), in which the implicit function theorem can be easily exploited and the existence of a Nash equilibrium (NE) of the proposed game can be proved. Moreover, this analysis ensures the well-posedness of the two efficiency measures used to evaluate the effectiveness of the decentralized strategy, the Price of Anarchy (PoA) and the Price of Connectedness (PoC). In an extended part of our work, we also incorporate a critical factor in the management of epidemics - the availability and adequacy of healthcare resources, with a particular emphasis on intensive care units (ICUs). Technically, these elements are integrated into the decision-making process through the notion of coupled constraints, which leads us to explore a generalized form of the game. As a result, we extend our analysis to the study of the generalized Nash equilibrium of this new game, wherein specific conditions pertaining to the existence of such an equilibrium are explored and established.

As mentioned in the introduction, decentralized epidemic management is a complex issue, as demonstrated by the global response to the SARS-Cov2 virus in 2020. Governments around the world implemented stringent measures, often uniformly across large geographical areas such as countries. However, this approach had inherent drawbacks, namely the mismatch between the severity of the measures imposed and the local situation. This mismatch led to avoidable local economic losses, potential psychological damage and subsequent frustration, ultimately reducing the effectiveness of the measures. As we approach 2021, accumulated experience has suggested a more localized approach to decision-making, even when it comes to vaccinations. Thus, different countries have adopted varied control strategies, focusing on aspects such as education, social welfare, the economy or health. Even within one country, regions have implemented measures tailored to their local situation, reflecting an attempt to strike a balance between socio-economic and health aspects.

In light of these observations, we present a mathematical model that examines the effects of decentralization on epidemic management. In our proposed framework, each region or country is a decision-maker where the virus spreads according to a networked epidemic models [31, 32, 33], [34, Chapter 9.3]. Our model, while relatively simple, captures key effects, which is based on a strategic-form game drawn from a networked Susceptible-Infected-Recovered (SIR) compartmental model [12, 13]. Here, each player represents a geographical region with the goal of deciding social-distancing rules to minimize associated costs, thereby implementing a trade-off between socio-economic losses and health losses. A thorough analysis of Nash equilibrium is conducted, and the effectiveness of the decentralized strategy is evaluated through the

efficiency metrics - the Price of Anarchy (PoA) and the Price of Connectedness (PoC). In an advanced extension of our work, we incorporate a crucial component of epidemic management, i.e., the availability and adequacy of healthcare resources, with particular attention to intensive care units (ICUs). These factors are integrated into the decision-making process, enabling us to examine a generalized form of the game. Consequently, we extend our analysis to study the generalized Nash equilibrium of this new game, identifying and establishing specific conditions for its existence.

This chapter is organized as follows : Sec. 2.1 offers a detailed description of the networked SIR epidemic model we consider and presents the strategic form game model designed to highlight the primary trade-offs, along with the selected measures of global efficiency. Sec. 2.2 delves into a thorough investigation of the Nash equilibria, both in terms of its existence and uniqueness. A substantial theoretical analysis is proposed to investigating the issue of decentralized epidemic management under the constraints imposed by Intensive Care Units (ICUs). Lastly, Section 2.4 demonstrates the practical application of our proposed game model through numerical simulations for a scenario reminiscent of Covid-19, and discusses the potential effects of implementing a decentralization strategy in the decision-making process.

The results of this chapter corresponds to the publication [40].

2.1 Problem statement

We consider a set of $K > 1$ interconnected regions (e.g., provinces, states, or cities) that are affected by an epidemic ; the region index is denoted by $k \in \mathcal{K} := \{1, \dots, K\}$. The epidemic propagation within a region is assumed to follow a SIR model. This section provides both the model that we consider for the epidemic dynamics in the presence of interconnected regions (Sec. 2.1.1) and the game proposed to model the fact that the epidemic management is decentralized (Sec. 2.1.2). The proposed game model intends to be simple while capturing a key feature, which is the tradeoff between socio-economic losses, and health aspects.

2.1.1 Epidemic Model

For Region $k \in \mathcal{K}$, we respectively denote by β_{kk} and γ_k the virus (endogenous) transmission rate and the removal/recovery rate ($\frac{1}{\gamma_k}$ is called the average recovery period). For $k \neq \ell$, the quantity $\beta_{k\ell}$ denotes the transmission rate from Region ℓ to Region k. The action of Region k on the epidemics is represented by a scalar control action denoted by $u_k \in \mathcal{U}_k$ where $\mathcal{U}_k := [U_k^{\min}, U_k^{\max}] \subset [0, 1)$ is compact. **The control action u_k is assumed to be constant over the time period of interest (working phase) which is the interval $[0, T]$, $T > 0$.** In this chapter, we restrict our attention to the study over a single phase ; a phase may typically last few weeks. In practice, the action would need to be updated for each phase. This corresponds to considering a blockwise constant management strategy, which is the easiest to implement

in practice. We will denote by u the control action profile or vector : $u := (u_1, \ldots, u_K) \in \mathcal{U}$ where $\mathcal{U} := \mathcal{U}_1 \times \ldots \times \mathcal{U}_K$ and we will also use the notation u_{-k} to refer to the reduced action profile $u_{-k} := (u_1, \ldots, u_{k-1}, u_{k+1}, \ldots, u_K)$. The fractions of susceptibles, infected, and recovered for Region k are respectively denoted by $s_k(t, u_k, u_{-k}) \in [0, 1]$, $i_k(t, u_k, u_{-k}) \in [0, 1]$, and $r_k(t, u_k, u_{-k}) \in [0, 1]$. With this notation, the continuous-time dynamics for the epidemic in Region k in presence of interconnection is assumed to be given by $\forall T \in \mathbb{R}_{\geq 0}$, $u \in \mathcal{U}$:

$$\begin{cases} \dfrac{\partial s_k}{\partial t}(t,u) = -s_k(t,u)\Big[(1-u_k)\displaystyle\sum_{\ell=1}^{K} \beta_{k\ell} i_\ell(t,u)\Big] \\ \dfrac{\partial i_k}{\partial t}(t,u) = -\dfrac{\partial s_k}{\partial t}(t,u) - \gamma_k i_k(t,u) \\ \dfrac{\partial r_k}{\partial t}(t,u) = \gamma_k i_k(t,u) \\ s_k(t,u) + i_k(t,u) + r_k(t,u) = 1, \end{cases} \tag{2.1}$$

where the initial fractions of susceptibles and infected are chosen as $s_k^0 > 0$ and $i_k^0 \geq 0$.

For the sake of simplicity we assume that the social distancing rules imposed in Region k (namely, u_k) affects uniformly all the infected population of each region in contact with the susceptibles of Region k, i.e., $(1 - u_k)\beta_{k\ell}$ is the controlled rate at which the infected individuals of Region ℓ infects the susceptibles in Region k. In practice, it would be quite difficult to measure its value, or to assign it a prescribed value. Then, we assume policy makers of each Region k would apply a social-distancing rule close enough to the abstract quantity u_k.

2.1.2 Game Model

Each region is assumed to seek for a tradeoff between the socio-economic losses and the local health impact of the epidemic, induced by the sanitary rules. This amounts to considering a cost function that comprises three terms. Precisely, we assume that a region aims at minimizing the following composite cost :

$$J_k(u) := \underbrace{a_k u_k + b_k u_k^2}_{\textbf{socio-economic losses}} + \underbrace{c_k\Big[s_k^0 - s_k(T,u)\Big]}_{\textbf{health losses}}, \tag{2.2}$$

where $(a_k, b_k, c_k) \in \mathbb{R}^3_{\geq 0}$ are constant. The reasoning behind this choice is that social-distancing strategies induce both health and socio-economic losses. In particular, we assume the socio-economic cost is a sum of linear and quadratic terms w.r.t the social distancing rules, as motivated in the related literature of optimal control applied to epidemic that spreads in a single region (see e.g., [80], [5, Section 2.4]) ; this assumption seems to be commonly accepted in economic studies, according to [81, Eq. 8 in Section 2.2.2]. On the other hand, we consider the health

losses to be proportional to the final size of the epidemic after a working phase. In particular, the decision of each node has an impact on its neighbors, through the network structure and the epidemic dynamics. The strategic form (see e.g., [63]) of the static game under consideration is therefore given by :

$$\mathcal{G} := \Big(\mathcal{K}, \big(\mathcal{U}_k\big)_{1\leq k\leq K}, \big(J_k\big)_{1\leq k\leq K}\Big), \tag{2.3}$$

in which the players (nodes of the network) are the regions of a country (or simply countries) ; the action space for Player k is given by $\mathcal{U}_k = [U_k^{\min}, U_k^{\max}] \subset (0,1)$; the individual cost function of Player $k \in \mathcal{K}$ is given by J_k in (2.2). Region $k \in \mathcal{K}$ expresses its interests by setting the triple (a_k, b_k, c_k), whereas the set of action $\mathcal{U}_k$ is imposed by a social planner (e.g., a country or an international organization, depending on the nature of the player). In the case where players are countries, we assume that the social planner might be a worldwide organization such as the WHO (World Health Organization). In addition, we emphasize that the theoretical results established in this chapter hold for a multistage game setup in which the one-shot game is repeated at each stage (for which the parameters are updated) and different constant control actions are applied during it.

2.1.3 Efficiency measures

One of the main objectives of this chapter is to assess the potential inefficiencies that might be induced by letting each region choose its control action. A famous and well-used measure of global efficiency is given by the Price of Anarchy (PoA) of a game [78].

Before defining the PoA, let us remind the definition of a Nash equilibrium (NE). An action profile u^{NE} is an NE if : $\forall k \in \mathcal{K}, \forall u'_k \in \mathcal{U}_k$,

$$J_k(u^{\mathrm{NE}}) \leq J_k(u'_k, u^{\mathrm{NE}}_{-k}).$$

The PoA is defined by :

$$\mathrm{PoA} := \frac{\max\limits_{u\in\mathcal{U}^{\mathrm{NE}}} \sum\limits_{k=1}^{K} J_k(u)}{\min\limits_{u\in\mathcal{U}} \sum\limits_{k=1}^{K} J_k(u)}, \tag{2.4}$$

where $\mathcal{U}^{\mathrm{NE}}$ is the set of NE of $\mathcal{G}$. The function $\sum_{k=1}^{K} J_k$ is often referred as the social cost of the game. The PoA thus compares the performance of the worst NE to the performance of the centralized solution. Implicitly, the PoA assumes that the social cost is a relevant metric to measure the global performance. In particular, when the PoA is too high the decentralization strategy will not be effective at the risk of observing selfish behavior from Players.

To have a second measure of global efficiency, we also introduce the Price of Connectedness (PoC), which is defined as follows :

$$\mathrm{PoC} := \frac{\max\limits_{u \in \mathcal{U}^{\mathrm{NE}}} \sum\limits_{k=1}^{K} J_k(u)}{\sum\limits_{k=1}^{K} \min\limits_{u_k \in \mathcal{U}_k} \widetilde{J}_k(u_k)}, \tag{2.5}$$

where $\widetilde{J}_k(u_k)$ is the cost that Region k would obtain if they do not consider the influence of the network i.e., the crossing transmission rates $\beta_{k\ell}$, $k \neq \ell$, would be vanishing in (2.1). This therefore corresponds to the performance that Region k would expect to obtain by neglecting the interactions with the other regions while these actually exist, hence the term PoC. Such as for the other efficiency measure, we consider that when the PoC is too high, regions should take into account the network structure before taking a decision.

2.2 Nash equilibrium analysis

Since one of our main objectives is to measure efficiency at NE through the PoA and PoC in (2.4)-(2.5), it is necessary to conduct the complete equilibrium analysis of the NE. This analysis includes the study of the existence and uniqueness of the NE.

2.2.1 Existence

In this section, we state our main result concerning the existence of a pure NE. Notice that the existence of a mixed NE is ensured by the continuity of the cost functions J_k, $k \in \mathcal{K}$ (see [63]), but it is of no practical interest in our setting. The existence of a pure NE is strongly related to the geometrical properties of the cost functions J_k, $k \in \mathcal{K}$, such as the quasi-convexity properties. Since the dependency of the third term of J_k on u_k is not explicit, the quasi-convexity analysis of J_k appears to be a non-trivial problem. This is the reason why we define a working regime in which it is possible to prove that J_k is quasi-convex w.r.t. u_k.

*Weak Interconnection regime (**WIR**)* : The game $\mathcal{G}$ is said to be in the **WIR**, if $\forall (k, \ell) \in \mathcal{K}^2 : \ \ell \neq k$ there exists $\nu_{\beta,k} > 0$ such that $\beta_{k\ell} \leq \nu_{\beta,k}$ and J_k is quasi-convex w.r.t. u_k on $\mathcal{U}_k$ (i.e, $\forall u_{-k} \in \mathcal{U}_{-k}$, $\forall \lambda \in \mathbb{R}$, the lower level set $\mathcal{L}^k(u_{-k}, \lambda) := \{u_k \in \mathcal{U}_k : \ J_k(u_k, u_{-k}) \leq \lambda\}$ is convex).

The motivation behind the definition of the **WIR** is given by the following result.

Proposition 1. *In the **WIR** the game $\mathcal{G}$ has at least one pure NE.*

Proof. See Appendix 2.6.1. ■

An important practical question would be : "When is the game in the **WIR** ?". To answer this technical question, let us introduce the following working assumption.

Assumption 1. *Let* $\forall(k,\ell) \in \mathcal{K}^2, \rho_{k\ell} := \dfrac{\beta_{k\ell}}{\gamma_\ell}$.
Condition (i) : The matrix $\widehat{\boldsymbol{B}}$ *whose entries are given by :* $\widehat{\boldsymbol{B}}_{k,\ell} = \beta_{k\ell}$*, is non-singular.*
Condition (ii) : $\forall k$, $\forall u$, $\forall T \in \mathcal{T}$ *one has that* $s_k(t,u) > 0$.
Condition (iii) : $\mathcal{T} = \mathbb{R}_{\geq 0}$ *where*

$$\mathcal{T} := \left\{ t \in \mathbb{R}_{\geq 0} : \forall k,\ \forall u,\ (1-u_k)s_k(t,u) \leq \frac{1}{\sum_{\ell=1}^{K} \rho_{k\ell}} \right\}.$$

Condition (i) is ensured when $\widehat{\boldsymbol{B}}$ is strictly diagonally dominant (which is often the case in practice because intra-regions interactions are much stronger than inter-regions ones).

Condition (ii) is trivially satisfied as far as the epidemic does not affect the entire population.

Condition (iii) is needed to characterize a bound for the inter-regions interactions i.e., to quantitatively describe the **WIR** with $\nu_{\beta,k} := \left(\frac{\min_{\ell\in\mathcal{K}} \gamma_\ell}{(1-U_k^{\min})s_k^0} - \beta_{kk} \right) \Big/ (K-1)$. In what follows, we propose to exhibit a sufficient condition such that the game is in the **WIR**.

To establish the corresponding result, a few notations are in order. Let $T \in \mathcal{T}$, $u \in \mathcal{U}$ and

$$\begin{cases} s(T,u) = (s_1(T,u), \ldots, s_K(T,u))^\top, \\ i(T,u) = (i_1(T,u), \ldots, i_K(T,u))^\top, \\ r(T,u) = (r_1(T,u), \ldots, r_K(T,u))^\top. \end{cases}$$

To be able to express the derivative of s_k w.r.t. u_k and exploit the implicit function theorem, let us introduce the two square matrices $\boldsymbol{B} := \mathrm{diag}(1-u)\widehat{\boldsymbol{B}}$ and $\boldsymbol{\Gamma} := \mathrm{diag}(\gamma)$, where $\gamma := (\gamma_1, \ldots, \gamma_K)$. The reformulated system (2.1) in a collective dynamics form : $\forall t \in [0,T]$,

$$\begin{cases} \dfrac{\partial s}{\partial t}(t,u) = -\mathrm{diag}(s(t,u))\boldsymbol{B}i(t,u) \\ \dfrac{\partial i}{\partial t}(t,u) = \mathrm{diag}(s(t,u))\boldsymbol{B}i(t,u) - \boldsymbol{\Gamma}i(t,u) \\ \dfrac{\partial r}{\partial t}(t,u) = \boldsymbol{\Gamma}i(t,u). \end{cases} \tag{2.6}$$

Using (2.6) and [12, Section 2], one can write the following identity :

$$\frac{\mathrm{d}}{\mathrm{d}t}[\boldsymbol{B}\boldsymbol{\Gamma}^{-1}(s(t,u) + i(t,u)) - \ln(s(t,u))] = 0. \tag{2.7}$$

Therefore, by integrating (2.7) on $[0, T]$, one has that

$$\boldsymbol{B\Gamma^{-1}}(s(T,u) + i(T,u) - x^0) = \ln(s(T,u)) - \ln(s^0),$$

where $s^0 = s(0,\cdot)$, $i^0 = i(0,\cdot)$ and $x^0 = s^0 + i^0$. Let $F : \mathcal{U} \times (0,1]^{2K} \to \mathbb{R}^K$ such that, for any $k \in \mathcal{K}$, the k^{th}-component of F is given by $F_k : \mathcal{U} \times (0,1]^{2K} \to \mathbb{R}$:

$$F_k(u,s,i) = (1-u_k)\sum_{\ell=1}^{K} \rho_{k\ell}\left(s_\ell + i_\ell - x_\ell^0\right) + \ln\left(\frac{s_k^0}{s_k}\right).$$

We define the set of non-monotonic players as $\mathcal{K}_{\text{NM}} := \{k \in \mathcal{K} : J_k \text{ is not monotone w.r.t. } u_k\}$, (i.e., $k \in \mathcal{K}_{\text{NM}}$ if the assigned weights of socio-economic and health losses are such as J_k is non-monotone w.r.t. u_k).

Now that we have introduced all the notations needed to establish the main result of this chapter, let us exhibit the following key Lemma that provides, $\forall k \in \mathcal{K}$, a lower-bound on the derivative of s_k w.r.t. u_k.

Lemma 2. *Under Assumption 1, $\forall T \in \mathcal{T},\ \forall u \in \mathcal{U}$ and $\forall (k,\ell) \in \mathcal{K}^2$ one has*

$$\frac{\partial s_k}{\partial u_\ell}(T,u) \geq 0$$

and

$$\frac{\partial s_k}{\partial u_k}(T,u) \geq \frac{s_k(T,u)\ln\left(\dfrac{s_k(T,u)}{s_k^0}\right)}{(1-u_k)\left[(1-u_k)\rho_{kk}s_k(T,u) - 1\right]}.$$

Proof. See Appendix 2.6.2. ■

The following Theorem establishes the main result of this chapter, by ensuring that the game $\mathcal{G}$ is in the **WIR**.

Theorem 5. *Let $T \in \mathcal{T}$. Suppose Assumption 1 holds and the less restrictive action profile $u_{\min} = (U_1^{\min}, ..., U_K^{\min}) \in [0,1)^K$ verifies that, $\forall k \in \mathcal{K}_{\text{NM}}$,*

$$(1 - U_k^{\min})s_k(T, u_{\min}) \geq 1/(2\rho_{kk}). \tag{2.8}$$

*Then, the game $\mathcal{G}$ is in the **WIR**.*

Proof. See Appendix 2.6.3. ■

The additional condition we introduce means that if the epidemics are sufficiently controlled, then the game $\mathcal{G}$ is a quasi-convex game that ensures the existence of a pure NE, according

to Proposition 1. In practice, that would mean that the social planner would need to track the regions at least partially (e.g., by imposing some minimum epidemic management measures).

2.2.2 Uniqueness

In practice having the uniqueness of the NE may be a useful feature for a government (when players are the regions) or for an international organization (when players are countries). It is typically convenient to be able to predict the outcome of the game. If the game models the interactive situation sufficiently well, an NE can be effectively observed. If there is only one NE, the situation becomes predictable, which is not the case in the presence of multiple equilibria. It is known that uniqueness typically requires additional conditions ([63]). The following result establish the uniqueness property of the NE, and the convergence of the sequential best-response dynamics.

Theorem 6. *Suppose that* $\forall k \in \mathcal{K}$*,*

$$\frac{\partial^2 J_k}{\partial {u_k}^2}(u) > \sum_{\ell=1,\ell\neq k}^{K} \left| \frac{\partial^2 J_k}{\partial u_k \partial u_\ell}(u) \right|.$$

Then $\mathcal{G}$ *has a unique NE, and the sequential best-response dynamics converges to this equilibrium.*

Proof. See Appendix 2.6.4. ■

We should note that, if the conditions of Theorem 5 hold for all $k \in \mathcal{K}$, then J_k is strictly convex w.r.t. u_k that is, $\frac{\partial^2 J_k}{\partial {u_k}^2}(u) > 0$. Here, the additional condition of Theorem 6 requires that the dependency of the second derivative of J_k w.r.t. the control actions of the other regions is sufficiently small. The latter is both useful to predict the epidemic tendency when its management is decentralized and to compute the NE (so the PoA and PoC).

Remark. If the game is not in the **WIR** but $\mathcal{K}_{\mathrm{NM}} = \emptyset$, the costs J_k are all individually quasi-convex and the existence of a pure NE is ensured. Moreover, there is a unique pure NE which lies at the extreme of the interval $\mathcal{U}$, in particular whatever the values of $\beta_{k\ell}$.

2.3 Game analysis under ICUs constraints

One critical aspect of epidemic control is the availability and capacity of healthcare resources, particularly intensive care units (ICUs), which play a vital role in treating severe cases and reducing mortality rates. Motivated by the coupled constraint ICU scenario, we consider a generalized form game that captures the strategic interactions among different entities involved in resource allocation and decision-making under ICU constraints. The generalized strategic

form of the game when integrating all the constraints write as :

$$\widetilde{\mathcal{G}} := \left(\mathcal{K}, \left(\mathcal{U}_k\right)_{1\leq k\leq K}, \left(\mathcal{C}_k\right)_{1\leq k\leq K}, \left(J_k\right)_{1\leq k\leq K} \right),$$

in which the players (nodes of the network) are the regions of a country (or simply countries); the action space for Player k is given by $\mathcal{U}_k = [U_k^{\min}, U_k^{\max}] \subset (0,1)$; the individual cost function of Player $k \in \mathcal{K}$ is given by J_k in (2.2); $\forall u_{-k} \in \mathcal{U}_{-k}$, $\mathcal{C}_k(u_{-k}) := \{u_k \in \mathcal{U}_k : \forall t,\ i_k(t,u) \leq \frac{1}{\sigma_k}\mathrm{i_{cu,k}}\}$. The parameter $\mathrm{i_{cu,k}}$ and σ_k represents the maximum proportion of ICU patients and the proportion of infected individuals who require intensive care in the context of the epidemic. In France, it has been reported that the highest recorded number of ICU patients reached $7\,148$ on April 8, 2020. However, it is worth noting that the overall capacity of ICU beds across the entire country has been evaluated to exceed $15\,000$, indicating the healthcare system's capability to accommodate the increased demand for intensive care during that period. The following theorem ensures the existence of at least one Generalized Nash equilibrium (GNE) in the game $\widetilde{\mathcal{G}}$ (See Definition 27).

Theorem 7. *Let $T \in \mathcal{T}$. Suppose Assumption 1 holds and the less restrictive action profile $u_{\min} = (U_1^{\min}, ..., U_K^{\min}) \in [0,1)^K$ verifies that, $\forall k \in \mathcal{K}$,*

$$(1 - U_k^{\min}) s_k(T, u_{\min}) \geq 1/(2\rho_{kk}). \tag{2.9}$$

Then, the game $\widetilde{\mathcal{G}}$ has at least one GNE.

Proof. Based on the Theorem 5 and [79], we derive the desired result. See Appendix 2.6.5. ■

2.4 Numerical performance analysis

The goal of this section is to quantify the PoA and PoC numerically for a Covid-19-type scenario. The proposed methodology can be applied to other epidemic scenarios where multiple regions are involved. Motivated by a scenario which has been studied by the French government in May 2020.

Influence of the epidemic graph on the PoA :

In this particular example, our focus is on a graph made up of ten interconnected nodes ($K = 10$). Our objective is to investigate the impact of the graph's structure on the Price of Anarchy (PoA), a metric that measures the efficiency of resource allocation. To facilitate our analysis, we establish several assumptions and parameter settings. Firstly, we assume a uniform value of $\gamma_k = 0.14$, for all nodes k. Additionally, for all $k \in \mathcal{K}$, we set $a_k = b_k = 1$ and regions$k \in \{6,7,8,9,10\} =: \mathcal{K}_{\mathrm{NM}}$ are assigned a value of $c_k = 1000$, while for all $k \in \mathcal{K} \setminus \mathcal{K}_{\mathrm{NM}}$, $c_k = 0$.

For the epidemic phase, we consider a time horizon of $T = 30$ days. To ensure compliance with Theorem 5, we introduce the concept of minimal action, denoted as $U_k^{\min}$, which is determined by setting $U_k^{\min}$ such that $\beta_{k\ell} \leq \nu_{\beta,k}$. Here, the weights $\beta_{k\ell}$ are assigned in a manner that yields the matrix $\widehat{\boldsymbol{B}}$ obtained by element-wise multiplication of the matrix $\widetilde{\boldsymbol{A}}$ i.e., $\widehat{\boldsymbol{B}} = \boldsymbol{B}^0 \odot \widetilde{\boldsymbol{A}}$. The matrix $\boldsymbol{B}^0$ and $\widetilde{\boldsymbol{A}}$ are defined as follows :

$$\boldsymbol{B}^0 = 10^{-3} \times \begin{pmatrix} 20 & 38 & 50 & 32 & 8 & 51 & 21 & 39 & 46 & 46 \\ 29 & 36 & 4 & 12 & 11 & 27 & 32 & 32 & 16 & 21 \\ 36 & 17 & 22 & 20 & 31 & 42 & 40 & 23 & 10 & 34 \\ 4 & 17 & 21 & 34 & 15 & 29 & 41 & 10 & 4 & 24 \\ 30 & 35 & 3 & 7 & 36 & 18 & 24 & 36 & 11 & 29 \\ 28 & 19 & 30 & 10 & 32 & 21 & 3 & 18 & 7 & 3 \\ 10 & 25 & 26 & 14 & 19 & 26 & 1 & 0.1 & 19 & 29 \\ 11 & 7 & 11 & 8 & 22 & 5 & 16 & 18 & 1 & 22 \\ 12 & 14 & 17 & 17 & 9 & 8 & 12 & 11 & 6 & 1 \\ 13 & 11 & 2 & 18 & 11 & 18 & 18 & 1 & 5 & 8 \end{pmatrix},$$

$$\text{and } [\widetilde{\boldsymbol{A}}]_{k\ell} = \begin{cases} 1 & \text{if } k \text{ and } \ell \text{ are connected} \\ & \text{in the epidemic graph,} \\ 10^{-10} & \text{otherwise.} \end{cases}$$

To generate a suitable graph structure, we employ the Watts-Strogatz model, specifically the Small-world graph. By varying the average degree per agent, denoted as $\overline{Deg}$, with values of 2, 4, 6, 8, and 10, and maintaining a fixed connection probability of 0.5, we randomly generate 5000 adjacency matrices denoted as $\widetilde{\boldsymbol{A}}$. This approach enables us to explore different graph configurations and their influence on the observed PoA.

In Fig. 2.1, we observe the interpolation of the PoA with respect to the quantity $\sum_{k\in\mathcal{K}} \sum_{\ell\in\mathcal{N}_k} \frac{\beta k\ell}{\gamma_k}$, where $\mathcal{N}_k$ represents the set of neighbors of Region k. It can be seen that the Price of Anarchy increases with the average degree per agent in the graph, reaching values as high as 1.5 for highly connected graphs. Consequently, the implication of this result is that the social planner should not decentralize decision-making in such cases.

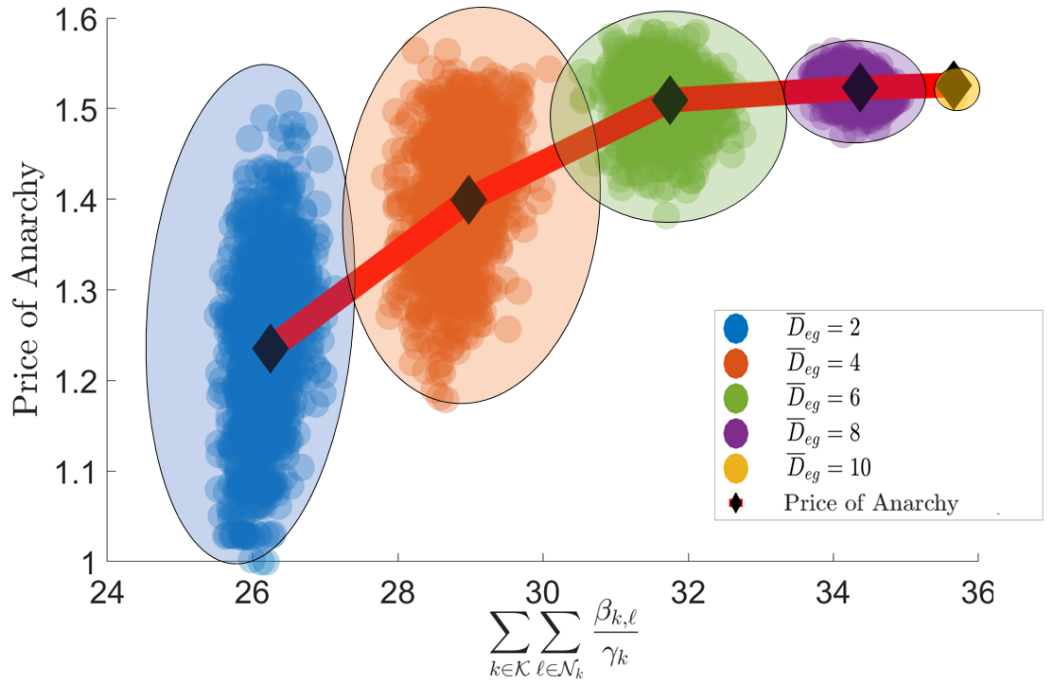

FIGURE 2.1 – Relationship between the Price of Anarchy (PoA) and the sum of the epidemic graph coefficients $\sum_{k\in\mathcal{K}}\sum_{\ell\in\mathcal{N}k}\frac{\beta_{k,\ell}}{\gamma_k}$ for random graphs generated using the Watts-Strogatz model. The average degree per agent $\overline{Deg}$ is varied in the range $\overline{Deg}\in\{2,4,6,8,10\}$ to observe the influence of the epidemic graph on the PoA.

Influence of the inter-region virus transmission rates on the PoA :

We assume that France is divided in $K=5$ regions and we propose to observe the influence of the inter-region virus transmission rates $\beta_{k\ell}$ on the PoA and PoC. To choose the epidemic's parameters, we have exploited the studies on Covid-19 that have been conducted in [5, 82, 83]. We assume that : Regions $k\in\{1,2\}$ have selected the weight a_k, b_k and c_k such that only the socio-economic losses matter; Regions $k\in\{3,4,5\}$ weighted the weights of each of the losses such that $\mathcal{K}_{\text{NM}}=\{3,4,5\}$; see the Table 2.1.

k	γ_k	β_{kk}	s_k^0	i_k^0	a_k	b_k	c_k
1	0.15	$3\gamma_1$	0.8	0.2	2	0	0
2	0.15	$2\gamma_2$	0.9	0.1	0.5	0	0
3	0.15	$1.5\gamma_3$	0.9	0.005	5	2	50
4	0.15	$1.2\gamma_4$	0.9	0.002	2	5	70
5	0.15	$1\gamma_5$	0.9	0.001	3	5	70

TABLE 2.1 – Influence of inter-region virus transmission rates on the PoA in Chapter 2 : Epidemic and game parameters

The time horizon of the considered epidemic phase is set to $T=30$ days [84, 85, 86]. The

coupled SIR model is implemented by using the Matlab ODE45 solver with the Runge-Kutta scheme. The action space is chosen by the social planner such as : $\forall k \in \mathcal{K}$, $U_k^{\max} = 0.9$, $u_{\min} = (0.6, 0.51, 0.35, 0.2, 0.1)$ and $\mathcal{U}_k = \{U_k^{\min}, (U_k^{\max} - U_k^{\min}) \cdot 0.1, \ldots, U_k^{\max}\}$. In view of the Table 2.1, the Theorem 5 holds, when the inter-region virus transmission rates $\beta_{k\ell}$ are lower than the constant threshold $\nu_{\beta,k} = \frac{1}{4} \cdot (\frac{\gamma_k}{(1-U_k^{\min})s_k^0} - \beta_{kk})$, which is reasonable in view of the situation in France provided by the National Institute of Statistics and Economic Studies (INSEE) in [87, Table 6-8]. By applying an exhaustive search to find the NE and the social optimal, we show in Fig. 2.2 and 2.3 the interpolation of the PoA, PoC w.r.t $\beta_{k\ell}$, $\forall k \neq \ell$. Each curve corresponds to a scenario where all incoming transmission rates from a given region vary uniformly (i.e.,$\forall \ell \neq k$, $\beta_{k\ell} \in \{0, 1 \cdot 10^{-3}, \ldots, 1.2 \cdot 10^{-2}\}$), whereas the other transmission rates are fixed at the threshold value $\nu_{\beta,k}$. We observe that the PoA can be as large as 1.2 for crossing rates greater than 0.2%. Therefore, the outcome in this case is that the social planner should not decentralize the decision making. We emphasize that, when $\beta_{k\ell} \geq \nu_{\beta,k}$ the simulationCHAP2 does not fit into our theoretical setup. The PoC measures the impact of ignoring the connection with other regions is even larger and reaches values as large as 3, which shows that a region has a strong interest in accounting for the crossing rates to manage the epidemic locally.

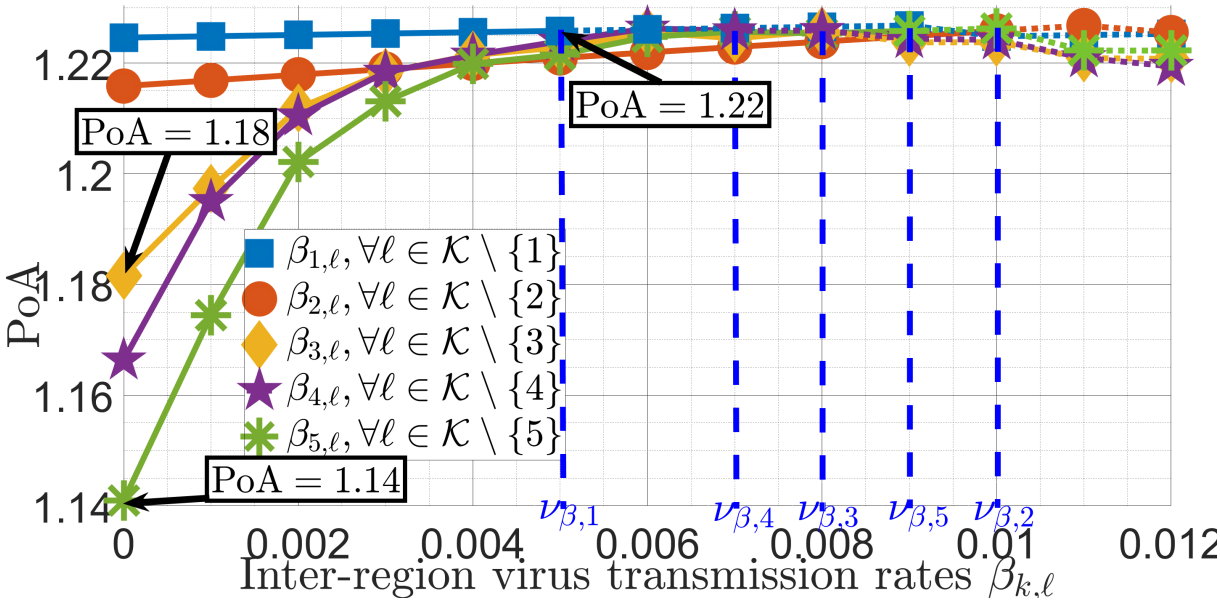

FIGURE 2.2 – Interpolation of PoA by varying uniformly the incoming transmission rates of each Region k. The dotted curves do not fit into our theoretical setup.

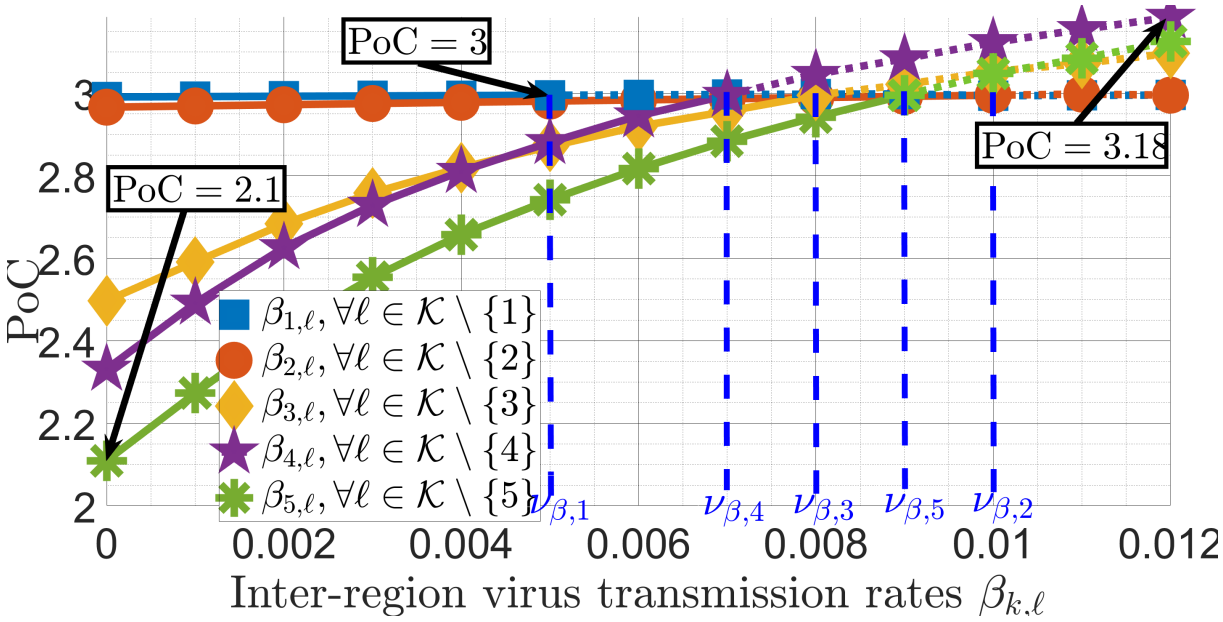

FIGURE 2.3 – Interpolation of PoC by varying uniformly the incoming transmission rates of each Region k. The dotted curves do not fit into our theoretical setup.

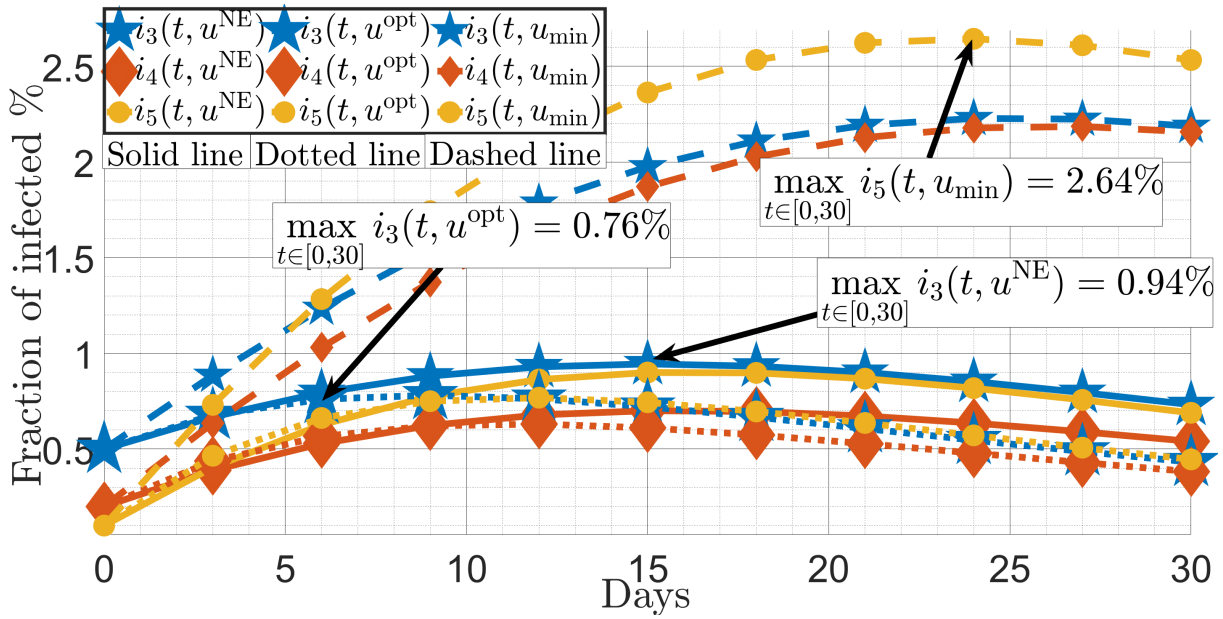

FIGURE 2.4 – Interpolation of infected proportions in each Regions $k \in \{3, 4, 5\}$. u^{NE}= Nash equilibrium strategy ; u^{opt}= optimal centralized strategy ; $u_{\min}$= less restrictive policy.

In view of the weights a_k, b_k, c_k given in the Table 2.1, a natural question should be raised : "How is the epidemic spreading in the regions $k \in \{3, 4, 5\}$?" Fig. 2.4 shows the evolution over the time of i_k, for $k \in \{3, 4, 5\}$, when different strategy is considered and $\forall k \neq \ell,\ \beta_{k\ell} = \nu_{\beta,k}$. Quantitatively we observe that : when either the NE or optimal strategy is applied, the maximum

proportion of infected in Regions $k \in \{3,4,5\}$ is less that 0.94%, i.e. if the population sizes in Regions $k \in \{3,4,5\}$ are similar to the region "Île-de-France", then the infected proportions are upper-bounded by $112\ 800$ cases, when policy-makers apply either NE or centralized strategy.

Influence of the ICUs constraints on the PoA :

In this numerical example, we consider an epidemic scenario where the underlying graph is structured into a total of $K = 5$ regions. The main focus of our investigation lies in examining the impact of ICU constraints on the GNE strategy with respect to three key aspects : the Price of Anarchy (PoA), and the dynamics of the epidemic itself. To facilitate a comprehensive analysis, we provide the specific parameters associated with the epidemic and the game in Table 2.2. By studying this illustrative scenario, we aim to gain insights into how ICU constraints can shape resource allocation strategies and subsequently influence the overall dynamics of the epidemic.

k	γ_k	β_{kk}	s_k^0	i_k^0	a_k	b_k	c_k
1	0.15	$3.5\gamma_1$	0.9	0.1	0	0	$7 \cdot 10^3$
2	0.15	$2.7\gamma_2$	0.9	0.1	0	0	$7 \cdot 10^3$
3	0.15	$2.05\gamma_3$	0.995	0.005	5	2	0
4	0.15	$2\gamma_4$	0.998	0.002	2	5	0
5	0.15	$1\gamma_5$	0.999	0.001	3	5	0

TABLE 2.2 – Influence of the ICUs constraints on the PoA in Chapter 2 : Epidemic and Game parameters

We investigate an epidemic management approach comprising $N = 3$ distinct phases across $K = 5$ regions. Each phase requires the adjustment of actions, denoted as $u(n)$, to effectively address the evolving situation. The time horizon for each epidemic phase is set to $T = 30$ days. At the start of each phase, the initial condition, represented as $x((n-1)T) := (s((n-1)T), i((n-1)T), r((n-1)T))$, is updated to reflect the outcomes of the previous phase and serves as the basis for subsequent decision-making processes. To model the epidemic dynamics, we employ a coupled SIR (Susceptible-Infected-Recovered) model, utilizing the Matlab ODE45 solver with the Runge-Kutta scheme. The action space is determined by the social planner and defined as follows : $\forall k \in \mathcal{K}$, the maximum action is set as $U_k^{\max} = 0.9$, while the minimum action is defined as $u_{\min} = (0.75, 0.7, 0.7, 0.6, 0.2)$ and The action space for each region is defined as $\mathcal{U}_k = \{U_k^{\min}, (U_k^{\max} - U_k^{\min}) \cdot 0.1, \ldots, U_k^{\max}\}$. In the context of inter-region virus transmission rates, we assume that for all regions $\forall k$ and $\ell \neq k$, $\beta_{k\ell} = \nu_{\beta,k} = \frac{1}{4} \cdot (\frac{\gamma_k}{(1-U_k^{\min})s_k^0} - \beta_{kk})$. This relationship satisfies the conditions outlined in Theorem 7, ensuring the existence of a GNE. Moreover, for each region $k \in \{1,2\}$ the ICU occupancy, denoted as $\mathrm{i_{cu,1}} = \mathrm{i_{cu,2}} = \infty$ whereas for $k \in \{3,4,5\}$, $\mathrm{i_{cu,k}} := i_k(0)$ and

$\sigma_3 = \sigma_4 = \sigma_5 = \sigma$ is a parameter that varies throughout the analysis. In order to evaluate the effectiveness of the GNE for each epidemic stage, we redefine the price of anarchy such as : $\forall n \in \{1, 2, 3\}$

$$\widetilde{\mathrm{PoA}}(n) := \max_{u \in \widetilde{\mathcal{U}}^{\mathrm{NE}}(n)} \sum_{k=1}^{K} \widetilde{J}_k(u, x^{\mathrm{GNE}}(n-1)) \Big/ \min_{u \in \mathcal{C}} \sum_{k=1}^{K} \widetilde{J}_k(u, x^{\star}(n-1)),$$

where :

- $\widetilde{\mathcal{U}}^{\mathrm{NE}}(n)$ is the set of GNE of $\widetilde{\mathcal{G}}$ at the n^{th}-stage of the epidemic ;
- for $n > 1$, $\widetilde{J}_k(u, x(n-1)) := a_k u_k + b_k u_k^2 + c_k(s_k((n-1)T, u(n-1)) - s_k(T, u))$, and for $n = 1$ we have $\widetilde{J}_k(u, x(0)) = J_k(u)$;
- $\mathcal{C} := \{u \in \mathcal{U} : \ \forall k \in \{3, 4, 5\}, \ \forall t \in [(n-1)T, nT], \ i_k(t, u) \leq \dfrac{1}{\sigma} \mathrm{i}_{\mathrm{cu,k}}\}$.

In Tab. 2.3 and Tab. 2.4, the Price of Anarchy (PoA) and the social cost evaluated at the GNE, have been presented across three different stages of the epidemic and for different values of σ. As the ICU constraints increase (which is represented by an increase in $1/\sigma$), the PoA and the social cost at the GNE also increase but the social cost evaluated at the optimal centralized strategy remains constant. This suggests that more flexible ICU constraints can lead to more inefficient outcomes if regions make decisions in a decentralized manner and does not impact the optimal centralized strategy. This scenario is akin to the Braess paradox (see the example in Section 1.2.2), where adding extra capacity can lead to overall poorer performance in terms of social cost. To better understand this phenomenon, we compare the GNE strategies with the optimal centralized strategies for each phase of the epidemic, considering different values of σ, specifically $\sigma \in \{0.0857, 0.15, 0.75\}$, as depicted in Table 2.5 and Figure 2.5.

Upon assessing the relative weights of the parameters c_k for regions $k \in \{1, 2\}$ and a_k and b_k for regions $k \in \{3, 4, 5\}$, there is a considerable discrepancy. This contrast illustrates the emphasis on health-related concerns in regions 1 and 2, as opposed to the predominantly socio-economic concerns in regions 3, 4 and 5. When decision-making is centralized, a central authority is likely to impose stricter restrictions in regions 3, 4 and 5 during the initial epidemic phase in order to minimize healthcare costs in regions 1 and 2, even at the expense of socio-economic impact in regions 3, 4 and 5. Such strict initial restrictions in regions 3, 4 and 5 result in a higher proportion of susceptible individuals, $s_k(T, u^{\star})$, in these regions at the end of the first phase of epidemic management. In contrast, under a decentralized decision-making structure, regions 3, 4, and 5, primarily concerned with minimizing their socio-economic costs, may display a lower interest in their health-related costs. As a result, under a decentralized decision-making process, the chosen strategies u_k^{GNE} for regions 3, 4, and 5 would tend to be less restrictive, reflecting their priority to minimize socio-economic costs. This lower emphasis on health-related restrictions leads to a smaller proportion of susceptible individuals, $s_k(T, u^{\mathrm{GNE}})$, in these regions

after the initial epidemic phase. This divergence in the initial management of the epidemic subsequently inflates the Price of Anarchy (PoA) for the second and third stages of epidemic mitigation.The central planner's initial emphasis on health considerations initiates a cascade of events that precipitate increased systemic inefficiencies in subsequent stages. Moreover, a decrease in the σ parameter accentuates the manifestation of the Braess paradox, highlighting the inefficiencies resulting from the strategic choices made in the preliminary phase of epidemic management.

	Epidemic stage →			
	σ	Stage $n=1$	Stage $n=2$	Stage $n=3$
← ICUs parameter σ decreases	0.7500	1.0032	1.0342	1.0899
	0.6000	1.0079	1.0861	1.1620
	0.5000	1.0130	1.1470	1.2444
	0.4286	1.0183	1.2206	1.3420
	0.3750	1.0239	1.3015	1.4457
	0.3333	1.0296	1.3871	1.5524
	0.3000	1.0348	1.4702	1.6541
	0.2727	1.0367	1.5036	1.7006
	0.2500	1.0388	1.5498	1.7648
	0.2308	1.0410	1.5983	1.8308
	0.2143	1.0431	1.6452	1.8932
	0.2000	1.0453	1.6926	1.9549
	0.1875	1.0474	1.7415	2.0169
	0.1765	1.0496	1.7903	2.0776
	0.1667	1.0506	1.8143	2.1076
	0.1579	1.0513	1.8310	2.1285
	0.1500	1.0521	1.8480	2.1498
	0.1429	1.0529	1.8786	2.1918
	0.1364	1.0537	1.8965	2.2138
	⋮	⋮	⋮	⋮
	0.0968	1.0604	2.0544	2.3988
	0.0937	1.0611	2.0712	2.4175
	0.0909	1.0618	2.0880	2.4361
	0.0882	1.0625	2.1049	2.4546
$\widetilde{\mathrm{PoA}}(n)$	0.0857	1.0628	2.1117	2.4619

TABLE 2.3 – The table illustrates the relationship between the Price of Anarchy (PoA) and a parameter denoted as σ. This parameter is introduced in the Intensive Care Units (ICUs) constraint for players in regions $\forall k \in \{3,4,5\}$, where $u_k \in \mathcal{C}k(u{-}k) = \{u_k \in \mathcal{U}k : \ \forall t,\ i_k(t,u) \leq \frac{1}{\sigma}\mathrm{icu,k}\}$. As the parameter σ decreases, indicating increased flexibility in the ICU constraints, there is an observed increase in the Price of Anarchy (PoA). This finding suggests the presence of the Braess paradox, as discussed in the example in Section 1.2.2.

	Epidemic stage →			
	σ	Stage $n=1$	Stage $n=2$	Stage $n=3$
↓ ICUs parameter σ decreases	0.7500	592.9415	37.5362	13.3500
	0.6000	595.6906	39.6782	14.3575
	0.5000	598.6444	42.1056	15.4752
	0.4286	601.7956	44.8097	16.6889
	0.3750	605.1148	47.7794	17.9785
	0.3333	608.4652	50.9211	19.3058
	0.3000	611.5475	53.9722	20.5703
	0.2727	612.7350	55.5884	21.3487
	0.2500	613.9823	57.2966	22.1547
	0.2308	615.2834	59.0914	22.9832
	0.2143	616.5262	60.8240	23.7661
	0.2000	617.7788	62.5778	24.5406
	0.1875	619.0595	64.3821	25.3192
	0.1765	620.3325	66.1883	26.0809
	0.1667	620.9463	67.0767	26.4572
	0.1579	621.3659	67.6912	26.7203
	0.1500	621.7969	68.3201	26.9872
	0.1429	622.2389	68.9632	27.2576
	0.1364	622.6912	69.6201	27.5314
	⋮	⋮	⋮	⋮
	0.0968	626.6748	75.4158	29.8323
	0.0937	627.0956	76.0316	30.0648
	0.0909	627.5178	76.6501	30.2959
	0.0882	627.9411	77.2713	30.5257
$\max_{u\in\widetilde{\mathcal{U}}^{\mathrm{NE}}(n)} \sum_{k=1}^{K} \widetilde{J}_k(u, x^{\mathrm{GNE}}(n-1))$	0.0857	628.1103	77.5197	30.6170

TABLE 2.4 – The table presents the relationship between the social cost, evaluated at the worst Generalized Nash Equilibrium (GNE) for each stage n, and a parameter denoted as σ. This parameter is introduced in the Intensive Care Units (ICUs) constraint for players in regions $\forall k \in \{3,4,5\}$, where $u_k \in \mathcal{C}k(u-k) = \{u_k \in \mathcal{U}k : \ \forall t,\ i_k(t,u) \leq \frac{1}{\sigma}\mathrm{icu}, \mathrm{k}\}$. As the parameter σ decreases, indicating increased flexibility in ICU constraints, there is an observed increase in the social cost. This finding suggests the presence of the Braess paradox, as discussed in the example in Section 1.2.2.

TABLE 2.5 – The table illustrates the correlation between the Generalized Nash Equilibrium (GNE) strategy and the optimal centralized strategy for each epidemic stage, with respect to the parameter σ from the set $\{0.0857, 0.15, 0.75\}$. As the value of σ decreases, indicating an increase in the ICU constraint, it becomes apparent that the GNE strategy for regions 3, 4, and 5 tends to be more relaxed, while the optimal centralized strategy remains unchanged regardless of the value of σ.

(a) GNE strategy (u^{GNE}) when $\sigma = 0.75$ for each epidemic stage.

	Epidemic stage →		
	Stage 1	Stage 2	Stage 3
Region 1	0.90	0.90	0.90
Region 2	0.90	0.90	0.90
Region 3	0.86	0.70	0.70
Region 4	0.86	0.60	0.60
Region 5	0.85	0.20	0.20

(b) Optimal strategy ($u^\star$) when $\sigma = 0.75$ for each epidemic stage.

	Epidemic stage →		
	Stage 1	Stage 2	Stage 3
Region 1	0.90	0.90	0.90
Region 2	0.90	0.90	0.90
Region 3	0.90	0.76	0.70
Region 4	0.90	0.60	0.60
Region 5	0.85	0.20	0.20

(c) GNE strategy (u^{GNE}) when $\sigma = 0.15$ for each epidemic stage.

	Epidemic stage →		
	Stage 1	Stage 2	Stage 3
Region 1	0.90	0.90	0.90
Region 2	0.90	0.90	0.90
Region 3	0.70	0.70	0.70
Region 4	0.60	0.60	0.60
Region 5	0.40	0.20	0.20

(d) Optimal strategy ($u^\star$) when $\sigma = 0.15$ for each epidemic stage.

	Epidemic stage →		
	Stage 1	Stage 2	Stage 3
Region 1	0.90	0.90	0.90
Region 2	0.90	0.90	0.90
Region 3	0.90	0.77	0.70
Region 4	0.90	0.60	0.60
Region 5	0.73	0.20	0.20

(e) GNE strategy (u^{GNE}) when $\sigma = 0.0857$ for each epidemic stage.

	Epidemic stage →		
	Stage 1	Stage 2	Stage 3
Region 1	0.90	0.90	0.90
Region 2	0.90	0.90	0.90
Region 3	0.70	0.70	0.70
Region 4	0.60	0.60	0.60
Region 5	0.20	0.20	0.20

(f) Optimal strategy ($u^\star$) when $\sigma = 0.0857$ for each epidemic stage.

	Epidemic stage →		
	Stage 1	Stage 2	Stage 3
Region 1	0.90	0.90	0.90
Region 2	0.90	0.90	0.90
Region 3	0.90	0.76	0.70
Region 4	0.90	0.60	0.60
Region 5	0.77	0.20	0.20

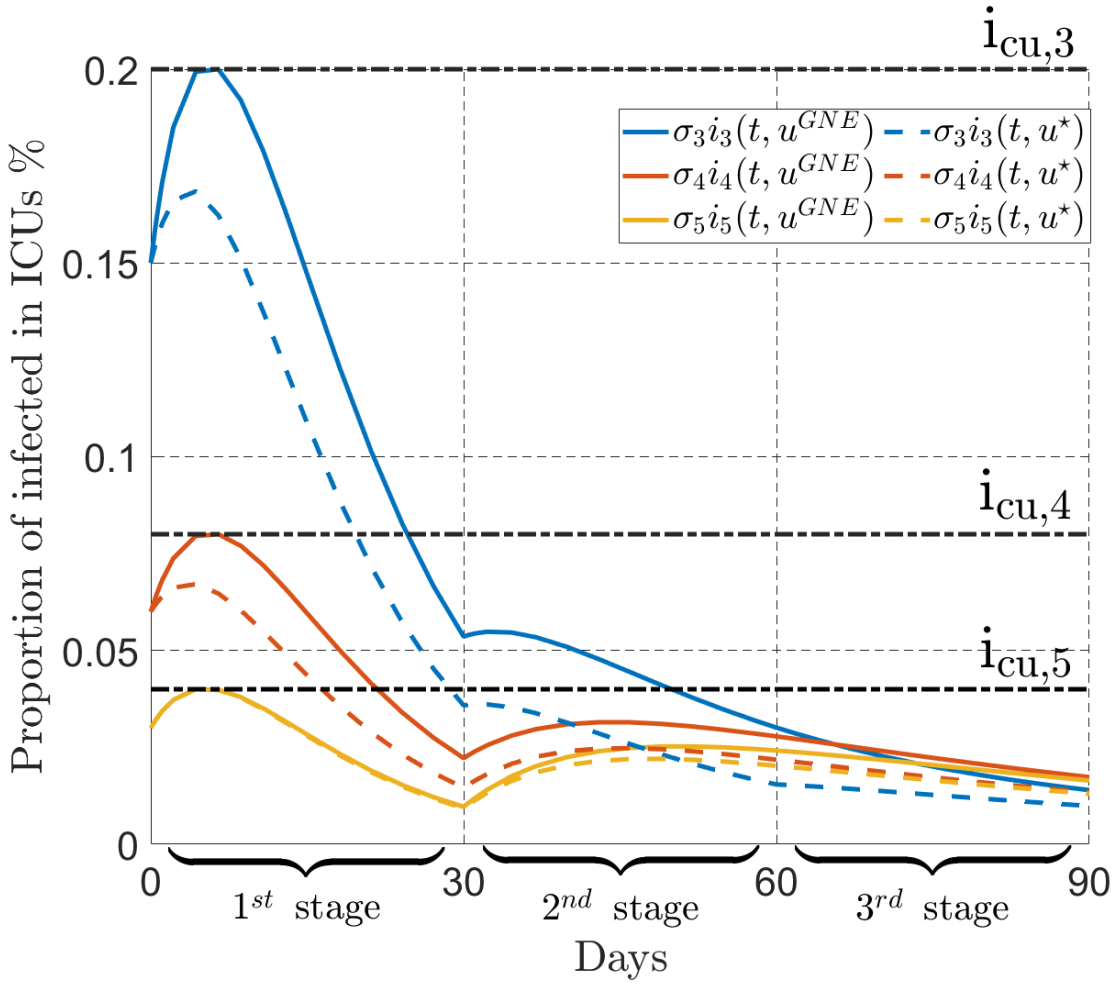

(a) Interpolation of the proportion of infected individuals admitted to ICUs in Region $k \in \{3, 4, 5\}$ under the GNE and the optimal centralized strategies : $\sigma = 0.75$.

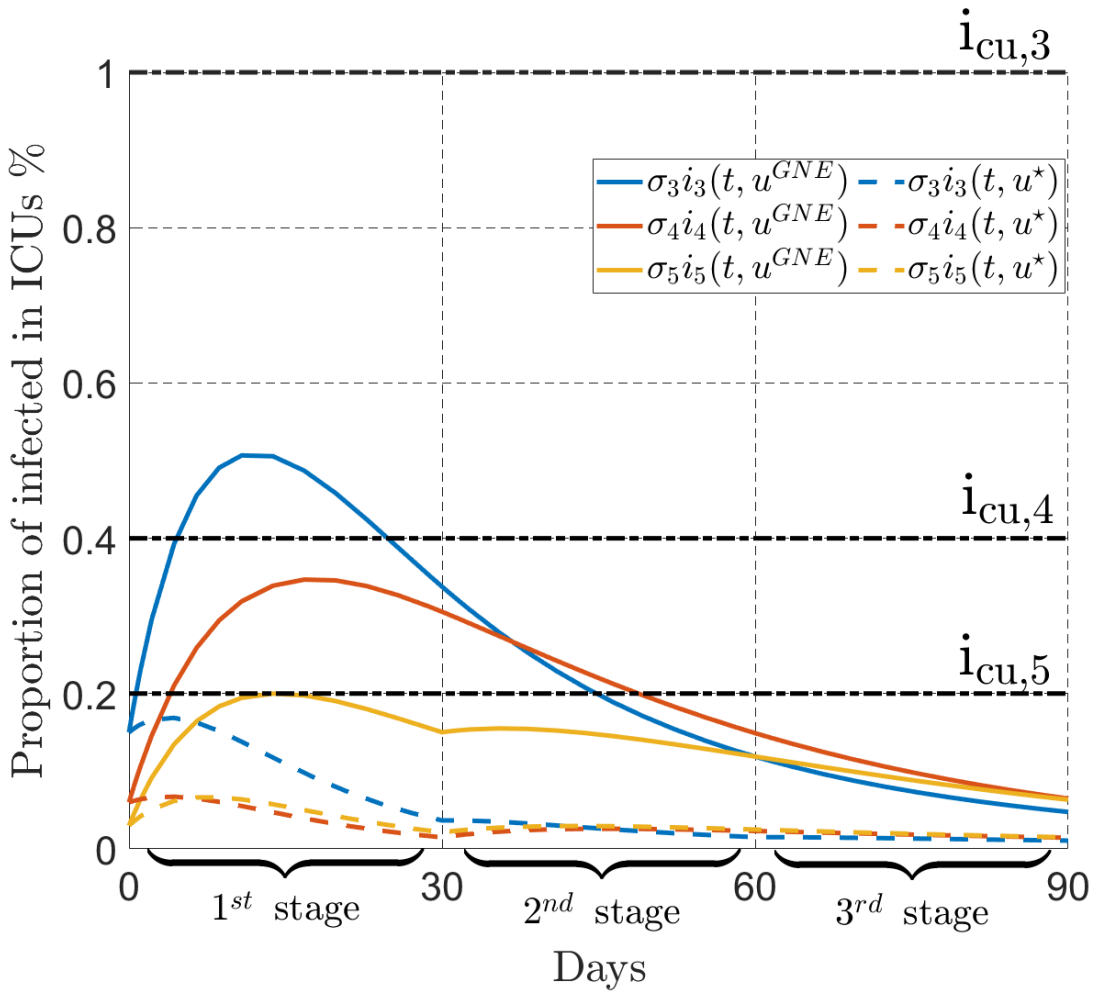

(b) Proportion of infected individuals admitted to ICUs in Region 3,4 and 5 when the GNE and optimal centralized strategies are applied with $\sigma = 0.15$.

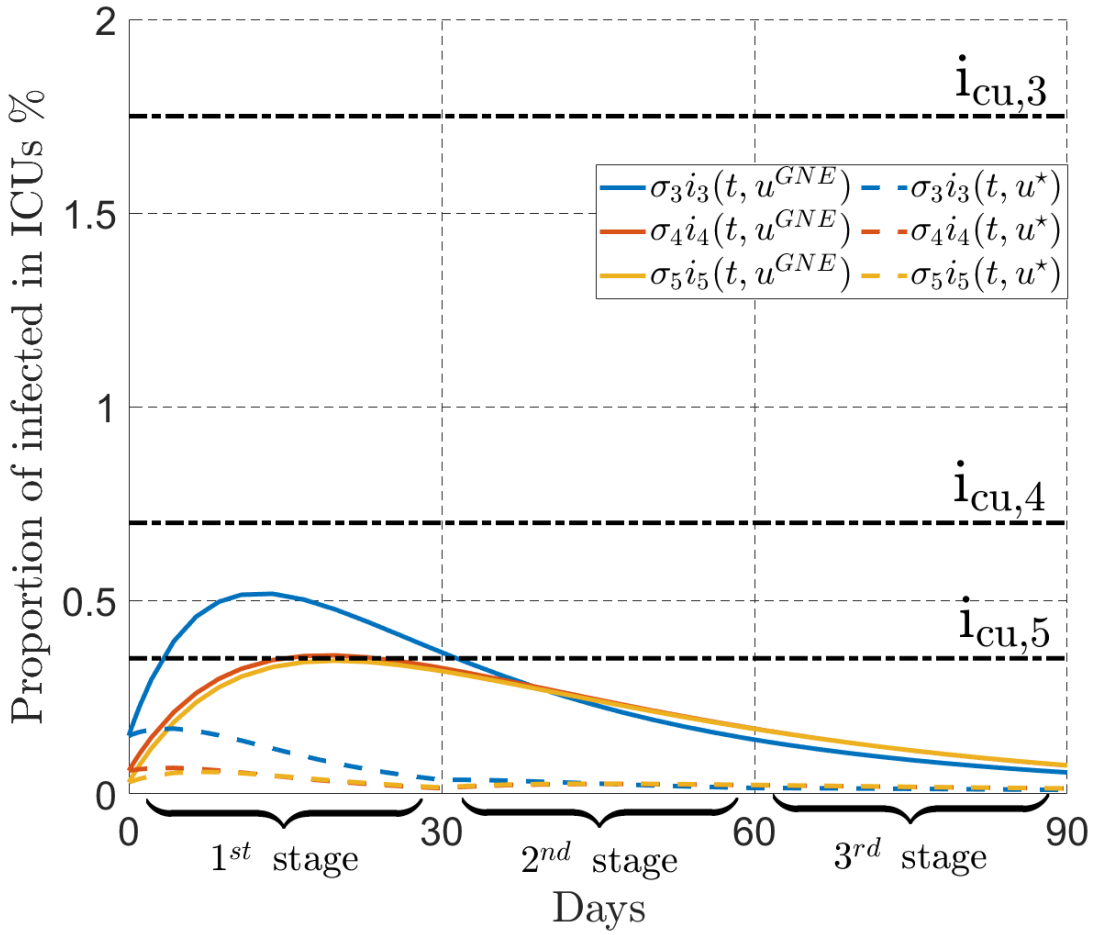

(c) Evolution of the proportion of infected individuals admitted to ICUs in Region $k \in \{3, 4, 5\}$ under the GNE and optimal centralized strategies : $\sigma = 0.0857$.

FIGURE 2.5 – Temporal evolution of the proportion of infected individuals admitted to Intensive Care Units (ICUs) in Region $k \in \{3, 4, 5\}$ under Generalized Nash Equilibrium (GNE) and optimal centralized strategies for different values of $\sigma \in \{0.75, 0.15, 0.0857\}$. The graph illustrates how the proportion of infected individuals admitted to ICUs changes over time, highlighting the impact of varying σ values on the strategies employed and their corresponding outcomes.

2.5 Conclusion

In this chapter, we present a mathematical model that examines the effects of decentralization on epidemic management. In our proposed framework, each region or country is a decision-maker where the virus spreads according to a networked epidemic models. Our model, while relatively simple, captures key effects, which is based on a strategic-form game drawn from a networked Susceptible-Infected-Recovered (SIR) compartmental model. Here, each player re-

presents a geographical region with the goal of deciding social-distancing rules to minimize associated costs, thereby implementing a trade-off between socio-economic losses and health losses. The conducted Nash equilibrium (NE) analysis of the proposed game largely relies on the individual quasi-convexity of the cost function of a region. Because one cannot express the state of the fraction of "susceptibles" as a function of the control actions, this analysis turns out to be non-trivial. We exhibit a regime called Weak Interconnection Regime (WIR) in terms of inter-region transmission rates in which existence is guaranteed; this regime appears to be non-limiting for real scenarios. A thorough analysis of Nash equilibrium is conducted in Theorem 5, Proposition 2 and Theorem 6. The assessment of decentralized epidemic management efficiency in this chapter revolves around two key metrics : the Price of Anarchy (PoA) and the Price of Connectedness (PoC). These metrics serve as quantitative indicators to evaluate the performance of the Nash Equilibrium (NE) strategy in comparison to the optimal centralized strategy, and to highlight the significance of considering the graph structure in decentralized decision-making processes. In an advanced extension of our work, we incorporate a crucial component of epidemic management, i.e., the availability and adequacy of healthcare resources, with particular attention to intensive care units (ICUs). These factors are integrated into the decision-making process, enabling us to examine a generalized form of the game. Consequently, in Theorem 7, we extend our analysis to study the generalized Nash equilibrium of this new game, identifying and establishing specific conditions for its existence. The numerical analysis allows one to clearly quantify what is lost when regions or countries decide by themselves the way to manage the epidemic locally, without coordination. By simulating the Nash Equilibrium (NE) using different graph structures and inter-region transmission rates, and comparing the losses incurred by decentralization, the influence of graph connectivity on decision-making has been examined. The findings unanimously indicate that the interconnection between regions plays a crucial role in the effectiveness of decentralized decision-making, highlighting the critical impact of graph connectivity on the efficiency of the NE. Furthermore, the numerical analysis performed by solving the game with ICUs constraints unveiled the existence of a Braess Paradox (see Section 1.2.2).

2.6 Appendix of Chapter 2

2.6.1 Proof of Proposition 1

Since the action space of each player $\mathcal{U}_k$ is a convex, compact and non-empty set; the costs J_k are jointly continuous that is continuous w.r.t. the action profile $u \in \mathcal{U}$; the costs J_k are quasi-convex w.r.t. u_k on $\mathcal{U}_k$. Then, the game $\mathcal{G}$ is a quasi-convex game. By Debreu-Fan-Glicksberg theorem for quasi-convex games [63, Theorem 50], the existence of a pure NE is guaranteed.

2.6.2 Proof of Lemma 2

Let $k \in \mathcal{K}$, $u \in \mathcal{U}$, $T \in \mathcal{T}$ and, $X := \Big(u, s(T,u), i(T,u)\Big) \in \mathcal{U} \times (0,1]^K \times (0,1]^K$ such that $F(X) = 0$. In what follows, we denote by :

$$\begin{aligned} \boldsymbol{D} &:= \left(\mathrm{diag}(s(T,u))^{-1} - \mathrm{diag}(\boldsymbol{B\Gamma^{-1}})\right)^{-1}, \\ \overline{\boldsymbol{B}} &:= \boldsymbol{B} - \mathrm{diag}(\boldsymbol{B}). \end{aligned}$$

In view of the expression of F, we have that :

$$\begin{cases} \dfrac{\partial F}{\partial s}(X) = -\boldsymbol{D^{-1}}\left(\boldsymbol{I}_K - \boldsymbol{D}\overline{\boldsymbol{B}}\boldsymbol{\Gamma^{-1}}\right) \\ \dfrac{\partial F}{\partial u}(X) = -\mathrm{diag}(\underline{1} - u)^{-1}\mathrm{diag}\left(\ln\left(s(T,u)\right) - \ln\left(s^0\right)\right). \end{cases}$$

According to Condition (iii) in Assumption 1, we derive that,

$$\left\|\boldsymbol{D}\overline{\boldsymbol{B}}\boldsymbol{\Gamma^{-1}}\right\|_\infty = \max_{k\in\mathcal{K}} \sum_{\ell=1,\ell\neq k}^{K} \left|\frac{(1-u_k)\rho_{k\ell}}{s_k(T,u)^{-1} - (1-u_k)\rho_{kk}}\right| < 1.$$

Therefore, the Neumann series converges and,

$$\left(\boldsymbol{I}_K - \boldsymbol{D}\overline{\boldsymbol{B}}\boldsymbol{\Gamma^{-1}}\right)^{-1} = \sum_{k=0}^{+\infty}\left(\boldsymbol{D}\overline{\boldsymbol{B}}\boldsymbol{\Gamma^{-1}}\right)^k.$$

According to the implicit function theorem, it follows that,

$$\frac{\partial s}{\partial u}(T,u) = -\left[\frac{\partial F}{\partial s}(X)\right]^{-1}\frac{\partial F}{\partial u}(X).$$

We denote by $\widehat{\dfrac{\partial s}{\partial u}}(T,u)$ the approximation of $\dfrac{\partial s}{\partial u}(T,u)$ at the first order of the Neumann series, such that,

$$\forall k,\ell,\ \widehat{\frac{\partial s}{\partial u}}(T,u) := \left(\boldsymbol{I}_K + \boldsymbol{D}\overline{\boldsymbol{B}}\boldsymbol{\Gamma^{-1}}\right)\boldsymbol{D}\frac{\partial F}{\partial u}(X).$$

Therefore, $\forall k,\ell$,

$$\frac{\partial s_k}{\partial u_\ell}(T,u) \geq \widehat{\frac{\partial s_k}{\partial u_\ell}}(T,u) \geq 0,$$

since Condition (iii) of Assumption 1 holds. The lower bound of $\dfrac{\partial s_k}{\partial u_k}(T,u)$ given in Lemma 2 corresponds to $\widehat{\dfrac{\partial s_k}{\partial u_k}}(T,u)$.

2.6.3 Proof of Theorem 5

The goal of this proof is to ensure that $\forall k \in \mathcal{K}$, J_k is quasi-convex w.r.t $u_k \in \mathcal{U}_k$. We know that, $\forall k \in \mathcal{K} \setminus \mathcal{K}_{\rm NM}$, J_k quasi-convexity property holds. In what follows, we are interest in to show the convexity of costs J_k for Players $k \in \mathcal{K}_{\rm NM}$. Therefore, we propose to analyze in a first step the convexity of i_k w.r.t u_k, which allows us to discuss about the concavity of s_k w.r.t u_k for $k \in \mathcal{K}_{\rm NM}$.

Let $k \in \mathcal{K}_{\rm NM}$, $u \in \mathcal{U}$, $T \in \mathcal{T}$ and $X := \Big(u, s(T,u), i(T,u)\Big) \in \mathcal{U} \times (0,1]^K \times (0,1]^K$ such that $F(X) = 0$. By following the same reasoning as in Lemma 2, we apply the implicit function theorem to the function $F : \mathcal{U} \times (0,1]^K \times (0,1]^K \to \mathbb{R}^K$ with :

$$\frac{\partial F}{\partial i}(X) = \mathrm{diag}(1-u)\widehat{\boldsymbol{B}}\Gamma.$$

Hence, we derive that

$$\frac{\partial i_k}{\partial u_k}(T,u) = \left[\frac{\partial F}{\partial i}^{-1}(X)\frac{\partial F}{\partial u}(X)\right]_{k,k} = \frac{\gamma_k b_{kk}^{\rm inv} \ln\left(\dfrac{s_k(T,u)}{s_k^0}\right)}{(1-u_k)^2},$$

where $b_{kk}^{\rm inv}$ is the $(k,k)^{\rm th}$ element of $\widehat{\boldsymbol{B}}^{-1}$.

Let $u_{-k} \in \mathcal{U}_{-k}$, $\lambda \in \mathbb{R}$,

$$(\underline{u}_k, \overline{u}_k) \in \Big\{u_k \in \mathcal{U} : \frac{\partial i_k}{\partial u_k}(T,u) \leq \lambda\Big\},$$

such that $\underline{u}_k \leq \overline{u}_k$.

Given that :

$$(i)\ \forall \alpha \in [0,1],\ \underline{u}_k \leq \alpha\underline{u}_k + (1-\alpha)\overline{u}_k \leq \overline{u}_k$$

$$(ii)\ s_k \text{ is increasing w.r.t. } u_k$$

we derive the quasi-convexity of $\dfrac{\partial i_k}{\partial u_k}$ w.r.t u_k, since the following holds.

$$\frac{\partial i_k}{\partial u_k}(T, \alpha\underline{u}_k + (1-\alpha)\overline{u}_k, u_{-k}) \leq \frac{\gamma_k b_{kk}^{\rm inv} \ln\left(\dfrac{s_k(T,\overline{u}_k,u_{-k})}{s_k^0}\right)}{(1-\underline{u}_k)^2} \leq \lambda.$$

Let us write the second derivative of i_k w.r.t. u_k,

$$\frac{\partial^2 i_k}{\partial u_k^2}(T,u) = \frac{\gamma_k b_{kk}^{\text{inv}} \left(\frac{\partial s_k}{\partial u_k}(T,u)(1-u_k) + 2s_k(T,u) \ln \left(\frac{s_k(T,u)}{s_k^0} \right) \right)}{(1-u_k)^3 s_k(T,u)}.$$

By combining with the lower-bound of $\frac{\partial s_k}{\partial u_k}$ given in Lemma 2, we derive that

$$\frac{\partial^2 i_k}{\partial u_k^2}(T,u) \geq \frac{\gamma_k b_{kk}^{\text{inv}} \ln \left(\frac{s_k(T,u)}{s_k^0} \right)}{(1-u_k)^3} G_k(u)$$

where

$$G_k(u) := \left(\frac{-\gamma_k}{\gamma_k - s_k(T,u)(1-u_k)\beta_{kk}} + 2 \right).$$

In view of the condition given in Theorem 5, it follows that

$$G_k(u_{\min}) \leq 0 \Rightarrow \frac{\partial^2 i_k}{\partial u_k^2}(T,u_{\min}) \geq 0.$$

Since $\frac{\partial i_k}{\partial u_k}$ is quasi-convex w.r.t. u_k, then $\forall T \in \mathcal{T}$ and $\forall u \in \mathcal{U}$,

$$\frac{\partial^2 i_k}{\partial u_k^2}(T,u) \geq 0.$$

Since, $\forall k \in \mathcal{K}$,

$$r_k(T,u) = \int_0^T \gamma_k i_k(t,u) \mathrm{dt},$$

it follows from the Leibniz's rule for differentiation under the integral sign that

$$\frac{\partial^2 r_k}{\partial u_k^2}(T,u) = \int_0^T \gamma_k \frac{\partial^2 i_k}{\partial u_k^2}(t,u) \mathrm{dt} \geq 0.$$

Hence, $\forall T \in \mathcal{T},\ \forall u \in \mathcal{U}$,

$$\frac{\partial^2 s_k}{\partial u_k^2}(T,u) \leq 0,$$

since $s_k = -i_k - r_k$.

To conclude this proof, $\forall k \in \mathcal{K}$, J_k is quasi-convex then by definition the game $\mathcal{G}$ is in the **WIR**.

2.6.4 Proof of Theorem 6

According to [88, Section 2.5-2.6], a sufficient condition to ensure the contraction of the Best-response mapping given by, $\mathrm{BR}(\cdot) = \left(\underset{u\in\mathcal{U}_1}{\operatorname{argmin}}\ J_1(u,\cdot), \ldots, \underset{u\in\mathcal{U}_K}{\operatorname{argmin}}\ J_K(u,\cdot)\right)$ is to verify the strict diagonal dominance condition, which yields that :

$$\left[\nabla^2 J\right]_{1\leq k,\ell\leq K} = \left[\frac{\partial^2 J_k}{\partial u_k \partial u_\ell}\right]_{1\leq k,\ell\leq K} > 0 \Rightarrow \nabla^2 J + \nabla^2 J^\top > 0.$$

Hence, according to [74, Theorem 2 and Theorem 6], the diagonally strictly convexity (DSC) condition is verified that ensures the uniqueness of the NE. Moreover, in view of [88, Section 2.5], the sequential best-response algorithm converges to the unique Nash equilibrium of the game $\mathcal{G}$.

2.6.5 Proof of Theorem 7

In order to establish the proof for the existence of a Generalized Nash Equilibrium (GNE) in the game $\widetilde{\mathcal{G}} = \left(\mathcal{K}, (\mathcal{U}_k)_{k\in\mathcal{K}}, (\mathcal{C}_k)_{k\in\mathcal{K}}, (J_k)_{k\in\mathcal{K}}\right)$, it is essential to recall the definitions of upper and lower semicontinuity of a set-valued map.

Definition 30. *Let us consider a set-valued map, denoted as $F : \mathcal{X} \to 2^{\mathcal{Y}}$.*

- *F is said to be upper semicontinuous at a point $x \in \mathcal{X}$ if, for any open set $\mathcal{V} \subseteq \mathcal{Y}$ containing $F(x)$, there exists an open neighborhood $\mathcal{W} \subset \mathcal{X}$ of x such that $F(x') \subseteq \mathcal{V}$ for all $x' \in \mathcal{W}$.*
- *F is said to be lower semicontinuous at a point $x \in \mathcal{X}$if, for any open set $\mathcal{V} \subseteq \mathcal{Y}$ containing $F(x)$, there exists an open neighborhood $\mathcal{W} \subset \mathcal{X}$ of x such that $F(x') \cap \mathcal{V} \neq \emptyset$ for all $x' \in \mathcal{W}$.*

According to [79, Theorem 3.1], the game $\widetilde{\mathcal{G}}$ has at least one GNE if the following conditions hold :

(i) For all $k \in \mathcal{K}$, $\mathcal{U}_k = [U_k^{\min}, U_k^{\max}]$ is nonempty, convex and compact subset of a Euclidean space.

(ii) For all $k \in \mathcal{K}$ and $u_{-k} \in \mathcal{U}_{-k}$, the set valued-map $\mathcal{C}_k(u_{-k}) = \{u_k \in \mathcal{U}_k : \forall t,\ \sigma_k i'_k(t,u) \leq \mathrm{i}_{\mathrm{cu,k}}\}$ is both u.s.c. and l.s.c. in u_{-k}.

(iii) For all $k \in \mathcal{K}$ and $u_{-k} \in \mathcal{U}_{-k}$, the set valued-map $\mathcal{C}_k(u_{-k})$ is nonempty, closed, convex.

(iv) For all $k \in \mathcal{K}$, J_k defined in (2.2) is continuous w.r.t. u and quasi-convex w.r.t. u_k on $\mathcal{C}_k(u_{-k})$.

The non-triviality of conditions (ii), (iii), and (iv) arises due to the complexity inherent in the expressions of $\mathcal{C}_k$ and J_k. However, based on the proof of Theorem 5 and the equation (2.9),

it can be inferred that conditions (iii) and (iv) hold true. This conclusion is supported by the convexity of J_k and i_k with respect to u_k, as demonstrated for all $k \in \mathcal{K}$. Moreover, as established in [79, Proposition 4.1] and [79, Proposition 4.2], condition (ii) is satisfied in view of the continuity of i_k w.r.t. u on the set $\mathcal{U}$, as well as the convexity of i_k w.r.t. u_k on the set $\mathcal{U}_k$.

Chapter 3

On the Efficiency of Decentralized Epidemic Management in the Presence of Opinion Dynamics

In this chapter, we propose a mathematical model to evaluate the effects of decentralization on epidemic management in terms of global efficiency when the epidemic dynamic is coupled with an opinion dynamic, the latter modelling variations due the social behavior changes or vaccination effects. We consider a relatively simple mathematical model that captures the main features of interest, consisting of a generalized strategic form game built from a networked Susceptible-Infected-Recovered (SIR) compartmental model [12, 13] coupled with a time varying opinion dynamics model [14, 15, 11, 16, 17, 18]. Each player represents a geographical area takes a decision that verify a coupling constraint which minimizes individual cost, by implementing a given trade-off between socio-economic losses, global/local losses in terms of the reproduction number of the virus [19, 20, 21, 22], awareness costs, and an average opinion cost. We note that the proposed game model is a generalized strategic form game played in one shot i.e., the sanitary control actions are fixed over a finite time horizon, and $N+1$ awareness campaigns are applied by each region to influence the beliefs of antagonistic individuals in the social network. The guaranteed existence and uniqueness of the Generalized Nash Equilibrium (GNE) are demonstrated by assuming a strongly connected epidemic graph and a posynomial cost structure in an auxiliary game. Additionally, an algorithm is presented that converges to the GNE, and it is proven that the centralized management problem can be converted into a convex optimization problem. These results allow us to assess through numerical results the loss (measured in terms of Price of Anarchy (PoA)) induced either by decentralization with or without taking into account the opinion dynamic.

The previous chapter addressed the decentralization of decision-making in epidemic control under the assumption of strict compliance to sanitary rules by the population. This chapter will delve into another key facet of epidemic propagation. Specifically, it explores the role of individual behavior within various regions, an aspect that was not considered in the earlier discussion. The Covid-19 outbreak offers a prime example of this behavior, as people independently adopted practices such as reducing social contact, staying home when feasible, applying stricter hygiene and social distancing measures, or wearing masks, irrespective of government-imposed regulations. These behaviors, often influenced by social trends or 'fads', have shown to affect the effectiveness of government actions. As demonstrated by previous studies [5, 6], these behavioral modifications can induce controllable changes in policy outcomes when mediated through social networks.

The goal of this chapter is to evaluate the efficiency of decentralized epidemic management in the presence of opinion dynamics. For this purpose, the game model considered in this chapter, is a one-shot game that is based from a networked SIR epidemic model (e.g., [36, 37, 38, 39, 40, 41]) coupled with a time-varying opinion dynamics model including behavioral drifts. Each player represents a geographical area which minimizes individual cost, by implementing a given trade-off between socio-economic losses, global/local losses in terms of the reproduction number of the virus [19, 20, 21, 22]. A complete analysis of the static and generalized strategic form game is conducted through the Generalized Nash equilibrium (GNE).

The chapter presents a detailed description of the model in Sec. 3.1, a complete analysis of the corresponding GNE in Sec. 3.2, and a numerical analysis of the game's effectiveness in a Covid-19-type scenario in Sec. 3.3.

3.1 Problem Statement

We consider a set of $K \geq 2$ interconnected regions (e.g., countries, "länder", metropolis, provinces, "régions", or states) that are affected by an epidemic ; the region index is denoted by $k \in \mathcal{K} := \{1, \ldots, K\}$. The time evolution of the epidemic of each region is governed by a dynamical model which is chosen to be as described in Sec. 3.1.1 ; more precisely, the epidemic propagation within a region is assumed to follow a SIR-type model. The corresponding dynamical equations are coupled since regions are interconnected and thus exchanges between regions in terms of infected people exist. Additionally, we assume : the existence of an opinion dynamics for each region ; that these dynamics are linear and not only coupled among themselves but also with the epidemic propagation dynamic. The epidemic management is assumed to be decentralized decision-wise, which means that each region chooses the way the epidemic is mitigated or controlled over its own geographical territory. To model the underlying decision process, we propose a static game model whose strategic form is provided in Sec. 3.1.2.

3.1.1 Dynamical System Model

The proposed epidemic propagation model is based on a SIR-model. For Region $k \in \mathcal{K}$, the fractions of susceptibles, infected, and recovered are respectively denoted by $s_k \in [0, 1]$, $i_k \in [0, 1]$, and $r_k \in [0, 1]$. Considering two regions $(k, \ell) \in \mathcal{K}^2$, we denote by : $\beta^0_{k\ell}$ the natural virus transmission rate from Region k to ℓ ; γ_k the removal/recovery rate within Region k ($\frac{1}{\gamma_k}$ is called the average recovery period) ; $\widehat{\beta}_{k\ell}$ the maximum amplitude of the perturbation induced by the presence of the opinion dynamics on the virus propagation dynamics. Before providing the assumed dynamical model, it is useful to notice that an hybrid dynamical system is considered namely, we both consider a time-continuous dynamics and a discrete-time dynamics. In terms of decisions, Region k applies a direct epidemic control policy over Region ℓ which is denoted by a scalar quantity $u_{k\ell} \in \mathcal{U}_{k\ell}$, $\mathcal{U}_{k\ell} := [u^{\min}_{k\ell}, u^{\max}_{k\ell}] \subseteq [0, \beta^0_{k\ell}]$ and assumed to be constant over a time interval $[0, T]$, $T > 0$. During the Covid-19 epidemics in 2020 control measures were typically constant over a period of a couple of weeks and updated from period to period ; for this example of epidemics, choosing $u_{k\ell} = u^{\max}_{k\ell}$ would correspond to very severe lockdown and social distancing measures. The set where the control action $u_k = (u_{k1}, \ldots, u_{kK})$ lies in is denoted by $\mathcal{U}_k = \prod_{\ell \in \mathcal{K}} \mathcal{U}_{k\ell}$. Over a given time interval, the quantities $s_k \in [0, 1]$, $i_k \in [0, 1]$, and $r_k \in [0, 1]$ evolve in continuous time and t will be used as the corresponding time variable. Within each interval, each region is also allowed to implement influence control campaigns at given discrete time instants denoted by $t_n \in [0, T]$, $n \in \{0, \ldots, N\}$, $N > 1$, $t_{n+1} > t_n$. The opinion of Region k is assumed to evolve in a discrete-time manner and the opinion at time t_n is denoted by $\theta_k(n) \in [0, 1]$. The natural influence in terms of opinion of Region ℓ

on Region k at time t_n is assumed to follow a linear model and is represented by a weight $p_{k\ell}(n) \in [0,1]$. This influence is also weighted by the influence control intensity performed by each region : the influence action control exerted by Region k on the influence from Region ℓ at instant t_n is denoted by $v_{k\ell}(n) \in \mathcal{V}_{k\ell}$, $\mathcal{V}_{k\ell} := [v_{k\ell}^{\min}, v_{k\ell}^{\max}] \subseteq [0,1]$. For example, choosing $v_{k\ell}(n) = v_{k\ell}^{\min}$ would mean that Region k tries to minimize as much as possible the influence of Region ℓ ; in practice this can be done by posting a large number of messages to counterbalance the influence of the other region or by simply applying information withholding. By denoting $v_k(n) = (v_{k1}(n), v_{k2}(n), \ldots, v_{kK}(n))$, the set where the control action $v_k = (v_k(0), \ldots, v_k(N))$ lies in is $\mathcal{V}_k^{N+1}$, where $\mathcal{V}_k = \prod_{\ell \in \mathcal{K}} \mathcal{V}_{k\ell}$. At last, we use the notations $\mathcal{N}_k$ and $\widehat{\mathcal{N}}_k(n)$ to respectively refer to the sets of neighbors of Region k for the epidemic propagation and the influence propagation. For the influence propagation, the set of neighbors is allowed to vary over time. To establish some analytical results, some additional assumptions on the epidemic propagation and influence propagation graph will be added ; these assumptions are provided throughout the chapter. Equipped with all these notations introduced so far, the hybrid dynamics for the epidemic in Region k in presence of interconnections and opinion dynamics, can be written as follows : $\forall (k,\ell),\ \forall n,\ \forall t \in [t_n, t_{n+1}),\ \forall (u_{k\ell}, v_{k\ell}(n)) \in \mathcal{U}_{k\ell} \times \mathcal{V}_{k\ell}$,

$$\begin{cases} \dfrac{\mathrm{d}s_k}{\mathrm{dt}} = -s_k(t) \displaystyle\sum_{\ell \in \mathcal{N}_k} \left[\beta_{k\ell}^0 - u_{k\ell} + \theta_k(n)\widehat{\beta}_{k\ell}\right] i_\ell(t), \\ \dfrac{\mathrm{d}i_k}{\mathrm{dt}} = -\dfrac{\mathrm{d}s_k}{\mathrm{d}t} - \gamma_k i_k(t), \\ \dfrac{\mathrm{d}r_k}{\mathrm{dt}} = \gamma_k i_k(t), \\ \theta_k(n+1) = \displaystyle\sum_{\ell \in \widehat{\mathcal{N}}_k(n)} v_{k\ell}(n) p_{k\ell}(n) \theta_\ell(n) \end{cases} \tag{3.1}$$

We now introduce some useful vector and matrix notations. For the vector notations : $s = (s_1, \ldots, s_K)^\top$; $i = (i_1, \ldots, i_K)^\top$; $r = (r_1, \ldots, r_K)^\top$; $\theta = (\theta_1, \ldots, \theta_K)^\top$; $u_k = (u_{k1}, \ldots, u_{kK})$; $u = (u_1, \ldots, u_K)$; $u_{-k} := (u_1, \ldots, u_{k-1}, u_{k+1}, \ldots, u_K)$; $v_{-k} := (v_1, \ldots, v_{k-1}, v_{k+1}, \ldots, v_K)$; $v = (v_1, \ldots, v_K)$; $\gamma := (\gamma_1, \ldots, \gamma_K)$. For the matrix notations : $\boldsymbol{B}^0 = [\beta_{k\ell}^0]_{1 \le k,\ell \le K}$; $\widehat{\boldsymbol{B}} = \left[\widehat{\beta}_{k\ell}\right]_{1 \le k,\ell \le K}$; $\boldsymbol{D}_\gamma = \mathrm{Diag}(\gamma)$; $\boldsymbol{P}(n) = [p_{k\ell}(n)]_{1 \le k,\ell \le K}$; the epidemic control action matrix $\boldsymbol{U}$ is defined by the entries $U_{k\ell} = \begin{cases} u_{k\ell} \text{ if } \ell \in \mathcal{N}_k \\ 0 \text{ otherwise} \end{cases}$;

the influence control action matrix at time t_n is defined by the entries $V_{k\ell}(n) = \begin{cases} v_{k\ell}(n) \text{ if } \ell \in \widehat{\mathcal{N}}_k(n) \\ 0 \text{ otherwise} \end{cases}$.

With these notations, the system dynamics rewrites in the following compact form : $\forall t \in$

$[t_n, t_{n+1}),\ n \in \{0, \dots, N\}$,

$$\begin{cases} \dfrac{\mathrm{d}s}{\mathrm{d}t} = -\mathrm{Diag}(s(t)) \left[\boldsymbol{B^0} - \boldsymbol{U} + \mathrm{Diag}(\theta(n)) \widehat{\boldsymbol{B}} \right] i(t) \\ \dfrac{\mathrm{d}i}{\mathrm{d}t} = -\dfrac{\mathrm{d}s}{\mathrm{d}t} - \boldsymbol{D}_\gamma i(t) \\ \dfrac{\mathrm{d}r}{\mathrm{d}t} = \boldsymbol{D}_\gamma i(t), \\ \theta(n+1) = [\boldsymbol{V}(n) \odot \boldsymbol{P}(n)]\, \theta(n). \end{cases} \tag{3.2}$$

To conclude the presentation of the considered dynamical model, several mild conditions are assumed to be met.

Assumption 2. *Condition (i) :* $\forall k, \ell,\ \beta^0_{k\ell} = 0 \iff \widehat{\beta}_{k\ell} = 0$.
Condition (ii) $\forall n \in \{0, \dots, N\}$, $\boldsymbol{P}(n)$ *is a row-stochastic matrix.*
Condition (iii) : $\forall n \in \{0, \dots, N+1\}$, *the matrix* $\boldsymbol{D}_\gamma^{-1}[\boldsymbol{B}^0 - \boldsymbol{U} + \mathrm{Diag}(\theta(n))\widehat{\boldsymbol{B}}]$ *is non-negative and irreducible.* □

Condition (i) means that if the virus is not physically transmitted between two regions, it is also not transmitted through a change in behavior between the two regions and vice-versa. Condition (ii) imposes that $\forall n, k\ \sum_{\ell \in \widehat{\mathcal{N}}_k(n)} p_{k\ell}(n) = 1$, which is a very classical assumption in the literature of opinion dynamics. Condition (iii) is verified when the controlled epidemic graph is strongly connected. This condition is very reasonable since $\forall k \neq \ell,\ \beta^0_{k\ell} - u_{k\ell} = 0$ means there is no physical interactions from Region k to Region ℓ.

3.1.2 Generalized Strategic Form Game Model

The first equation of (3.1) shows that the fraction of susceptibles in Region k depends on the fraction of infected in the neighboring regions. Therefore the control actions of the neighbors of Region k impact what happens in Region k and thus its decision. This decision interdependency situation is referred to as a game. The most simple mathematical model for a game is given by the strategic form game model (see e.g., cite [63]). A strategic form game comprises three components : the set of players, the sets of strategies, and the players' cost functions. When one wants to study a situation where each player has a range of actions that depends on the actions of other players, one needs to add one more component, the set of coupled constraints. This model with four components is called the generalized strategic form (see e.g., [89, 79]). Here, we first describe the three conventional components and then, after describing the assumed cost functions, we describe the set of coupled constraints. The set of players here is the set of regions $\mathcal{K} = \{1, \dots, K\}$. In the assumed setting, the sets of strategies coincide with the set of actions ; the action of Region k is given by the vector (u_k, v_k) that is, the set of actions is $\mathcal{U}_k \times \mathcal{V}_k$. The cost function of a player is chosen to be a tradeoff between a cost associated with the control

actions, the local virus reproduction number, the global virus reproduction number, and a loss term due to the perturbation induced by the opinion. First, we provide the expression of these cost functions and then we provide some explanations about its construction. The cost function for Region k is chosen to be :

$$\begin{aligned} J_k(u,v) := \quad & -a_k \sum_{\ell \in \mathcal{N}_k} \log\left(1 - \frac{u_{k\ell}}{\beta^0_{k\ell}}\right) \\ & + b_k^{\text{local}} \sum_{n=0}^{N+1} \sum_{\ell \in \mathcal{N}_k} \frac{\beta^0_{k\ell} - u_{k\ell} + \theta_k(n)\widehat{\beta}_{k\ell}}{\gamma_k} \\ & + b_k^{\text{global}} \sum_{n=0}^{N+1} \rho\left(\boldsymbol{D}_\gamma^{-1}\left(\boldsymbol{B^0} - \boldsymbol{U} + \text{Diag}(\theta(n))\widehat{\boldsymbol{B}}\right)\right) \\ & - c_k \sum_{n=0}^{N} \sum_{\ell \in \widehat{\mathcal{N}}_k(n)} \log(v_{k\ell}(n)) + d_k \sum_{n=0}^{N+1} \theta_k(n), \end{aligned} \tag{3.3}$$

where $(a_k, b_k^{\text{local}}, b_k^{\text{global}}, c_k, d_k) \in \mathbb{R}^5_{\geq 0}$ are non-negative parameters and $\rho(\boldsymbol{M})$ stands for the spectral radius (i.e., the largest eigenvalue) of the matrix $\boldsymbol{M}$. Additionally, motivated by practical considerations such as those encountered with the management of Covid-19 epidemics, we assume the existence of a set constraints which includes a coupled constraint (in the sense of Rosen [74]) on the game. The game action profile (u, v) has to meet the following constraints : $(u,v) \in \mathcal{C} := \prod_{k=1}^{K} \mathcal{C}_k(u_{-k}, v_{-k})$ where

$$\mathcal{C}_k(u_{-k}, v_{-k}) := \Big\{ (u_k, v_k) \in \mathcal{U}_k \times \mathcal{V}_k : \ \forall n \in \{0, \dots, N\},\ m \in \{0, \dots, N+1\}$$

$$\begin{aligned} & \sum_{\ell \in \mathcal{N}_k} \frac{u_{k\ell}}{\beta^0_{k\ell}} \leq \phi_k, \ \sum_{\ell \in \widehat{\mathcal{N}}_k(n)} \frac{1}{v_{k\ell}(n)} \geq \widehat{\phi}_k(n), \\ & \sum_{\ell \in \mathcal{N}_k} \frac{\beta^0_{k\ell} - u_{k\ell} + \widehat{\beta}_{k\ell}\theta_k(m)}{\gamma_k} \leq \mathrm{R}_k^{\max},\ \theta_k(m) \leq \theta_k^{\max} \Big\}. \end{aligned} \tag{3.4}$$

At this point, some comments on the construction of the cost functions and the additional set of constraints are in order.

Remark 1. First, let us comment on the choice of the costs associated with the control action (namely, the first and fourth terms of J_k). A common choice is to assume a monotonic linear or quadratic costs (see e.g., [81, Section 2.2.2][40]). Here we assume a logarithmic cost. This choice not only allows one to still have a smooth, monotonic, and convex cost but also offers some posynomiality property, which makes possible the non-trivial analysis of the GNE of the game. Interestingly, for some typical ranges for the control actions as those used for the Covid-

19 case, the approximation of the log function by a linear function is very reasonable. For instance, when $u_{k\ell} \leq 0.53\beta^0_{k\ell}$ (or $v_{k\ell}(n) \geq 0.53$) the relative difference between $-\log(\frac{\beta^0_{k\ell}-u_{k\ell}}{\beta^0_{k\ell}})$ and $\frac{u_{k\ell}}{\beta^0_{k\ell}}$ (or $-\log(v_{k\ell}(n))$ and $-v_{k\ell}(n)$) is less than 30%. In other words, by restricting the action space of each player, one can assume that considering the logarithmic form to penalize the control action is equivalent to considering a linear structure.

Remark 2. The second and third terms of the J_k can respectively be interpreted as a local reproduction number (see [22]) and a global reproduction number (see [20]). In particular, it can be checked that if the global reproduction number $\rho\left(\boldsymbol{D}_\gamma^{-1}\left(\boldsymbol{B^0}-\boldsymbol{U}+\mathrm{Diag}(\theta(n))\widehat{\boldsymbol{B}}\right)\right)$ is strictly less than 1, the epidemic dies out in all the regions. Depending on the values for the parameters b_k^{local} and b_k^{global}, a region will assign more (or less) importance to the local or the global situation of the epidemics.

Remark 3. We have added two budget constraints on the control actions u_k and v_k. Notice that these individual constraints could have been directly integrated into the definition of the action sets for the players. But, the structure of the budget constraint on v_k is easier to be understood after knowing about the cost function structure. Indeed, the constraint $\sum_{\ell\in\widehat{\mathcal{N}}_k(n)}\frac{1}{v_{k\ell}(n)} \geq \widehat{\phi}_k(n)$ can be rewritten, with a change of variable, as $-\sum_{\ell\in\widehat{\mathcal{N}}_k(n)}\log(v_{k\ell}(n)) \leq \widehat{\psi}_k(n)$. At last, note that the constraints on the local reproduction numbers and those on $\theta_k(m)$ are coupled constraints because of the presence of $\theta_k(m)$, which leads us to consider the GNE as a suitable solution concept for the considered game. Finally, the generalized strategic form of the game when integrating all the constraints writes as :

$$\mathcal{G} := \left(\mathcal{K}, \left(\mathcal{U}_k \times \mathcal{V}_k\right)_{1\leq k\leq K}, \left(\mathcal{C}_k\right)_{1\leq k\leq K}, \left(J_k\right)_{1\leq k\leq K}\right). \tag{3.5}$$

3.2 Generalized Nash Equilibrium Analysis

A GNE for the generalized strategic form game $\mathcal{G}$ is defined as follows.

Definition 31. *A GNE for the game $\mathcal{G}$ is a point $(u^\star, v^\star)$ such that $\forall k \in \mathcal{K}$,*

$$(u_k^\star, v_k^\star) \in \underset{(u_k,v_k)\in\mathcal{C}_k(u^\star_{-k},v^\star_{-k})}{\mathrm{argmin}} J_k(u_k, v_k, u^\star_{-k}, v^\star_{-k}). \tag{3.6}$$

A fundamental issue for the equilibrium analysis is the existence issue. There are useful existence theorems for strategic form games whose cost functions are individually convex or quasi-convex (see e.g., [63]). Such geometrical properties are not available here, which makes the existence analysis non-trivial and not a special case of existing general theorems. Remarkably, it turns out to be possible to construct an auxiliary game whose existence property gua-

rantees, by equivalence, the existence of an equilibrium in $\mathcal{G}$. The auxiliary game even allows the uniqueness issue to be treated and to build an algorithm to determine the unique NE of $\mathcal{G}$. In addition to conducting the equilibrium analysis in this section (existence, uniqueness, determination), we also provide the equilibrium efficiency measures retained for the numerical analysis section. To facilitate the reading and make the results easy to exploit, the choice made by the authors is to state here only the derived results and to provide all the technical aspects and details in the Appendix section (Appendix-A).

3.2.1 Existence and Uniqueness Analysis

To prove the existence and uniqueness of a GNE in $\mathcal{G}$, first, it is assumed that the less trivial term of J_k is always present that is, $\forall k,\ b_k^{\text{global}} > 0$. Second, we introduce an auxiliary game $\widetilde{\mathcal{G}}$ which is obtained from $\mathcal{G}$ by performing appropriate changes of variables. The rationale for making these changes of variables is to exploit the posynomiality property of the opinion state $\theta_m(n)$ w.r.t. the influence control action v_k (see Appendix-A). These changes of variables are as follows : $\forall n \in \{0, \ldots, N\}$ and $\forall (k, \ell_n, \ldots, \ell_0) \in \mathcal{K}^{n+2}$, $\omega_{k\ell_n \ldots \ell_0}(n) = v_{k\ell_n}(n) \times v_{\ell_n \ell_{n-1}}(n-1) \times \ldots \times v_{\ell_1 \ell_0}(0)$; $\xi_{\omega_{k\ell_n \ldots \ell_0}}(n) = \log\left(\omega_{k\ell_n \ldots \ell_0}(n)\right)$; $\xi_{y_{k\ell}} = \log\left(\beta_{k\ell}^0 - u_{k\ell}\right)$. The auxiliary game $\widetilde{\mathcal{G}}$ has the following form :

$$\widetilde{\mathcal{G}} = \left(\mathcal{K} \cup \{K+1\}, \left(\mathbf{\Pi}_k \widetilde{\mathcal{C}}\right)_{1 \leq k \leq K+1}, \left(\widetilde{J}_k\right)_{1 \leq k \leq K+1}\right) \tag{3.7}$$

where $\mathcal{K} \cup \{K+1\}$ represents the set of auxiliary players ; $\widetilde{J}_k$ corresponds to the auxiliary individual cost functions given in (3.15) ; $\mathbf{\Pi}_k \widetilde{\mathcal{C}}$ is the projection of the coupled constraint set $\widetilde{C}$ on the action vector of the k^{th}-player in (3.16). Exploiting the introduced auxiliary game, we have the following result.

Proposition 2. *The game $\mathcal{G}$ possesses a unique* GNE*; which is denoted by* $(u^\star, v^\star)$. □

Proof. The proof is provided in Appendix-B. Therein, it is proved that a GNE in $\mathcal{G}$ becomes, by change of variables, a GNE of $\widetilde{\mathcal{G}}$ and conversely. One then proves that there exists a unique GNE in $\widetilde{\mathcal{G}}$.

3.2.2 Efficiency Measures

One of the main objectives of this chapter is to assess the potential inefficiencies that might be induced by decentralizing the management or control of an epidemic. A famous and well-used measure of global efficiency is given by the Price of Anarchy (PoA) of a game [78]. For the sake of clarity, let us introduce the sum-cost function $J = \sum_{k=1}^{K} J_k$. To refine our efficiency analysis, we not only consider the original version of the PoA (which is denoted by PoA_{uv}) but

also two useful variants of it :

$$\mathrm{PoA}_{uv} = \frac{J(u^\star, v^\star)}{\min\limits_{(u,v)\in\mathcal{C}} J(u,v)} \tag{3.8}$$

in which both u and v are controlled partially by the players and the uniqueness result is exploited;

$$\mathrm{PoA}_{u} = \frac{J(u^\star(1_{K^2(N+1)}), 1_{K^2(N+1)})}{\min\limits_{(u,v)\in\mathcal{C}} J(u,v)} \tag{3.9}$$

where v is set to the vector of ones $1_{K^2(N+1)}$, which means that no influence/opinion control is allowed;

$$\mathrm{PoA}_{v} = \frac{J(0_{K^2}, v^\star(0_{K^2}))}{\min\limits_{(u,v)\in\mathcal{C}} J(u,v)}. \tag{3.10}$$

where u is set to the vector of zeros 0_{K^2}, which means that no epidemic control is allowed.

Computing the above quantities relies on being able to globally minimize the sum-cost J. It is known that the sum-cost minimization problem is generically hard. For the game under consideration, it is possible to exploit the auxiliary game to dramatically decrease the computational complexity associated with the global minimization of J. This is what is stated through the next proposition.

Proposition 3. *The global minimum of the sum-cost function J can be found by solving a convex optimization problem.* □

Proof. See Appendix-C. ■

In the next subsection, we tackle the computation problem of the GNE of $\mathcal{G}$.

3.2.3 GNE Determination Algorithm

In Sec. 3.2.1, we have shown that the game $\mathcal{G}$ has a unique GNE. Here, we propose an algorithm to find this unique equilibrium point. To compute the GNE of $\mathcal{G}$ we again resort to the auxiliary game $\widetilde{\mathcal{G}}$ for which the GNE is much easier to compute. Indeed, one of the key ingredients of the algorithm is to use a gradient-type updating rule for minimizing $\widetilde{J}_k$, which is relevant since the auxiliary game is convex in the sense of Rosen [74]. The function $\widetilde{J}_k$ is not only individually convex (i.e., w.r.t. (u_k, v_k)) but also jointly convex (i.e., w.r.t. (u, v)), which is exploited to exhibit a Lyapunov function for the convergence analysis of the proposed algorithm. Using the notations introduced in Appendix-A, we denote by $\xi = (\xi_1, \ldots, \xi_K, \xi_{K+1})$ such that $\forall k \in \mathcal{K}$, $\xi_k = (\xi_{y_k}, \xi_{\omega_k})$, where : $\xi_{y_k} = (\xi_{y_{k1}}, \ldots, \xi_{y_{kK}})$ such that $\xi_{y_{k\ell}} \in \mathbb{R}$; $\xi_{\omega_k} := (\xi_{\omega_k}(0), \ldots, \xi_{\omega_k}(N))$ where $\forall n \in \{0, \ldots, N\}, \xi_{\omega_k}(n) := (\xi_{\omega_{k1,\ldots,1}}(n), \xi_{\omega_{k1,\ldots 2}}(n), \ldots, \xi_{\omega_{kK\ldots K}}(n))$

such that $\forall(\ell_n, \ldots, \ell_0) \in \mathcal{K}^{(n+1)}$, $\xi_{\omega_{k\ell_n\ell_{n-1}\cdots\ell_0}}(n) \in \mathbb{R}$. For $k = K+1$ we denote by $\xi_{K+1} = (\xi_\lambda, \xi_x)$ where : $\xi_\lambda = (\xi_\lambda(0), \ldots, \xi_\lambda(N+1))$ such that $\forall n,\ \xi_\lambda(n) \in \mathbb{R}$ and $\xi_x = (\xi_x(0), \ldots, \xi_x(N+1))$ such that $\forall \ell \in \mathcal{K}$ and $\forall n$, the ℓ^{th}-component of $\xi_x(n)$ is given by $\xi_{x_\ell}(n) \in \mathbb{R}$.

Since the proposed algorithm is an iterative procedure, a natural question is whether the algorithm converges and to which convergence point. The following proposition provides the corresponding result.

Proposition 4. *The Generalized Nash equilibrium seeking algorithm given in Tab. 1 converges to the* GNE *of* $\mathcal{G}$. □

Proof. See Appendix-D. ■

Algorithm 1 Generalized Nash equilibrium seeking algorithm for $\mathcal{G}$

Initialization : $t = 0$,
$\forall (k,\ell) \in \mathcal{K}^2, \forall n \in \{0,\dots,N\}, \forall (\ell_n,\dots,\ell_0) \in \mathcal{K}^{n+1}$,
$\xi^{(0)}_{y_{k\ell}} \in \mathcal{Y}_{k\ell}$, $\xi^{(0)}_{\omega_{k\ell_n\ell_{n-1}\dots\ell_0}}(n) \in \mathcal{W}_{k\ell_n\ell_{n-1}\dots\ell_0}(n)$
$\xi^{(0)}_{\lambda}(n) \in \mathbf{\Lambda}$, $\xi^{(0)}_{x}(n) \in \mathcal{X}$.
Let $\overline{\delta} = (\overline{\delta}_1,\dots,\overline{\delta}_K,\overline{\delta}_{K+1}) > 0$.

Process : $\forall k \in \mathcal{K} \cup \{K+1\}$,

$$\frac{\mathrm{d}\xi_k}{\mathrm{d}t} = -\overline{\delta}_k \nabla_{\xi_k} \widetilde{J}_k + \sum_{j \in \{1 \le i \le M:\ \widetilde{h}_i(\xi) > 0\}} \overline{\mu}_j \nabla_{\xi_k} \widetilde{h}_j(\xi),$$

where :
$\forall k \in \mathcal{K} \cup \{K+1\}$, $\widetilde{J}_k$ is given in (3.15) ;
$\widetilde{h}$ is given in (3.16), $M = \dim(\widetilde{h})$ and $\widetilde{M} = \dim(\xi)$
$\forall j \in \{1,\dots,M\}$, $\widetilde{h}_j$ is the j^{th}-component of $\widetilde{h}$;
$\overline{\mu}_j$ is the j^{th}-nonzeros element of $\overline{\mu} \in \mathbb{R}^{\overline{M}}_{\le 0}$ where $\overline{M} \le M$
and $\overline{\mu}(\xi) = \left[\overline{\boldsymbol{H}}(\xi)^\top \overline{\boldsymbol{H}}(\xi)\right]^{-1} \overline{\boldsymbol{H}}(\xi)^\top g(\xi,\overline{\delta}) \le 0$
where the matrix $\overline{\boldsymbol{H}}(\xi) \in \mathbb{R}^{\widetilde{M}\times\overline{M}}$ is composed by
$\overline{M} \le M$ linearly independent columns of
$\boldsymbol{H}(\xi) = [\nabla_\xi \widetilde{h}_1(\xi), \nabla_\xi \widetilde{h}_2(\xi), \dots, \nabla_\xi \widetilde{h}_M(\xi)]$
selected from $\nabla_\xi \widetilde{h}_j(\xi)$
for $j \in \{i \in \{1,\dots,M\} :\ \widetilde{h}_i(\xi) > 0\}$.

Output : $\forall (k,\ell) \in \mathcal{K}^2$ and $\forall n \in \{0,\dots,N\}$,

$$u^\star_{k\ell} = \beta^0_{k\ell} - \lim_{t\to+\infty} \exp(\xi^{(t)}_{y_{k\ell}})$$

$$v^\star_{k\ell}(n) = \lim_{t\to+\infty} \Big[\exp(\xi^{(t)}_{\omega_{k\ell k\dots k}}(n)) - \exp(\xi^{(t)}_{\omega_{\ell k\dots k}}(n-1)) \Big].$$

3.3 Numerical Performance Analysis

The goal of this section is to assess numerically the efficiency measures introduced in Section 3.2.2. The numerical analysis is conducted for Covid-19-type scenarios but **the proposed methodology may be applied to other types of epidemics including viral marketing-type ones.** To choose the parameters of the epidemic model, we have in part exploited the studies on Covid-19 that have been conducted in [5, 82, 83]. We assume a territory that is divided into $K = 10$ geographical regions; the time horizon of the considered epidemic phase is set to $T = 40$ days and regions apply 3 awareness/influence campaigns at $t_1 = 10$ days, $t_2 = 20$ days, $t_3 = 30$ days. For simplicity we assume that $\forall k \in \mathcal{K}$ and $n \in \{1, 2, 3\}$, $\theta_k^{\max} = \mu_k = \widehat{\nu}_k(n) = \mathrm{R}_k^{\max} = +\infty$. For the epidemic model parameters, it is assumed that : $\forall k \in \mathcal{K}$, $\gamma_k = 0.2$. When the degree per agent in the social network equals 0, we take $\forall n,\ \boldsymbol{P}(n) = \boldsymbol{I}_K$; in the other cases $\forall n$,

$$p_{k\ell}(n) = \begin{cases} 1/\text{Degree} & \text{if } k \text{ and } \ell \text{ are connected} \\ & \text{in the social network,} \\ 0 & \text{otherwise.} \end{cases}$$

The perturbation matrix $\widehat{\boldsymbol{B}}$ is given by $\widehat{\boldsymbol{B}} = 0.5\boldsymbol{B}^0$ where $\boldsymbol{B}^0 = \boldsymbol{B} \odot \widetilde{\boldsymbol{A}}$ and

$$\boldsymbol{B} = \begin{pmatrix} 0.37 & 0.03 & 0.06 & 0.01 & 0.02 & 0.02 & 0.01 & 0.08 & 0.01 & 0.08 \\ 0.05 & 1.00 & 0.08 & 0.22 & 0.15 & 0.25 & 0.27 & 0.19 & 0.05 & 0.26 \\ 0.07 & 0.14 & 1.00 & 0.13 & 0.14 & 0.08 & 0.05 & 0.04 & 0.15 & 0.07 \\ 0.22 & 0.21 & 0.01 & 0.88 & 0.05 & 0.23 & 0.14 & 0.01 & 0.16 & 0.21 \\ 0.01 & 0.11 & 0.20 & 0.09 & 0.72 & 0.18 & 0.10 & 0.18 & 0.15 & 0.11 \\ 0.21 & 0.17 & 0.06 & 0.08 & 0.06 & 0.90 & 0.19 & 0.23 & 0.17 & 0.16 \\ 0.02 & 0.06 & 0.05 & 0.07 & 0.07 & 0.07 & 0.24 & 0.08 & 0.02 & 0.03 \\ 0.15 & 0.10 & 0.22 & 0.26 & 0.01 & 0.13 & 0.03 & 1.00 & 0.15 & 0.13 \\ 0.04 & 0.01 & 0.01 & 0.04 & 0.01 & 0.01 & 0.01 & 0.05 & 0.21 & 0.01 \\ 0.06 & 0.03 & 0.05 & 0.05 & 0.01 & 0.07 & 0.03 & 0.06 & 0.06 & 0.29 \end{pmatrix},$$

where $\boldsymbol{B}$ is diagonal dominant.

$$\text{and } [\widetilde{\boldsymbol{A}}]_{k\ell} = \begin{cases} 1 & \text{if } k \text{ and } \ell \text{ are connected} \\ & \text{in the epidemic graph,} \\ 10^{-10} & \text{otherwise.} \end{cases}$$

The initial state is given by

$$\theta(0)=(0.59, 0.25, 0.25, 0.46, 0.26, 0.68, 0.16, 0.24, 0.71, 0.6),$$
$$i(0)= 10^{-2} \cdot (0.2, 0.1, 2, 0.1, 3, 0.5, 2.5, 1, 2, 0.1),$$
$$s(0)= 1 - i(0).$$

Influence of the epidemic and influence graphs on the PoA.

PoA_{uv}		Influence graph			
Epidemic graph	Degree	0	2	6	10
	0	1.34	1.38	1.30	1.23
	2	1.46	1.60	1.67	1.66
	6	1.67	1.76	1.83	1.81
	10	1.78	1.85	1.92	1.91

TABLE 3.1 – The table illustrates the relationship between the Price of Anarchy ($\mathrm{PoA}_{\mathrm{uv}}$) and the degrees of the epidemic and influence graphs. The PoA becomes larger as the epidemic graph becomes more connected. On the other hand, the degree of the influence graph is seen not to have a significant impact.

In Tab. 3.1 we set $\forall k\ b_k^{\mathrm{local}} = d_k = 0$ and $a_k = c_k = 1$, $b_k^{\mathrm{global}} = 10$. Tab. 3.1 represents the PoA ($\mathrm{PoA}_{\mathrm{uv}}$) for different values for the degrees of the two graphs. The PoA is averaged over a total of 1600 realizations of the epidemic and social graphs. The simulation results show that the largest value for PoA_{uv} is 1.92 and is achieved when all regions are interconnected both for the epidemic graph and influence graph. The smallest value for PoA_{uv} value is 1.23 and is obtained when there is no interconnection in the epidemic graph and when the influence graph is fully connected. The study also reveals that there is no correlation between the average degree per agent in the influence graph and $\mathrm{PoA}_{\mathrm{uv}}$. However, an increase in the degree per agent in the epidemic graph results in an increase in $\mathrm{PoA}_{\mathrm{uv}}$. Notably, even when the epidemic graph and social network are not interconnected, the $\mathrm{PoA}_{\mathrm{uv}}$ value is still greater than one, indicating the presence of efficiency loss. The study highlights the importance of considering both the epidemic graph and the influence graph for designing decentralized decision-making processes for managing epidemics.

Influence of the cost function and control actions on the PoA. The cost function J_k comprises a collective term (namely, the term weighted by b_k^{global}) which is common to all the players whereas all the other terms are individual terms. To study the impact of the collective and individual terms on the PoA, we introduce the parameter $\alpha \in [0, 1]$ which is used for Fig.3.1 and Fig.3.2 and is defined as follows : $a_k = 1 - \alpha,\ b_k^{\mathrm{local}} = 0,\ b_k^{\mathrm{global}} = 10 \times \alpha,\ c_k = 1 - \alpha$

and $d_k = 0$ for all $k \in \mathcal{K}$. Additionally, for Fig.3.1 to Fig.3.4, we will assume $\boldsymbol{B}^0 = \boldsymbol{B}$ and $\forall n,\ [\boldsymbol{P}(n)]_{k\ell} = 1/10$. Fig. 3.1 represents the different efficiency measures ($\mathrm{PoA}_{\mathrm{uv}}$ in (3.8), $\mathrm{PoA}_{\mathrm{u}}$ in (3.9) and $\mathrm{PoA}_{\mathrm{v}}$ in (3.10)) against α. When $\alpha = 1$, the game becomes a team game and the GNE coincides with a local minimum point of the common cost function $J_k = b_k^{\mathrm{global}} \sum_{n=0}^{N+1} \rho\left(\boldsymbol{D}_\gamma^{-1}\left(\boldsymbol{B^0} - \boldsymbol{U} + \mathrm{Diag}(\theta(n))\widehat{\boldsymbol{B}}\right)\right)$; the fact that $\mathrm{PoA}_{\mathrm{uv}} = 1$ indicates the local minimum coincides with the global minimum and decentralization induces zero optimality loss. When the opinion is not controlled, this result is no longer true since the PoA is as large as almost 4, which is very significant. If the epidemic is not controlled and only the influence is controlled, the PoA reaches values as large as 11. Now, when both epidemic and influence are controlled, the largest value for the PoA is $\mathrm{PoA}_{\mathrm{uv}} \sim 2$, which is reached when $\alpha = 0.5$; this corresponding efficiency loss is still significant.

Fig. 3.2 depicts the average global reproduction number (Fig. 3.2.a) and total control cost (Fig. 3.2.b) against α for four distinct control strategies : the GNE strategy defined in (3.8)); the GNE strategy with no influence control (the strategy profile $(u^\star(1_{K^2(N+1)}), 1_{K^2(N+1)})$ defined in (3.9)); the GNE strategy with no epidemic control (the strategy profile $(0_{K^2}, v^\star(0_{K^2}))$ defined in (3.10)); and the optimal centralized strategy (the strategy profile that minimizes $\underset{(u,v)\in\mathcal{C}}{\mathrm{argmin}}\ J(u,v)$). The figure provides several insights. For example, one sees the impact on the global reproduction number of the fact that regions care about their individual socio-economic cost. For example, for $\alpha \sim 0.8$, a centralized solution would yield a value of less than 1 for the reproduction number whereas it reaches 2 for a decentralized management. If the opinion cannot be controlled, then this value becomes about 3.7, showing the importance of opinion influence. Now, when the epidemic cannot be directly controlled (namely, through u), the impact of the opinion influence becomes negligible and the reproduction number reaches values as large as 9.3 to 11.4. Fig. 3.2.b illustrates well the effect of decentralization and control actions on the total control cost.

Analysis of the control actions. For the preceding simulation results, the focus has been on the effect of decentralization and control actions on the global epidemic management efficiency. Here, we want to have more insights into the equilibrium control actions themselves both in space (over the regions) and time. For this, we define the aggregate GNE control action in $\%$ as follows : $\overline{u}_k^\star = \frac{100}{K} \times \sum_{\ell=1}^K \frac{u_{k\ell}^\star}{\beta_{k\ell}^0}$; $\overline{v}_k^\star(t_1) = \frac{100}{K} \times \sum_{\ell=1}^K (1 - v_{k\ell}(t_1))$. In Fig. 3.3 to Fig. 3.4, we set $a_k = 0.1$, $b_k^{\mathrm{local}} = 0$, $b_k^{\mathrm{global}} = 9$, $c_k = 0.1$, and $d_k = 0$ for all $k \in \mathcal{K}$. Fig. 3.4 depicts the value of the epidemic and opinion aggregate control actions for the 10 regions. These values have to be put in correlation with the parameters of the epidemics and, in particular, with the natural reproduction numbers namely, the elements of the diagonal of the $\boldsymbol{B}$ matrix : $(0.37, 1, 1, 0.88, 0.72, 0.9, 0.24, 1, 0.21, 0.29)$). The intuition that regions having a higher natural

reproduction number should undergo more severe measures is confirmed. But the proposed methodology says more than that since it has also the advantage of quantifying this relationship and thus providing the severity level each region should apply. Now, we look at the time aspect. In Fig. 3.3, we represent the evolution of the fractions of infected and the opinions of the regions. For the sake of clarity we represent the proportion of infected in each region by a blue shape rather than plotting 10 curves. The direct epidemic control actions and the influence control actions are fixed at the GNE strategy for the whole time period (40 days) by

$$\boldsymbol{U}^\star = 10^{-2} \times \begin{pmatrix} 36.3 & 2.8 & 5.6 & 0.5 & 2 & 2 & 0 & 8 & 0.5 & 7.5 \\ 4 & 99.4 & 7.4 & 21.4 & 15 & 25 & 26.2 & 18.8 & 4.4 & 24.9 \\ 6.6 & 14 & 99.4 & 13.3 & 13.7 & 8 & 4.5 & 4 & 13.6 & 6.3 \\ 21 & 20.8 & 0.9 & 88 & 5 & 22.7 & 13.3 & 0.1 & 15 & 20.6 \\ 0 & 11.0 & 19.7 & 8.6 & 72 & 17.8 & 9.2 & 17.8 & 13.7 & 9.5 \\ 20 & 16.7 & 5.5 & 8 & 6 & 90 & 18.4 & 22.7 & 16.0 & 16 \\ 1.1 & 6.4 & 4.7 & 6.6 & 6.5 & 6.7 & 23.6 & 0.2 & 1.2 & 2.4 \\ 14 & 9.8 & 22 & 25.7 & 0.5 & 13 & 2.7 & 99.4 & 14.4 & 12.8 \\ 3.8 & 0.9 & 0.5 & 4.5 & 1.4 & 0.2 & 0.5 & 5 & 20.1 & 1 \\ 5.2 & 2.9 & 4.6 & 4.9 & 0.6 & 7 & 2.1 & 6 & 5 & 28.4 \end{pmatrix},$$

$$\boldsymbol{V}^\star(1) = 10^{-2} \times \begin{pmatrix} 14 & 32 & 32 & 18 & 31 & 12 & 49 & 33 & 11 & 13 \\ 8 & 20 & 20 & 11 & 19 & 7 & 31 & 21 & 7 & 8 \\ 9 & 21 & 21 & 12 & 20 & 8 & 32 & 22 & 7 & 9 \\ 9 & 22 & 22 & 12 & 21 & 8 & 33 & 22 & 7 & 9 \\ 10 & 24 & 24 & 13 & 23 & 9 & 37 & 25 & 8 & 10 \\ 9 & 22 & 22 & 12 & 22 & 8 & 34 & 23 & 8 & 9 \\ 15 & 35 & 35 & 19 & 34 & 13 & 56 & 36 & 12 & 15 \\ 9 & 20 & 20 & 11 & 20 & 7 & 31 & 21 & 7 & 8 \\ 18 & 43 & 43 & 23 & 41 & 15 & 99 & 44 & 15 & 17 \\ 14 & 34 & 33 & 18 & 32 & 12 & 53 & 35 & 12 & 14 \end{pmatrix},$$

$\boldsymbol{V}^\star(2) \approx 1_K \times 1_K^\top$ and $\boldsymbol{V}^\star(3) = 1_K \times 1_K^\top$. The effect of the opinion influence is obvious. It is seen that the fractions of infected decrease significantly after only one influence campaign ; for example, the fraction of infected in the most infected region decreases from 40% to less than 10%. The impact of the subsequent campaigns is still positive but much less significant.

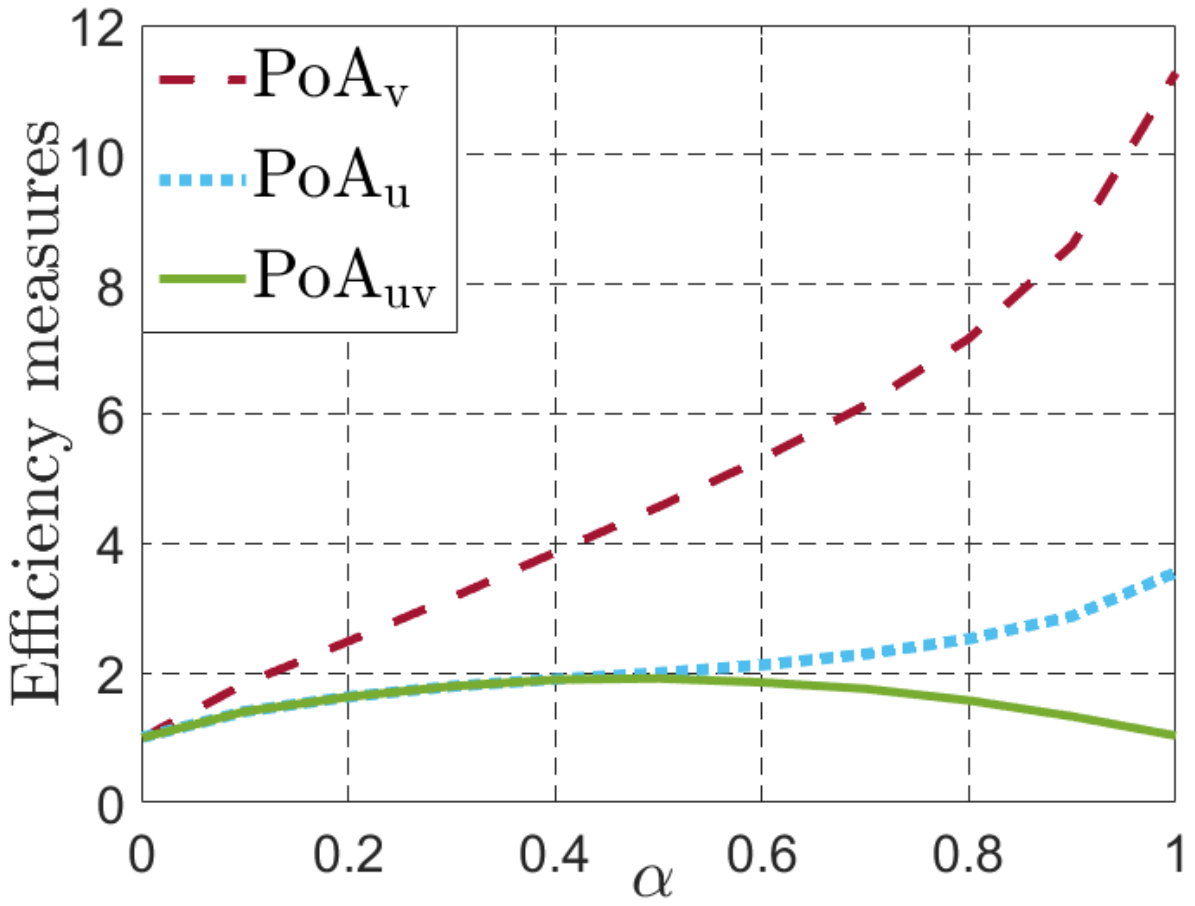

FIGURE 3.1 – The figure shows the impact of the cost function on the PoA, α being the weight assigned to the collective part of the cost functions J_k. It also shows the separate influence of the different control actions (direct epidemic control and influence control). In particular, when $\alpha = 1$, the PoA moves from 1 to 3.7 when the influence control is removed, showing the key role of opinion control when the epidemic management is decentralized.

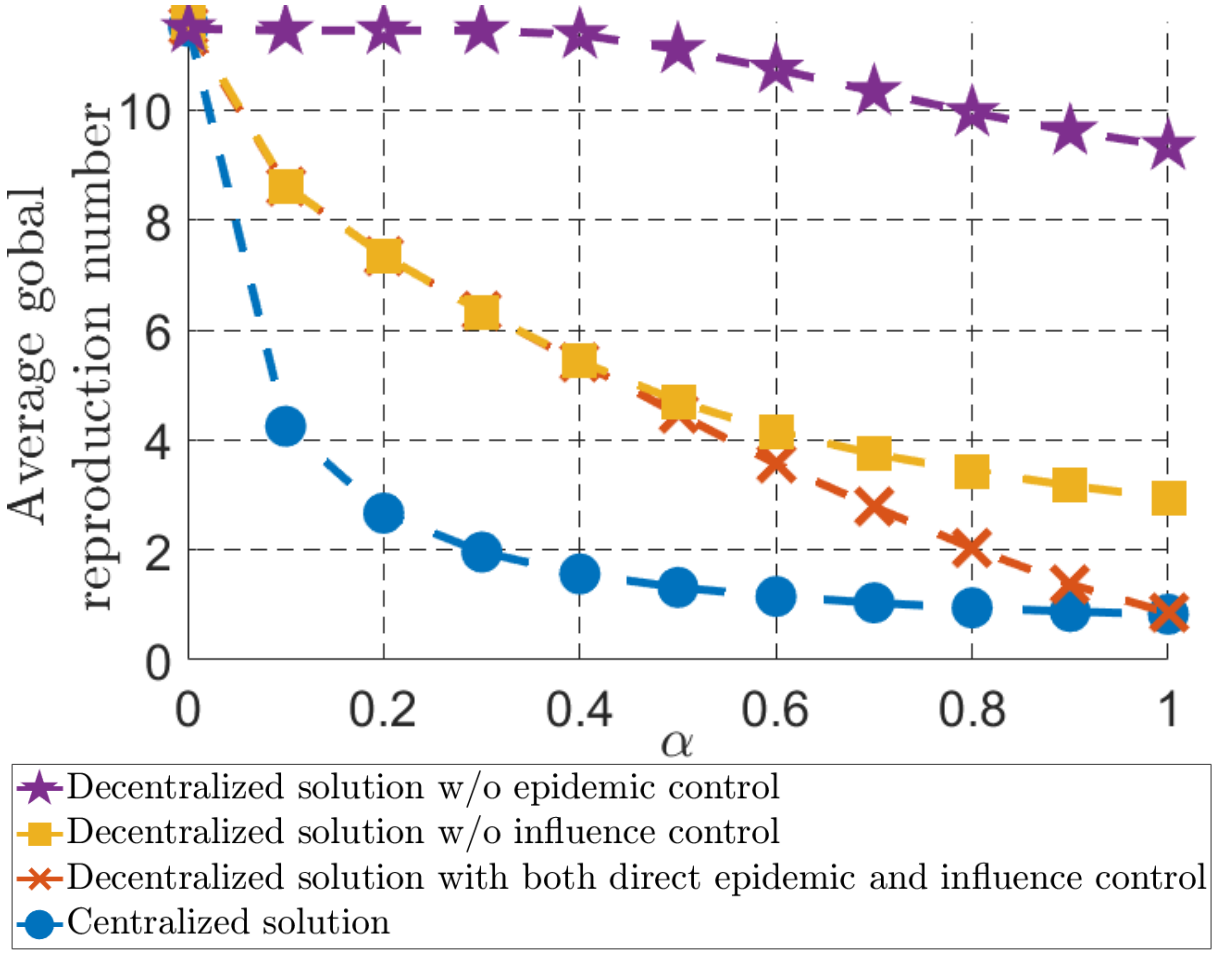

(a) Interpolation of $\sum_{n=0}^{N} \frac{\rho\left(\boldsymbol{D}_{\gamma}^{-1}\left(\boldsymbol{B^0}-\boldsymbol{U}+\mathrm{Diag}(\theta(n))\widehat{\boldsymbol{B}}\right)\right)}{N+1}$ w.r.t. α.

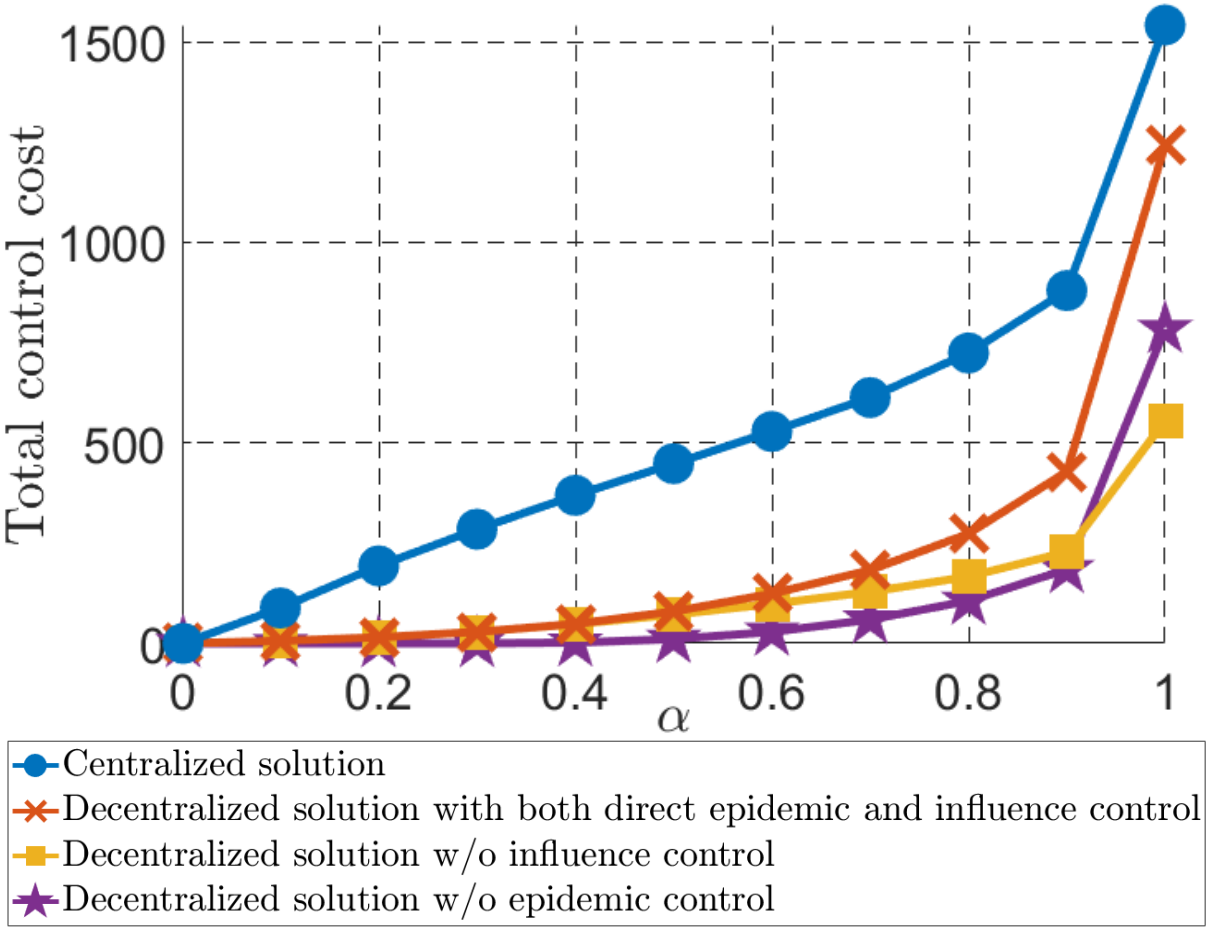

(b) Interpolation of $\sum_{k=1}^{K}\Big[-\sum_{\ell\in\mathcal{N}_k}\log(\frac{\beta^0_{k\ell}-u_{k\ell}}{\beta^0_{k\ell}})+\sum_{n=0}^{N}-\sum_{\ell\in\mathcal{N}_k^{\mathrm{S},n}}\log(v_{k\ell}(n))\Big]$ w.r.t. α.

FIGURE 3.2 – The figure shows the performance in terms of global reproduction number and total cost for four different management strategies.

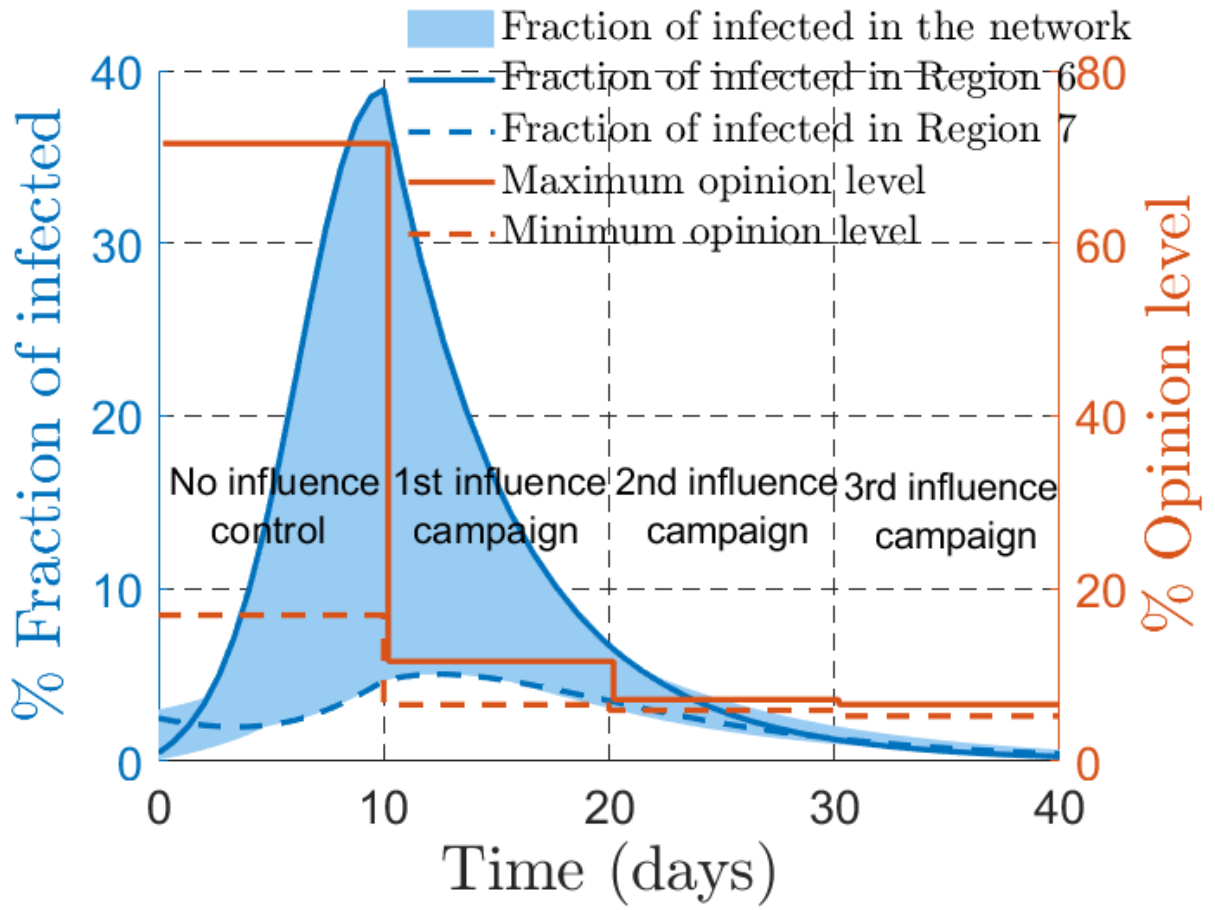

FIGURE 3.3 – Evolution of the fractions of infected and opinion levels for the different regions. The effect of influence campaigns on the fractions of infected appear very clearly.

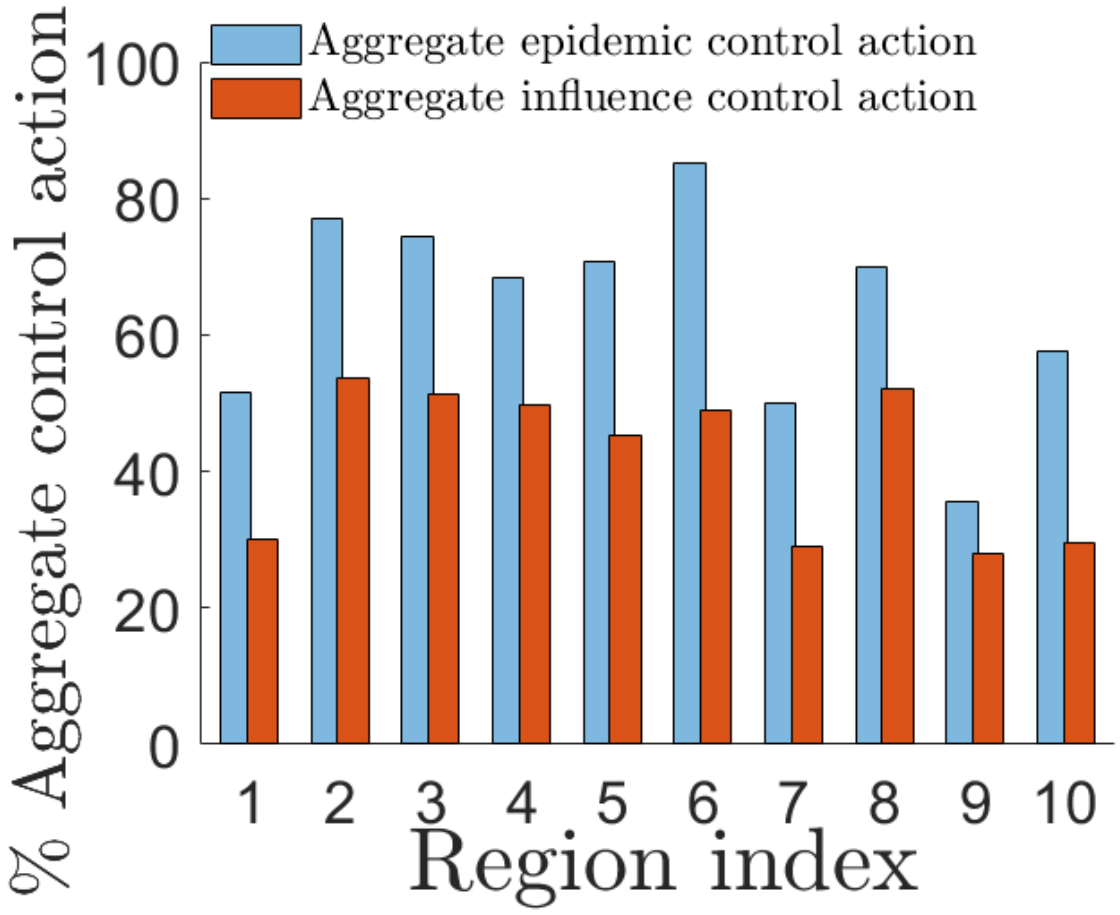

FIGURE 3.4 – The figure provides the control action intensity for the different regions. The corresponding values have to be put in correlation with the local situation of the epidemic, which is in part related to the values of the natural reproduction numbers.

3.4 Conclusion

In this chapter, we present a methodology for evaluating the impact of decentralization on epidemic management considering opinion dynamics. Our game model combines the classical networked SIR model, which captures the spread of the virus, with a time-varying opinion dynamics model. Each player in the game implements a trade-off between socio-economic losses, global/local losses represented by the reproduction number of the virus, and costs associated with awareness campaigns and opinions. The proposed game model is a generalized strategic form game played in one-shot, meaning that the sanitary actions are fixed over a finite time horizon, and $N + 1$ awareness campaigns are applied by each region to influence the beliefs of individuals in the social networks. The primary objective of this chapter is to undertake a comprehensive analysis of the Generalized Nash Equilibrium (GNE) within the framework of the proposed game model. To address this challenge, we introduce key assumptions regarding the

strong connectivity of the epidemic graph and the row stochastic property of the time-varying social network. Under these assumptions, we propose an equivalent auxiliary game that ensures the existence, uniqueness, and algorithm for the determination of the GNE. These results are established in Propositions 2 and 4. Furthermore, Proposition 3 reveals that the centralized management problem can be transformed into a convex optimization problem, allowing for efficient computation of optimal strategies. Finally, we exploit these analytical results to numerically assess the efficiency loss induced by decentralization. Conditions under which the PoA is small or large are clearly exhibited. The influence of graph connectivity and the cost function has been discussed. The key role of influence control for decentralized epidemic management is supported by many simulations. For example, in some situations, opinion control allows the PoA to be reduced from 3.7 to 1. If the epidemic is not managed through direct control measures, the role of opinion then becomes more secondary.

3.5 Appendix of Chapter 3

3.5.1 Auxiliary Game

In view of the dynamic of θ, $\forall k, n$ the drift $\theta_k(n)$ is a posynomial function w.r.t. the awareness action v i.e., $\theta_k(n+1) = \sum_{\ell_n \in \widehat{\mathcal{N}}_k(n)} \sum_{\ell_{n-1} \in \widehat{\mathcal{N}}_{\ell_n}(n-1)} \dots \sum_{\ell_0 \in \widehat{\mathcal{N}}_{\ell_0}(0)} \alpha_{k\ell_n\ell_{n-1}\dots\ell_0}(n) \times$
$v_{k\ell_n}(n) v_{\ell_n,\ell_{n-1}}(n-1) \dots v_{\ell_1,\ell_0}(0)\theta_{\ell_0}(0)$, where
$\alpha_{k,\ell_n,\ell_{n-1},\dots,\ell_0}(n) \geq 0$. In the sequel, we denote by : $\forall n \in \{0,\dots,N\}$ and $\forall (k,\ell_n,\dots,\ell_0) \in \mathcal{K}^{n+2}$, $\omega_{k\ell_n\ell_{n-1}\dots\ell_0}(n) = v_{k\ell_n}(n) v_{\ell_n,\ell_{n-1}}(n-1)\dots v_{\ell_1,\ell_0}(0)$. Let $\varepsilon_x > 0$ sufficiently small such that, from Assumption 2 and the theory of non negative matrix in [59], we use Perron-Frobenius lemma. For all $(u,v) \in \mathcal{U} \times \mathcal{V}$ and $n \in \{0,\dots,N\}$ we have :

$$
\begin{aligned}
\rho\left(\boldsymbol{D}_\gamma^{-1}\left(\boldsymbol{B^0} - \boldsymbol{U} + \operatorname{diag}(\theta(n))\widehat{\boldsymbol{B}}\right)\right) \quad & = \min_{\lambda^n, x^n} \lambda(n) \\
\text{s.t.} \quad & \boldsymbol{D}_\gamma^{-1}\left(\boldsymbol{B^0} - \boldsymbol{U} + \operatorname{diag}(\theta(n))\widehat{\boldsymbol{B}}\right) x(n) \leq \lambda(n) x(n), \\
& \textstyle\sum_{\ell=1}^K x_\ell(n) \leq 1, \\
& x_\ell(n) \geq \varepsilon_x.
\end{aligned}
\tag{3.11}
$$

Let us consider the following changes of variables such that $(k,\ell,\ell_n,\dots,\ell_0) \in \mathcal{K}^{n+3}$,

$$
\begin{aligned}
&\xi_{\omega_{k\ell_n\ell_{n-1}\dots\ell_0}}(n) = \log\left(\omega_{k\ell_n\ell_{n-1}\dots\ell_0}(n)\right), \\
&\xi_{y_{k\ell}} = \log\left(\beta^0_{k\ell} - u_{k\ell}\right).
\end{aligned}
\tag{3.12}
$$

In what follows, we define the operator $\operatorname{Exp}(\cdot)$ which corresponds to the component-wise exponential operator. Let $\rho^{\min} := \rho(\boldsymbol{D}_\gamma^{-1}(\boldsymbol{B^0} - \boldsymbol{U}^{\max}))$, $\rho^{\max} := \rho(\boldsymbol{D}_\gamma^{-1}(\boldsymbol{B^0} - \boldsymbol{U}^{\min}) + \widehat{\boldsymbol{B}})$,

where $\boldsymbol{U}^{\min,\max} = [u_{k\ell}^{\min,\max}]_{1\leq k,\ell\leq K}$. For all $k \in \mathcal{K}$, we denote the action profile of the k^{th} auxiliary player by $\xi_k := (\xi_{y_k}, \xi_{\omega_k})$, where : $\xi_{y_k} := (\xi_{y_{k,1}}, \ldots, \xi_{y_{k,K}})$ and $\forall \ell \in \mathcal{K},\ \xi_{y_{k\ell}} \in \mathcal{Y}_{k\ell} := [\log(\beta_{k\ell}^0 - u_{k\ell}^{\max}), \log(\beta_{k\ell}^0 - u_{k\ell}^{\min})]$; $\xi_{\omega_k} := (\xi_{\omega_k}(0), \ldots, \xi_{\omega_k}(n))$ and $\forall n \in \{0, \ldots, N\}$, $\xi_{\omega_k}(n) := (\xi_{\omega_{k,1,\ldots,1}}(n), \xi_{\omega_{k,1,\ldots,2}}(n), \ldots, \xi_{\omega_{k,K,\ldots,K}}(n))$ such that $\forall (\ell_n, \ldots, \ell_0) \in \mathcal{K}^{n+1}$, $\xi_{\omega_{k\ell_n\ell_{n-1}\ldots\ell_0}}(n) \in \mathcal{W}_{k\ell_n\ell_{n-1}\ldots\ell_0} := [\log(v_{k,\ell_n}^{\min}) + \ldots, \log(v_{\ell_1,\ell_0}^{\min}), \log(v_{k,\ell_n}^{\max}) + \ldots, \log(v_{\ell_1,\ell_0}^{\max})]$. We consider an additional player of index $K+1$ with the corresponding action profile $\xi_{K+1} := (\xi_\lambda, \xi_x)$ where : $\xi_\lambda := (\xi_\lambda(0), \ldots, \xi_\lambda(N+1))$ such that $\forall n \in \{0, \ldots, N+1\}$, $\xi_\lambda(n) \in \boldsymbol{\Lambda} := [\log(\rho^{\min}), \log(\rho^{\max})]$; $\xi_x := (\xi_x(0), \ldots, \xi_x(N+1))$ such that $\forall n \in \{0, \ldots, N+1\}$, $\xi_x(n) \in \mathcal{X} := [\log(\varepsilon_x), 0]^K$. In the following, we denote the complete auxiliary action profile by $\xi := (\xi_1, \ldots, \xi_K, \xi_{K+1})$ and for all $k \in \mathcal{K}$ and $n \in \{0, \ldots, N\}$,

$$\widetilde{\theta}_k(n+1) = \sum_{\ell_n \in \widehat{\mathcal{N}}_k(n)} \sum_{\ell_{n-1} \in \widehat{\mathcal{N}}_{\ell_n}(n-1)} \cdots \sum_{\ell_0 \in \widehat{\mathcal{N}}_{\ell_1}(0)} \Big[\alpha_{k\ell_n\ell_{n-1}\ldots\ell_0}(n) \exp(\xi_{\omega_{k\ell_n\ell_{n-1}\ldots\ell_0}}(n)) \theta_{\ell_0}(0) \Big]. \tag{3.13}$$

The generalized form of the auxiliary static game under consideration is therefore given by :

$$\widetilde{\mathcal{G}} := \Big(\mathcal{K} \cup \{K+1\}, \Big(\boldsymbol{\Pi}_k \widetilde{\mathcal{C}} \Big)_{1\leq k\leq K+1}, \big(\widetilde{J}_k \big)_{1\leq k\leq K+1} \Big), \tag{3.14}$$

where the action spaces and utilities are given in what follows.

$$\begin{aligned} \widetilde{J}_k(\xi) &:= -a_k \sum_{\ell \in \mathcal{N}_k} [\xi_{y_{k\ell}} - \log(\beta_{k\ell}^0)] + b_k^{\text{local}} \sum_{n=0}^{N+1} \sum_{\ell \in \mathcal{N}_k} \frac{\exp(\xi_{y_{k\ell}}) + \widehat{\beta}_{k\ell} \widetilde{\theta}_k(n)}{\gamma_k} \\ &- c_k \sum_{n=1}^{N} \sum_{\ell \in \widehat{\mathcal{N}}_k(n)} \Big[\xi_{\omega_{k\ell k\ldots k}}(n) - \xi_{\omega_{\ell\ldots k}}(n-1) \Big] - c_k \sum_{\ell \in \widehat{\mathcal{N}}_k(0)} \xi_{\omega_{k\ell}}(0) + d_k \sum_{n=0}^{N+1} \widetilde{\theta}_k(n+1). \\ \widetilde{J}_{K+1}(\xi) &:= \sum_{n=0}^{N+1} \exp(\xi_\lambda(n)). \end{aligned} \tag{3.15}$$

$$
\begin{aligned}
\widetilde{\mathcal{C}} := \Big\{ & \xi : \forall n \in \{0,\dots,N\}\ m \in \{0,\dots,N+1\},\ (k,\ell,\ell_n,...,\ell_0) \in \mathcal{K}^{n+3}, \\
& \boldsymbol{D}_\gamma^{-1}\left(\mathrm{Exp}(\xi_y) + \mathrm{diag}(\theta(m))\widehat{\boldsymbol{B}}\right)\mathrm{Exp}(\xi_x(m)) \odot \Big[\mathrm{Exp}(-\xi_\lambda(m)1_K - \xi_x(m))\Big] \leq 1_K \\
& -\xi_{y_{k\ell}} \leq -\log\left(\beta^0_{k\ell} - u^{\max}_{k\ell}\right) \\
& \xi_{y_{k\ell}} \leq \log\left(\beta^0_{k\ell} - u^{\min}_{k\ell}\right), \\
& -\xi_{\omega_{k\ell\ell_n\ell_{n-1}\dots\ell_0}}(n) \leq -\log(v^{\min}_{k\ell_n}) + \dots - \log(v^{\min}_{\ell_1\ell_0}) \\
& \xi_{\omega_{k\ell\ell_n\ell_{n-1}\dots\ell_0}}(n) \leq \log(v^{\max}_{k\ell_n}) + \dots + \log(v^{\max}_{\ell_1\ell_0}), \\
& -\xi_\lambda(m) \leq -\log(\rho^{\min}) \\
& \xi_\lambda(m) \leq \log(\rho^{\max}), \\
& -\xi_{x_\ell}(m) \leq -\log\left(\varepsilon_x\right), \\
& \textstyle\sum_{\ell=1}^K \exp\left(\xi_{x_\ell}(m)\right) \leq 1, \\
& \widetilde{\theta}_k(m) \leq \theta^{\max}_k, \\
& \displaystyle\sum_{\ell\in\mathcal{N}_k}\Big[\exp\left(\xi_{y_{k\ell}}\right) + \widehat{\beta}_{k\ell}\widetilde{\theta}_k(m)\Big]\Big/\gamma_k \leq \mathrm{R}^{\max}_k \\
& -a_k \sum_{\ell\in\mathcal{N}_k}[\xi_{y_{k\ell}} - \log(\beta^0_{k\ell})] \leq \phi_k, \\
& -c_k \sum_{\ell\in\widehat{\mathcal{N}}_k(n)}[\xi_{\omega_{k\ell k\dots k}}(n+1) - \xi_{\omega_{\ell k\dots k}}(n))] \leq \widehat{\psi}_k(n+1), \\
& -c_k \sum_{\ell\in\widehat{\mathcal{N}}_k(0)} \xi_{\omega_{k\ell}}(0) \leq \widehat{\psi}_k(0)\Big\} =: \{\xi : \widetilde{h}(\xi) \leq 0\},
\end{aligned}
\tag{3.16}
$$

where $\widetilde{h}(\xi)$ is jointly convex w.r.t. ξ. The auxiliary players are denoted by index $k \in \{1,\dots,K+1\}$ where the player $K+1$ is an additional player that we consider in our analysis; the action space for Player $k \in \mathcal{K} \cup \{K+1\}$ is given by $\mathbf{\Pi}_k\widetilde{\mathcal{C}}$ which is the projection of the sharing constraint set $\widetilde{\mathcal{C}}$ over the action profile of the auxiliary player k. It has to be noted that the game $\widetilde{\mathcal{G}}$ is a convex static and strategic game played in one shoot.

In this chapter, we show that the properties of the GNE of $\widetilde{\mathcal{G}}$ coincide with those of the game $\mathcal{G}$. The Definition of the GNE for the game $\widetilde{\mathcal{G}}$ is characterized by what follows. We call $\xi^{\mathrm{GNE}} \in \widetilde{\mathcal{C}}$ a Generalized Nash equilibrium point of $\widetilde{\mathcal{G}}$ if $\forall k \in \mathcal{K}$,

$$
\xi^{\mathrm{GNE}}_k \in \underset{\xi_k\in\mathbf{\Pi}_k\widetilde{\mathcal{C}}}{\mathrm{argmin}}\ \widetilde{J}_k(\xi_k, \xi^{\mathrm{GNE}}_{-k}). \tag{3.17}
$$

3.5.2 Proof of the Proposition 2

Existence of a GNE ***:***

According to [79, Thm. 3.1], the game $\widetilde{\mathcal{G}}$ has at least one GNE, $\xi^{\mathrm{GNE}} \in \widetilde{\mathcal{C}}$ since $\forall k \in \mathcal{K}$: $\mathbf{\Pi}_k\widetilde{\mathcal{C}}$ is nonempty, convex and compact subset of a Euclidean space; $\widetilde{\mathcal{C}}$ is both upper-

semicontinuous and lower-semicontinuous (e.g., [79, Proposition 4.1-4.2]) ; $\widetilde{\mathcal{C}}$ is nonempty, closed, convex ; $\widetilde{J}_k$ is continuous in $\widetilde{\mathcal{C}}$ and $\forall \xi_{-k} \in \prod_{-k} \widetilde{\mathcal{C}}$, $\xi_k \mapsto \widetilde{J}_k(\xi_k, \xi_{-k})$ is quasiconvex on $\mathbf{\Pi}_k \widetilde{\mathcal{C}}$.

Now, we will prove that the GNE strategies of $\mathcal{G}$ are given by those of $\widetilde{\mathcal{G}}$. Let ξ^{GNE} a Generalized Nash equilibrium of $\widetilde{\mathcal{G}}$ and we denote by $u^\star$ and $v^\star$ after the change of variable in (3.12). In view of (3.11) it follows that :

$$\widetilde{J}_{K+1}(\xi^{\mathrm{GNE}}) = \sum_{n=0}^{N} \rho(\mathbf{\Gamma^{-1}}(\boldsymbol{B^0} - \boldsymbol{U^\star} + \mathrm{diag}(\theta(n)^\star)\widehat{\boldsymbol{B}})),$$

and $\forall k \in \mathcal{K}$,

$$\begin{aligned}\widetilde{J}_k(\xi^{\mathrm{GNE}}) &= -a_k \sum_{\ell \in \mathcal{N}_k} \log\left(\frac{\beta^0_{k\ell} - u^\star_{k\ell}}{\beta^0_{k\ell}}\right) \\ &+ b_k^{\mathrm{local}} \sum_{n=0}^{N+1} \sum_{\ell \in \mathcal{N}_k} \Big[\frac{\beta^0_{k\ell} - u^\star_{k\ell} + \theta_k(n)^\star \widehat{\beta}_{k\ell}}{\gamma_k}\Big] \\ &- c_k \sum_{n=0}^{N} \sum_{\ell \in \widehat{\mathcal{N}}_k(n)} \log(v^\star_{k\ell}(n)) + d_k \sum_{n=0}^{N+1} \theta_k(n)^\star\end{aligned}$$

where $\forall k \in \mathcal{K}$,

$$[\boldsymbol{U^\star}]_{k\ell} = u^\star_{k\ell} := \begin{cases} \beta^0_{k\ell} - \exp(\xi^{\mathrm{GNE}}_{y_{k\ell}}) \text{ if } \ell \in \mathcal{N}_k \\ 0 \text{ otherwise,} \end{cases}$$

$\forall n \in \{0, \dots, N\}$,

$$\theta_k(n+1)^\star = \sum_{\ell_n \in \widehat{\mathcal{N}}_k(n)} \sum_{\ell_{n-1} \in \widehat{\mathcal{N}}_{\ell_n}(n-1)} \cdots \sum_{\ell_0 \in \widehat{\mathcal{N}}_{\ell_1}(0)} \Big[$$

$$\alpha_{k\ell_n\ell_{n-1}\dots,\ell_0}(n) \exp(\xi^{\mathrm{GNE}}_{\omega_{k\ell_n\ell_{n-1}\dots\ell_0}}(n))\theta_{\ell_0}(0)\Big],$$

and $\forall \ell \in \widehat{\mathcal{N}}_k(n)$, $v^\star_{k\ell}(n) :=$

$$\begin{cases} \exp(\xi^{\mathrm{GNE}}_{\omega_{k\ell k\dots k}}(n) - \xi^{\mathrm{GNE}}_{\omega_{\ell k\dots k}}(n-1)) \text{ if } n > 0 \\ \exp(\xi^{\mathrm{GNE}}_{\omega_{k\ell}}(0)) \text{ otherwise.} \end{cases}$$

Since ξ^{GNE} is a GNE of $\widetilde{\mathcal{G}}$, it follows from (3.17) that, $\forall k \in \mathcal{K}$ and $\xi_k \in \mathbf{\Pi}_k \widetilde{C}$,

$$\widetilde{J}_k(\xi^{\mathrm{GNE}}) \leq \widetilde{J}_k(\xi_k, \xi^{\mathrm{GNE}}_{-k})$$

and $\forall \xi_{K+1} \in \mathbf{\Pi}_{K+1} \widetilde{C}$,

$$\widetilde{J}_{K+1}(\xi^{\mathrm{GNE}}) \leq \widetilde{J}_{K+1}(\xi_{K+1}, \xi^{\mathrm{GNE}}_{-(K+1)}).$$

In view of (3.11), it follows that :

$$\begin{aligned} J_k(u^\star, v^\star) &= \widetilde{J}_k(\xi^{\mathrm{GNE}}) + b_k^{\mathrm{global}} \widetilde{J}_{K+1}(\xi^{\mathrm{GNE}}) \\ &\leq \widetilde{J}_k(\xi_k, \xi_{-k}^{\mathrm{GNE}}) + b_k^{\mathrm{global}} \widetilde{J}_{K+1}(\xi_{K+1}, \xi_{-(K+1)}^{\mathrm{GNE}}) \\ &= J_k(u_k, v_k, u_{-k}^\star, v_{-k}^\star). \end{aligned}$$

Hence, $(u^\star, v^\star)$ is a GNE of $\mathcal{G}$.

Uniqueness of the GNE ***:***

Let define a weighted non-negative sum of the function $\widetilde{J}_k$ given by $\sigma(\xi, \delta) := \sum_{k=1}^{K} \delta_k \widetilde{J}_k(\xi),\ \delta_k \in \mathbb{R}_{>0}$. Based on the Rosen's theory of uniqueness [74], the following Definition is used for exhibiting the desired property of the equilibrium point.

Definition 32. *$\sigma(\xi, \delta)$ is diagonally strictly convex (*DSC*) for $\xi \in \mathcal{E}$ and fixed $\delta \in \mathbb{R}_{\geq 0}^{K+1}$ if for every $\xi^0, \xi^1 \in \widetilde{\mathcal{C}}$ we have*

$$(\xi^1 - \xi^0)^\top (g(\xi^1, \delta) - g(\xi^0, \delta)) > 0,$$

where $g(\xi, \delta) := [\delta_1 \nabla_{\xi_1} \widetilde{J}_1(\xi), \ldots, \delta_{K+1} \nabla_{\xi_{K+1}} \widetilde{J}_{K+1}(\xi)]^\top$.

□

In what follows, we make use the following function : for $(\xi, \widehat{\xi}) \in \widetilde{\mathcal{C}}^2$ and $\delta \in \mathbb{R}_{\geq 0}^{K+1}$

$$\rho(\xi, \widehat{\xi}, \delta) := \sum_{k=1}^{K+1} \delta_k \widetilde{J}_k(\xi_1, \ldots, \xi_{k-1}, \widehat{\xi}_k, \xi_{k+1}, \ldots, \xi_K). \tag{3.18}$$

In the following we guarantee the uniqueness property of the GNE in the game $\widetilde{\mathcal{G}}$. In what follows, we denote by $M := \dim(\widetilde{h}(\xi))$. The Kuhn-Tucker conditions that verify (3.17) can now be expressed as follows : $\forall k \in \mathcal{K},\ \exists \mu_k^{\mathrm{GNE}} \in \mathbb{R}_{\leq 0}^{M}$ such that,

$$\widetilde{h}(\xi^{\mathrm{GNE}}) \leq 0 \tag{3.19a}$$

$$(\mu_k^{\mathrm{GNE}})^\top \widetilde{h}(\xi^{\mathrm{GNE}}) = 0 \tag{3.19b}$$

$$\delta_k \nabla_{\xi_k} \widetilde{J}_k(\xi^{\mathrm{GNE}}) + (\mu_k^{\mathrm{GNE}})^\top \nabla_\xi \widetilde{h}(\xi^{\mathrm{GNE}}) = 0. \tag{3.19c}$$

Let $\overline{\delta} \in \mathbb{R}^{K+1}_{>0}$. From the Definition of the DSC, we have for every $(\xi^0, \xi^1) \in \widetilde{\mathcal{C}}^2$,

$$
\begin{aligned}
&(\xi^1 - \xi^0)^\top (g(\xi^1, \overline{\delta}) - g(\xi^0, \overline{\delta})) = \textstyle\sum_{k=1}^{K} \overline{\delta}_k \Bigg[(N+2) \\
&\times \sum_{\ell=1}^{K} \Big[\frac{b_k^{\mathrm{local}} (\xi^1_{y_{k\ell}} - \xi^0_{y_{k\ell}})(\exp(\xi^1_{y_{k\ell}}) - \exp(\xi^0_{y_{k\ell}}))}{\gamma_k} \Big] + \sum_{n=0}^{N} \Big[\\
&\Big[\sum_{\ell=1}^{K} \frac{b_k^{\mathrm{local}} \widehat{\beta}_{k\ell}}{\gamma_k} + d_k \Big] \times \sum_{\ell_n \in \widehat{\mathcal{N}}_k(n)} \cdots \sum_{\ell_0 \in \widehat{\mathcal{N}}_{\ell_1}(0)} \big[\alpha_{k\ell_n \ldots \ell_0}(n) \times \\
&(\xi^1_{w_{k\ell_n \ldots \ell_0}}(n) - \xi^0_{w_{k\ell_n \ldots \ell_0}}(n)) \Big(\exp(\xi^1_{w_{k\ell_n \ldots \ell_0}}(n)) - \\
&\exp(\xi^0_{w_{k\ell_n \ldots \ell_0}}(n)) \Big) \theta_{\ell_0}(0) \big] \Big] + \overline{\delta}_{K+1} \times \\
&\sum_{n=0}^{N+1} \Big[(\xi^1_\lambda(n) - \xi^0_\lambda(n))(\exp(\xi^1_\lambda(n)) - \exp(\xi^0_\lambda(n))) \Big] > 0 \\
&\Rightarrow \sigma(\xi, \overline{\delta}) \text{ is DSC}, \ \forall \xi \in \widetilde{\mathcal{C}}
\end{aligned}
$$

In view of the geometric properties of $\widetilde{J}_k$, it follows that $\rho(\xi, \widehat{\xi}, \overline{\delta})$ is continuous in ξ and $\widehat{\xi}$ and convex in $\widehat{\xi}$ for every fixed $\xi \in \mathcal{E}$. Then by the Kakutani fixed point theorem, there exists $\xi^\star(\overline{\delta}) \in \widetilde{\mathcal{C}}$ such that

$$\rho(\xi^\star(\overline{\delta}), \xi^\star(\overline{\delta}), \overline{\delta}) = \min_{\xi \in \widetilde{\mathcal{C}}} \rho(\xi^\star(\overline{\delta}), \xi, \overline{\delta}).$$

Then by the necessary $\widetilde{h}(\xi^\star(\overline{\delta})) \leq 0$, it follows that $\exists \mu^\star \in \mathbb{R}^M_{\leq 0}$ such that, ${\mu^\star}^\top \widetilde{h}(\xi^\star(\overline{\delta})) = 0$ and $\forall k \in \mathcal{K}$,

$$\overline{\delta}_k \nabla_{\xi_k} \widetilde{J}_k(\xi^\star(\overline{\delta})) + \sum_{\ell=1}^{M} \mu^\star_\ell \nabla_{\xi_k} h_\ell(\xi^\star(\overline{\delta})) = 0,$$

which are the conditions (3.19a), (3.19b) and (3.19c) with $\xi^\star(\overline{\delta}) = \xi^{\mathrm{GNE}}$ and $\forall k \in \mathcal{K} \cup \{K+1\}$, $\ell \in \{1, \ldots, M\}$, $\mu^{\mathrm{GNE}}_{k\ell} = \mu^\star_\ell / \overline{\delta}_k$, which are sufficient to ensure that $\xi^\star(\overline{\delta})$ is a GNE (i.e., $\xi^\star(\overline{\delta})$ verifies (3.17)); according to [74, Thm. 4], $\xi^\star(\overline{\delta})$ is a unique normalized equilibrium point for the specified value of $\delta = \overline{\delta}$.

3.5.3 Proof of the Proposition 3

Let $\xi^\star \in \underset{\xi \in \widetilde{\mathcal{C}}}{\operatorname{argmin}} \sum_{k=1}^{K} [\widetilde{J}_k(\xi_1, \ldots, \xi_K) + b_k^{\mathrm{global}} \widetilde{J}_{K+1}(\xi_{K+1})]$ and $\xi \in \widetilde{\mathcal{C}}$. Let us denote by $\widetilde{\mathcal{C}}_{1:K}(\xi_{K+1}) := \{(\xi_1, \ldots, \xi_K) : \widetilde{h}(\xi) \leq 0\}$ and $\widetilde{\mathcal{C}}_{K+1}(\xi_1, \ldots, \xi_K) := \{\xi_{K+1} : \widetilde{h}(\xi) \leq 0\}$. It

follows that

$$\sum_{k=1}^{K}[\widetilde{J}_k(\xi_1,\dots,\xi_K)+b_k^{\text{global}}\widetilde{J}_{K+1}(\xi_{K+1})] \geq \min_{(\xi_1,\dots,\xi_K)\in\widetilde{\mathcal{C}}_{1:K}(\xi^\star_{K+1})} \Big[\sum_{k=1}^{K}\widetilde{J}_k(\xi_1,\dots,\xi_K)\Big] + b_k^{\text{global}} \min_{\xi_{K+1}\in\widetilde{\mathcal{C}}_{K+1}(\xi_1^\star,\dots,\xi_K^\star)} \big[\widetilde{J}_{K+1}(\xi_{K+1})\big].$$

According to the Perron-Frobenius lemma and the changed of variable in (3.12),

$$\min_{\xi_{K+1}\in\widetilde{\mathcal{C}}_{K+1}(\xi_1^\star,\dots,\xi_K^\star)} \widetilde{J}_{K+1}(\xi_{K+1}) = \sum_{n=0}^{N+1}\rho(\boldsymbol{D}_\gamma^{-1}(\text{Exp}(\xi_y^\star)+\text{diag}(\widetilde{\theta}(n)^\star)\widehat{\boldsymbol{B}}),$$

with $\forall n\in\{0,\dots,N\}$,

$$\widetilde{\theta}_k(n+1)^\star = \sum_{\ell_n\in\widehat{\mathcal{N}}_k(n)}\ \sum_{\ell_{n-1}\in\widehat{\mathcal{N}}_{\ell_n}(n-1)}\ \dots\ \sum_{\ell_0\in\widehat{\mathcal{N}}_{\ell_1}(0)}\Big[\alpha_{k\ell_n\ell_{n-1}\dots\ell_0}(n)\exp(\xi_{\omega_{k\ell_n\ell_{n-1}\dots\ell_0}}(n)^\star)\theta_{\ell_0}(0)\Big].$$

Furthermore, $\min_{(\xi_1,\dots,\xi_K)\in\widetilde{\mathcal{C}}_{1:K}(\xi^\star_{K+1})}\sum_{k=1}^{K}\widetilde{J}_k(\xi_1,\dots,\xi_K) = \sum_{k=1}^{K}\widetilde{J}_k(\xi_1^\star,\dots,\xi_K^\star)$. Finally, we derive that

$$\sum_{k=1}^{K}\left[\widetilde{J}_k(\xi_1^\star,\dots,\xi_K^\star)+b_k^{\text{global}}\sum_{n=0}^{N+1}\rho(\boldsymbol{\Gamma^{-1}}(\text{Exp}(\xi_y^\star)+\text{diag}(\widetilde{\theta}(n)^\star)\boldsymbol{B}^d)\right] = \min_{(u,v)\in\mathcal{C}}\sum_{k=1}^{K}J_k(u,v).$$

3.5.4 Proof of Proposition 4

We recall that $M=\dim(\widetilde{h}(\xi))$ and in what follows we denote $\widetilde{M}:=\dim(\xi)$. Let $\overline{\delta}\in\mathbb{R}_{>0}^{K+1}$. Consider the following differential equations, $\forall k\in\mathcal{K}\cup\{K+1\}$,

$$\frac{d\xi_k}{dt} = -\overline{\delta}_k\nabla_{\xi_k}\widetilde{J}_k+\sum_{j=1}^{M}\mu_j\nabla_{\xi_k}\widetilde{h}_j(\xi),\ \mu\in\mathcal{M}(\xi), \tag{3.20}$$

where $\mathcal{M}(\xi)\subset\mathbb{R}_{\leq 0}^{M}$ is bounded. We define $\boldsymbol{H}:\widetilde{\mathcal{C}}\to\mathbb{R}^{\widetilde{M}\times M}$ by

$$\boldsymbol{H}(\xi):=[\nabla_\xi\widetilde{h}_1(\xi),\nabla_\xi\widetilde{h}_2(\xi),\dots,\nabla_\xi\widetilde{h}_M(\xi)].$$

The matrix formulation of (3.20) is given by :

$$\frac{d\xi}{dt} = f(\xi,\mu,\overline{\delta}):=-g(\xi,\overline{\delta})+\boldsymbol{H}(\xi)\mu,\ \mu\in\mathcal{M}(\xi), \tag{3.21}$$

with

$$\mathcal{M}(\xi) := \underset{\mu}{\operatorname{argmin}} \ \|f(\xi,\mu,\overline{\delta})\| \quad \text{s.t.} \quad \begin{cases} \mu_j \leq 0 \text{ if } \widetilde{h}_j(\xi) > 0 \\ \mu_j = 0 \text{ otherwise.} \end{cases}$$

According to [74, Thm. 7], for every starting point $\xi(0) \in \widetilde{\mathcal{C}}$, the trajectory $\xi(t)$ of (3.21) exists and remains in $\widetilde{\mathcal{C}}$ at any time $t > 0$. In what follows, we show the convergence of (3.21) to the unique normalized equilibrium point $\xi^\star(\overline{\delta})$ associated to the value $\overline{\delta}$.

We consider an equilibrium point $\xi^\star$ of system (3.21) for a fixed $\overline{\delta} \in \mathbb{R}^{K+1}_{>0}$ such that $f(\xi^\star,\mu,\overline{\delta}) = 0,\ \mu \in \mathcal{M}(\xi^\star)$. In view of the proof of Proposition 2 and the definition of f, for $\xi^\star$ and $\mu \in \mathcal{M}(\xi^\star)$ such that $f(\xi^\star,\mu,\overline{\delta}) = 0$ is obviously a normalized equilibrium point associated to the fixed value $\overline{\delta}$. For all $\xi \in \widetilde{\mathcal{C}}$, we define $\overline{\mu}(\xi)$ such as the nonzeros elements of of $\mu \in \mathcal{M}(\xi)$ which are given by $\overline{\mu} \in \mathbb{R}^{\overline{M}}_{\leq 0}$, where $\overline{M} \leq M$ and $\overline{\mu}(\xi) = \left[\overline{\boldsymbol{H}}(\xi)^\top \overline{\boldsymbol{H}}(\xi)\right]^{-1} \overline{\boldsymbol{H}}(\xi)^\top g(\xi,\overline{\delta}) \leq 0$, where the matrix $\overline{\boldsymbol{H}}(\xi) \in \mathbb{R}^{\widetilde{M}\times\overline{M}}$ is composed by $\overline{M} \leq M$ linearly independent columns of $\boldsymbol{H}(\xi)$ selected from $\nabla_\xi \widetilde{h}_j(\xi)$ for $j \in \{i \in \{1,\dots,M\} :\ \widetilde{h}_i(\xi) > 0\}$. It follows that :

$$\frac{df(\xi,\mu,\overline{\delta})}{dt} = \left(-\boldsymbol{G}(\xi,\overline{\delta}) + \sum_{j=1}^{M} \mu_j \boldsymbol{Q}_j(\xi)\right)\frac{d\xi}{dt} + \overline{\boldsymbol{H}}(\xi)\frac{d\overline{\mu}}{dt}, \tag{3.22}$$

where $\boldsymbol{Q}_j(\xi)$ is the hessian of $\widetilde{h}_j(\xi)$; $\boldsymbol{G}(\xi,\overline{\delta})$ is the jacobian of $g(\xi,\overline{\delta})$; which are both positive semi-definite since $\forall k,\ \widetilde{J}_k$ and h are convex w.r.t. ξ. Let us consider $V : \widetilde{\mathcal{C}} \times \mathbb{R}^M_{\leq 0} \to \mathbb{R}_{\geq 0}$ as a Lyapunov function, given by $V(\xi,\mu) = \frac{1}{2}\|f(\xi,\mu,\overline{\delta})\|^2$, which is continuously differentiable positive definite function on $\widetilde{\mathcal{C}} \times \mathbb{R}^M_{\leq 0}$. By combining (3.21) with (3.22), we derive that,

$$\begin{aligned}
\frac{d}{dt}V(\xi,\mu) &= \frac{1}{2}\frac{d}{dt}(f(\xi,\mu,\overline{\delta})^\top f(\xi,\mu,\overline{\delta})) \\
&= f(\xi,\mu,\overline{\delta})^\top \frac{d}{dt} f(\xi,\mu,\overline{\delta}) \\
&= -f(\xi,\mu,\overline{\delta})^\top \boldsymbol{G}(\xi,\overline{\delta}) f(\xi,\mu,\overline{\delta}) + \sum_{j\in\{1\leq i\leq M:\ \widetilde{h}_i(\xi)>0\}} \overline{\mu}_j f(\xi,\mu,\overline{\delta})^\top \boldsymbol{Q}_j(\xi) f(\xi,\mu,\overline{\delta}) \\
&\quad + f(\xi,\mu,\overline{\delta})^\top \overline{\boldsymbol{H}}(\xi)\frac{d\overline{\mu}}{dt}.
\end{aligned}$$

From (3.21) and the expression of $\overline{\mu}$, it follows that,

$$\begin{aligned}
f(\xi,\mu,\overline{\delta})^\top \overline{\boldsymbol{H}}(\xi)\frac{d\overline{\mu}}{dt} &= \left[-g(\xi,\overline{\delta})^\top \overline{\boldsymbol{H}}(\xi) + \overline{\mu}^\top \overline{\boldsymbol{H}}(\xi)^\top \overline{\boldsymbol{H}}(\xi)\right]\frac{d\overline{\mu}}{dt} \\
&= \left[-g(\xi,\overline{\delta})^\top \overline{\boldsymbol{H}}(\xi) + g(v,\overline{\delta})^\top \overline{\boldsymbol{H}}(\xi)\right]\frac{d\overline{\mu}}{dt} \\
&= 0.
\end{aligned}$$

Since $\boldsymbol{Q_j}(\xi)$ and $\boldsymbol{G}(\xi, \overline{\delta})$ are positive semidefinite, it follows that,

$$\frac{d}{dt}V(\xi,\mu) = -f(\xi,\mu,\overline{\delta})^\top \boldsymbol{G}(\xi,\overline{\delta}) f(\xi,\mu,\overline{\delta}) + \sum_{j\in\{1\leq i\leq M:\ \widetilde{h}_i(\xi)>0\}} \overline{\mu}_j f(\xi,\mu,\overline{\delta})^\top \boldsymbol{Q}_j(\xi) f(\xi,\mu,\overline{\delta}).$$

Let $\mathcal{S} := \{(\xi,\mu) \in \widetilde{\mathcal{C}} \times \mathbb{R}^M_{\geq 0} : \ \frac{d}{dt}V(\xi,\mu) = 0\}$. Since, for a fixed $\overline{\delta}$, there exists a unique normalized equilibrium point $\xi^\star(\overline{\delta})$ that verifies the optimization problem given in

$$\xi^\star(\overline{\delta}) = \min_{\xi\in\widetilde{\mathcal{C}}} \rho(\xi^\star(\overline{\delta}), \xi, \overline{\delta}),$$

where ρ is given in (3.18). It follows that no solution of system (3.21) can stay identically in $\mathcal{S}$ other than the solution $\xi(t) = \xi^\star(\overline{\delta})$. Then, according to [90, Corollary 4.1], for any initial condition $\xi(t=0) \in \widetilde{\mathcal{C}}$, the system (3.21) converge asymptotically to the normalized equilibrium point $\xi^\star(\overline{\delta})$, which is the unique GNE of $\widetilde{\mathcal{G}}$.

Chapter 4

A Stackelberg Viral Marketing Design for Two Competing Players

In this chapter, we examine the viral marketing problem where two firms compete to obtain a greater market share by offering a service, good, or product to customers spread over multiple geographical regions. To this end, viral marketing is modeled as viral problem with multiple viruses and multiple decision-makers. For this, we exploit the concept of "winner takes all" [23], for which a particular case is given by the steady-state of a multi-virus SIS system [24]. It is worth noting that instances of such equilibria have been recorded in actual scenarios, a classic example being the competition between Facebook and Myspace, as detailed in [24]. One of the main objectives of this work is to characterize the advertising budget allocation strategy for each firm across regions to maximize its market share when competing. To achieve this goal, we introduce a Stackelberg game model that captures the principal effects of market share competition. By analyzing the equilibria of the two-level Stackelberg game in both pessimistic and optimistic settings, we provide the associated budget allocation strategy. Our analysis establishes the conditions under which the solution of the game leads to the "winner takes all" outcome. We complement our theoretical results with numerical simulations and provide an example to further illustrate our equilibrium characterization.

Chapters 2 and 3 meticulously formulate and analyze the issue of decentralizing decision-making with the objective of curbing an outbreak. This topic holds significance beyond epidemic control, extending to economic domains. For instance, when a company aims to maximize the dissemination of goods or services while delegating dissemination policies to local entities [7] or more generally for viral marketing [8].

The main goal of this chapter is to formulate a two-level Stackelberg game and characterize its solutions. The analysis does not rely on a specific dynamic for the information spreading but assumes that at the equilibrium the “winner takes all". We point out that the existing literature on multi-virus epidemic emphasize the aforementioned type of equilibrium [24, 43, 44]. We consider that two players compete over several regions to get a higher market share. The budget allocated by a firm to a certain region modifies the spreading rate of the associated service in that region. Note that we are analyzing the steady state revenue of each firm. This combined with the “winner takes all" behavior allows us to decouple the analysis of the investment strategy for each region. At the same time, we highlight that the design of the budget allocation strategy is subject to overall fixed budget constraints.

This chapter is structured as follows. Sec. 4.1 provides the problem formulation, going from the VM model up to the Stackelberg game analyzed in the chapter. The main result of this work is presented at the end of Sec. 4.1. Sec. 4.2 is devoted to the proof of the main result. A numerical example illustrates our theoretical findings in Sec. 4.3 and some concluding remarks are provided in Sec. 4.4.

4.1 Problem Statement

We consider a set of two firms competing over $K > 1$ regions (e.g., countries, provinces, or states) to maximize their market share. Let $\mathcal{K} := \{1, \dots, K\}$ and $\mathcal{M} := \{1, 2\}$ be the set of regions and firms, respectively. For a given region $k \in \mathcal{K}$ and a firm $m \in \mathcal{M}$, we respectively denote by (i) γ_{mk} the spreading rate of the service of Firm m in the region k; (ii) δ_{mk} the churn rate at which the individuals from Region k decide to dispense with the services of Firm m. In this work, we assume that there is a simple linear relationship between allocated budget and γ_{mk} dissemination rate, but more advanced and faithful models could be investigated in future work. In practice, the spread rate is influenced by numerous factors and it would be more accurate to

assume that firms focus on captivating content and identifying influential users or communities to indirectly influence the spread rate of viral marketing campaigns [91, 92, 93]. On top of this, we assume that Firm m has a given advertising budget B_m to allocate between the K regions in order to maximize the number of its subscribers. We denote by $\gamma_m := (\gamma_{m,1}, \dots, \gamma_{mk}) \in \mathbb{R}^K_{\geq 0}$ the action vector of Firm m such that $\sum_{k=1}^K \gamma_{mk} \leq B_m$ and $\gamma := (\gamma_1, \gamma_2) \in \mathbb{R}^{2K}_{\geq 0}$ the action profile. We also make a slight notation abuse by using the following notation : $\gamma := (\gamma_m, \gamma_{-m})$ for $m \in \mathcal{M}$.

Firm 1 will be referred to as the *leader* and Firm 2 as the *follower*. This is because the leader acts on the network first and the follower acts after a sufficiently long time such that it can observe and react to the action made by the leader.

4.1.1 Viral marketing model

By considering that the control action γ_{mk} is a constant on the working phase $[0, +\infty[$. Thus, the follower can be said to start influencing nodes at time 0. The fraction of individuals in Region $k \in \mathcal{K}$ who subscribe to the services of Firm $m \in \mathcal{M}$ is denoted by $x_{mk} \in [0, 1]$. For the interest of practicality, we consider the following assumption.

Assumption 3. *Each individual subscribes to at most one service.*

This assumption is justified by the consideration of average individual behavior, which aligns with the notion that individuals typically opt for a single subscription. The fraction of individuals in Region $k \in \mathcal{K}$ who have not subscribed to any services is denoted by $s_k \in [0, 1]$. In what follows we denote by $x^\infty_{mk} := \lim_{t \to \infty} x_{mk}(t)\ \forall k \in \mathcal{K}, \forall m \in \mathcal{M}$ and we suppose that :

$$(x^\infty_{1k}, x^\infty_{2k}) = \begin{cases} \left(1 - \dfrac{\delta_{1k}}{\gamma_{1k}}, 0\right) & \text{if } \dfrac{\gamma_{1k}}{\delta_{1k}} \geq \max\left(\dfrac{\gamma_{2k}}{\delta_{2k}}, 1\right) \\ \left(0, 1 - \dfrac{\delta_{2k}}{\gamma_{2k}}\right) & \text{if } \dfrac{\gamma_{2k}}{\delta_{2k}} \geq \max\left(\dfrac{\gamma_{1k}}{\delta_{1k}} + \pi, 1\right) \\ (0, 0) & \text{otherwise.} \end{cases} \tag{4.1}$$

The presence of $\pi > 0$ in (4.1) is motivated by practical reasons well-known in the economics literature [94, 95]. The leader has already established its market by the time when the follower enters the market. Thus, the follower has to invest a little more to convince the customers to switch services. In the economics literature π is called a barrier to entry. A barrier to entry is a condition that makes it difficult for new firms to enter a market and compete with established firms. Barriers can take various forms, such as economies of scale, brand loyalty, access to distribution channels, patents and copyrights, government regulations, and high capital requirements. The analysis in [24, Section 4.2] and [96] provide a bi-virus (Susceptible-Infected-Susceptible) SIS model applied for viral marketing, such that the system converges to a point closed to (4.1).

The main difference is that the case when $\frac{\gamma_{1k}}{\delta_{1k}} = \frac{\gamma_{2k}}{\delta_{2k}}$ leads to multiple equilibria, and is avoided in our model due to the barrier to entry π. Additionally, by setting the churn rates δ_{mk} to zero, the model corresponds to a Colonel Blotto game, which is commonly employed in viral marketing literature [97].

4.1.2 Game model

As previously stated, each Firm $m \in \mathcal{M}$ solves a budget allocation problem that maximizes a revenue under the global budget (denoted by B_m) constraint i.e., a feasible strategy for Firm m belong to the set $\Gamma_m := \{\gamma_m \in \mathbb{R}^K_{\geq 0} : \sum_{k=1}^K \gamma_{mk} \leq \mathrm{B_m}\}$. The budget B_m is imposed for practical reasons (e.g., a firm has a given finite investment budget).

Similar to [98], we consider the utility of each Firm $m \in \mathcal{M}$, such as given by

$$\begin{aligned} u_1(\gamma_1, \gamma_2) &:= \sum_{k=1}^{K} p_{1k} \left(1 - \frac{\delta_{1k}}{\gamma_{1k}}\right) \mathbb{1}_{\mathcal{H}_1(k,\gamma_{2k})}(\gamma_{1k}) \\ u_{2,\pi}(\gamma_2, \gamma_1) &:= \sum_{k=1}^{K} p_{2k} \left(1 - \frac{\delta_{2k}}{\gamma_{2k}}\right) \mathbb{1}_{\mathcal{H}_{2,\pi}(k,\gamma_{1k})}(\gamma_{2k}) \end{aligned} \tag{4.2}$$

where : (i) $\pi > 0$ is the barrier to entry for the follower, which is fixed ; (ii) p_{mk} the contribution of Region k to the revenue of firm m when all its individuals subscribe to the service m ; (iii) the quantity $\left(1 - \frac{\delta_{mk}}{\gamma_{mk}}\right)$ represents $x^{\infty}_{mk}(\gamma, \pi)$ in view of (4.1) and $\mathbb{1}$ is the indicator function, where

$$\mathcal{H}_1(k, \gamma_{2k}) := \left\{ \gamma_{1k} \in \mathbb{R}_{\geq 0} : \frac{\gamma_{1k}}{\delta_{1k}} \geq \max\left(\frac{\gamma_{2k}}{\delta_{2k}}, 1\right) \right\},$$

and

$$\mathcal{H}_{2,\pi}(k, \gamma_{1k}) := \left\{ \gamma_{2k} \in \mathbb{R}_{\geq 0} : \frac{\gamma_{2k}}{\delta_{2k}} \geq \max\left(\frac{\gamma_{1k}}{\delta_{1k}} + \pi, 1\right) \right\}.$$

In this chapter, we analyze a static Stackelberg game with a leader (Firm 1) and a follower (Firm 2). The utility of Firm 1 depends only on γ_1 as Firm 2 reacts with a best response strategy. We adopt a pessimistic approach for the leader, focusing on the analysis of weak Stackelberg equilibrium [99]. The leader's utility function, considering a given barrier to entry $\pi > 0$ for the follower, is formulated as :

$$\begin{aligned} u^S_{1,\pi}(\gamma_1) &:= \min_{\gamma_2 \in \mathrm{BR}_{2,\pi}(\gamma_1)} u_1(\gamma_1, \gamma_2), \\ \mathrm{BR}_{2,\pi}(\gamma_1) &= \operatorname*{argmax}_{\gamma_2 \in \Gamma_2} u_{2,\pi}(\gamma_2, \gamma_1). \end{aligned} \tag{4.3}$$

It should be noted that the analysis presented in this chapter also applies when considering an optimistic formulation for the leader, namely, strong Stackelberg equilibrium with $u^S_{1,\pi}(\gamma_1) =$

$\max_{\gamma_2 \in \mathrm{BR}_{2,\pi}(\gamma_1)} u_1(\gamma_1, \gamma_2)$. The goal of this work is to analyse a regular Stackelberg solution (S), for a given $\pi > 0$ of the game $\mathcal{G}_\pi^S := \left(\mathcal{M}, (\Gamma_m)_{1\leq m\leq 2}, (u_{m,\pi}^S)_{1\leq m\leq 2}\right)$ in which : the players are Firm 1 and Firm 2 ; the action space of Firm m is given by Γ_m ; the individual utility function of each firm is given by $u_{1,\pi}^S$ in (4.3) and $u_{2,\pi}^S = u_{2,\pi}$ in (4.2). Firm $m \in \mathcal{M}$ expresses its interests by setting the potential revenues $(p_{m,1}, \ldots, p_{mk}) \in \mathbb{R}_{\geq 0}^K$, whereas the set of action Γ_m is imposed by the capacity of investment of Firm m given by the budget $\mathrm{B_m}$. In addition, we emphasize that the theoretical results established in this chapter hold for a multistage game setup in which the one-shot game is repeated at each stage (for which the parameters are updated) and different constant control actions are applied during it.

Let us recall the definition of a weak Stackelberg solution. The strategy γ_π^{S} is a weak Stackelberg solution of the game $\mathcal{G}_\pi^S$ if it is a solution of the system of equations :

$$\gamma_{1,\pi}^{\mathrm{S}} \in \underset{\gamma_1 \in \Gamma_1}{\mathrm{argmax}}\ u_{1,\pi}^S(\gamma_1) \text{ and } \gamma_{2,\pi}^{\mathrm{S}} \in \underset{\gamma_2 \in \Gamma_2}{\mathrm{argmax}}\ u_{2,\pi}^S(\gamma_2, \gamma_{1,\pi}^{\mathrm{S}}).$$

4.1.3 Main result

As mentioned above, we investigate the weak Stackelberg solution of the game $\mathcal{G}_\pi^S$. In what follows, we denote by :

$$\mathrm{BR}_{2,\pi}^-(\gamma_1) := \underset{\gamma_2 \in \mathrm{BR}_{2,\pi}(\gamma_1)}{\mathrm{argmin}}\ u_1(\gamma_1, \gamma_2)$$

the best response of Firm 2 which minimizes the profit of the Firm 1 when it uses the strategy $\gamma_1 \in \Gamma_1$. Let $\mathrm{BR}_{2k,\pi}^-(\gamma_1) := \mathrm{P}_k(\mathrm{BR}_{2,\pi}^-(\gamma_1))$ where $\forall \gamma_2 \in \Gamma_2,\ k \in \mathcal{K}$ one has $\mathrm{P}_k(\gamma_2) = \gamma_{2k}$.

Let $\mathcal{K}_1 \in 2^K$ representing a given set of regions of investment under consideration by Firm 1, let us define the following set

$$\begin{aligned}\widehat{\Gamma}_{1,\pi}(\mathcal{K}_1) := \ \Bigg\{ \gamma_1 \in \mathbb{R}_{\geq 0}^K \Big| & \forall k \in \mathcal{K}_1,\ \frac{\gamma_{1k}}{\delta_{1k}} \geq \max\left(\frac{\mathrm{BR}_{2k,\pi}^-(\gamma_1)}{\delta_{2k}}, 1\right), \\ & \forall k \in \mathcal{K} \setminus \mathcal{K}_1,\ \frac{\gamma_{1k}}{\delta_{1k}} \leq \max\left(\frac{\mathrm{BR}_{2k,\pi}^-(\gamma_1)}{\delta_{2k}} - \pi, 1\right) \Bigg\},\end{aligned}$$

and

$$\widehat{S}_\pi(\mathcal{K}_1, \gamma_1) := \begin{cases} \sum_{k \in \mathcal{K}_1} p_{1k}\left(1 - \dfrac{\delta_{1k}}{\gamma_{1k}}\right) & \text{if } \gamma_1 \in \widehat{\Gamma}_{1,\pi}(\mathcal{K}_1) \neq \emptyset, \\ -1 & \text{otherwise.} \end{cases} \tag{4.4}$$

In simpler terms, the expression $\widehat{\Gamma}_{1,\pi}(\mathcal{K}_1)$ represents the set of investment options available to Firm 1 when Firm 2 applies a best response strategy. This set allows Firm 1 to determine the regions and values of investment that it can choose from. On the other hand, $\widehat{S}_\pi(\mathcal{K}_1, \gamma_1)$

represents the corresponding revenue that Firm 1 can generate based on its chosen investment strategy $\mathcal{K}_1$ and spread rate γ_1. We are now ready to state the main result of this chapter, which will be proven in the following section.

Theorem 8. *The Stackelberg strategy γ_π^S is obtained by solving :*

$$(\mathcal{K}_{1,\pi}^S, \gamma_{1,\pi}^S) := \underset{\mathcal{K}_1 \in 2^{\mathcal{K}}}{\operatorname{argmax}} \underset{\gamma_1 \in \Gamma_1}{\operatorname{argmax}} \widehat{S}_\pi(\mathcal{K}_1, \gamma_1) \tag{4.5}$$

where $\widehat{\Gamma}_{1,\pi}(\mathcal{K})$ is proven to be a convex set (see proof) for any $\mathcal{K}$ and the maximization problem $\max_{\gamma_1 \in \Gamma_1} \widehat{S}_\pi(\mathcal{K}_1, \gamma_1)$ is a convex OP for a given $\mathcal{K}_1$. The follower's strategy at the Stackelberg equilibria is given by $\gamma_{2k,\pi}^S = \dfrac{\sqrt{p_{2k}\delta_{2k}}}{\sum_{\ell \in \mathcal{K}_{2,\pi}^S} \sqrt{p_{2\ell}\delta_{2\ell}}} \mathrm{B}_2$ if $k \in \mathcal{K}_{2,\pi}^S$ and $\gamma_{2k,\pi}^S = 0$ otherwise, where

$$\mathcal{K}_{2,\pi}^S := \underset{\mathcal{K}_2 \in 2^{\mathcal{K}}}{\operatorname{argmax}} \sum_{k \in \mathcal{K}_2} p_{2k} \left(1 - \frac{\sqrt{\dfrac{\delta_{2k}}{p_{2k}}} \displaystyle\sum_{\ell \in \mathcal{K}_2} \sqrt{p_{2\ell}\delta_{2\ell}}}{\mathrm{B}_2} \right)$$
$$\text{s.t. } \mathcal{K}_2 \cap \mathcal{K}_{1,\pi}^S = \emptyset.$$

Proof. See the following section and Appendix. 4.5.3. ■

Remark 1. *In the perspective of studying the strong Stackelberg solution, it is enough to consider that the follower applies the strategy in $\mathrm{BR}_{2,\pi}^+(\gamma_1)$ where*

$$\mathrm{BR}_{2,\pi}^+(\gamma_1) := \underset{\gamma_2 \in \mathrm{BR}_{2,\pi}(\gamma_1)}{\operatorname{argmax}} u_1(\gamma_1, \gamma_2).$$

Remark 2. *Although the optimization problem specified in Equation* (4.5) *theoretically involves an exponential search space of 2^K regions. On one hand we provide just a methodology to solve such problems (that does not involve online solving and therefore computation time is not very important) and on the other hand, in many practical scenarios, the number of regions K in which firms compete is relatively small, typically around* 10*. Basically we can consider that USA, Europe, South America represent regions for competition at global level. If the competition is specific to a country than the number of regions will be also relatively small. This manageable number of regions significantly reduces the computational complexity associated with solving the optimization problem. A key result introduced in Theorem 8 is by ensuring that the maximization of $\widehat{S}_\pi(\mathcal{K}_1, \gamma_1)$, for a given $\mathcal{K}_1$ and for $\gamma_1 \in \Gamma_1$ can be effectively resolved*

through the utilization of a convex optimization algorithm.

In order to prove the main result of this chapter, we first characterize the best response strategy of Firm 2 and finally characterize the weak Stackelberg solution for a fixed barrier to entry $\pi > 0$.

4.2 Stackelberg strategy design

In this section, we propose a convex reformulation of the problem in (4.3). This allows us to obtain the optimal budget allocation solution for the follower and thus characterize the weak Stackelberg solution of the game $\mathcal{G}_\pi^S$.

For a given leader's strategy $\gamma_1 \in \Gamma_1$ we denote by $\widetilde{\Gamma}_{2,\pi}(\mathcal{K}_2, \gamma_1)$ as the set of strategy of Firm 2 to win the marketing battles in regions of $\mathcal{K}_2 \subseteq \mathcal{K}$ i.e.,

$$\begin{aligned}\widetilde{\Gamma}_{2,\pi}(\mathcal{K}_2, \gamma_1) := \Bigg\{ \gamma_2 \in \mathbb{R}_{\geq 0}^K \Bigg| & \forall k \in \mathcal{K}_2,\ \frac{\gamma_{2k}}{\delta_{2k}} \geq \max\left(\frac{\gamma_{1k}}{\delta_{1k}} + \pi, 1\right), \\ & \forall k \in \mathcal{K} \setminus \mathcal{K}_2,\ \frac{\gamma_{2k}}{\delta_{2k}} \leq \max\left(\frac{\gamma_{1k}}{\delta_{1k}}, 1\right) \Bigg\}.\end{aligned} \tag{4.6}$$

4.2.1 Follower's OP reformulation

The goal of this section is to reformulate the optimisation problem for the follower ($m = 2$) introduced in (4.3).

Proposition 5. *Let $\gamma_1 \in \Gamma_1$. The initial OP in* (4.3) *can be reformulated such as*

$$\max_{\gamma_2 \in \Gamma_2} u_{2,\pi}^S(\gamma_2, \gamma_1) = \max_{\mathcal{K}_2 \in 2^{\mathcal{K}}} \left[\begin{array}{c} \max\limits_{\gamma_2} \sum\limits_{k \in \mathcal{K}_2} p_{2k} \left(1 - \frac{\delta_{2k}}{\gamma_{2k}}\right) \\ \text{s.t.} \sum\limits_{k=1}^{K} \gamma_{2k} \leq \mathrm{B}_2 \\ \gamma_2 \in \widetilde{\Gamma}_{2,\pi}(\mathcal{K}_2, \gamma_1). \end{array} \right]$$

$$\text{s.t.} \exists \gamma_2 \in \widetilde{\Gamma}_{2,\pi}(\mathcal{K}_2, \gamma_1) : \sum_{k=1}^{K} \gamma_{2k} \leq \mathrm{B}_2 \tag{$P^\star$}$$

Remark 3. *It appears that, the condition "$\exists \gamma_2 \in \widetilde{\Gamma}_{2,\pi}(\mathcal{K}_2, \gamma_1) : \sum_{k=1}^{K} \gamma_{2k} \leq \mathrm{B}_2$" is verified, if and only if $\sum\limits_{k \in \mathcal{K}_2} \delta_{2k} \max\left(\frac{\gamma_{1k}}{\delta_{1k}} + \pi, 1\right) \leq \mathrm{B}_2$ i.e., the less restrictive strategy of $\widetilde{\Gamma}_{2,\pi}(\mathcal{K}_2, \gamma_1)$ verifies the budget constraint.*

Proof. See Appendix. 4.5.1. ■

4.2.2 Characterization of the follower's best response

The following proposition establishes the characterization of the best response $\mathrm{BR}_{2,\pi}$ in (4.3) for the follower and for a given strategy γ_1 of the leader.

Proposition 6. *Let $\gamma_1 \in \Gamma_1$. The Best response of the follower is characterized by :* $(\mathcal{K}_{2,\pi}^{\mathrm{BR}}(\gamma_1), \widetilde{\mathcal{K}}_{2,\pi}^{\mathrm{BR}}(\gamma_1)) \in$

$$\begin{aligned}
&\underset{\mathcal{K}_2,\widetilde{\mathcal{K}}_2}{\operatorname{argmax}} \sum_{k\in\mathcal{K}_2\setminus\widetilde{\mathcal{K}}_2} p_{2k}\left(1-\frac{1}{\max\left(\frac{\gamma_{1k}}{\delta_{1k}}+\pi,1\right)}\right)\\
&\qquad\qquad + \sum_{k\in\mathcal{K}_2} p_{2k}\left(1-\frac{\sqrt{\frac{\delta_{2k}}{p_{2k}}}\sum_{\ell\in\widetilde{\mathcal{K}}_2}\sqrt{p_{2\ell}\delta_{2\ell}}}{\mathrm{B}_2-\sum_{\ell\in\mathcal{K}_2\setminus\widetilde{\mathcal{K}}_2}\delta_{2\ell}\max\left(\frac{\gamma_{1\ell}}{\delta_{1\ell}}+\pi,1\right)}\right)\\
&\text{s.t.}\forall k\in\widetilde{\mathcal{K}}_2,\\
&\frac{\sqrt{p_{2k}\delta_{2k}}\left[\mathrm{B}_2-\sum_{\ell\in\mathcal{K}_2\setminus\widetilde{\mathcal{K}}_2}\delta_{2\ell}\max\left(\frac{\gamma_{1\ell}}{\delta_{1\ell}}+\pi,1\right)\right]}{\sum_{\ell\in\widetilde{\mathcal{K}}_2}\sqrt{p_{2\ell}\delta_{2\ell}}} > \delta_{2k}\max\left(\frac{\gamma_{1k}}{\delta_{1k}}+\pi,1\right).
\end{aligned}$$

Furthermore, any $\gamma_{2,\pi}^{\mathrm{BR}} \in \mathrm{BR}_{2,\pi}(\gamma_1)$ is defined by :

$$\gamma_{2k,\pi}^{\mathrm{BR}} = \begin{cases} 0 & \text{if } k\in\mathcal{K}\setminus\mathcal{K}_{2,\pi}^{\mathrm{BR}}(\gamma_1),\\ \delta_{2k}\max\left(\frac{\gamma_{1k}}{\delta_{1k}}+\pi,1\right) & \text{if } k\in\mathcal{K}_{2,\pi}^{\mathrm{BR}}(\gamma_1)\setminus\widetilde{\mathcal{K}}_{2,\pi}^{\mathrm{BR}}(\gamma_1),\\ \dfrac{\sqrt{p_{2k}\delta_{2k}}\left[\mathrm{B}_2-\sum_{\ell\in\mathcal{K}_{2,\pi}^{\mathrm{BR}}(\gamma_1)\setminus\widetilde{\mathcal{K}}_{2,\pi}^{\mathrm{BR}}(\gamma_1)}\gamma_{2\ell}^{\mathrm{BR}}\right]}{\sum_{\ell\in\widetilde{\mathcal{K}}_{2,\pi}^{\mathrm{BR}}(\gamma_1)}\sqrt{p_{2\ell}\delta_{2\ell}}}, & \text{if } k\in\widetilde{\mathcal{K}}_{2,\pi}^{\mathrm{BR}}(\gamma_1). \end{cases} \tag{4.7}$$

Proof. See Appendix 4.5.2. ■

4.3 Numerical performance analysis

The Colonel Blotto Game applied to the winner takes all model.

The Colonel Blotto Game presents an intriguing example for demonstrating the Stackelberg game formulated in this chapter, particularly in the context of the winner-takes-all problem. Please refer to the example provided in Section 1.2.2.

In this illustration, let us consider a scenario where two firms engage in competition to compete compete for market share across $K = 5$ regions. For each region $k \in \mathcal{K}$ and every Firm $m \in \mathcal{M}$, certain assumptions are made : the winning price $p_{mk} = 1$, the churn rates $\delta_{mk} = 10^{-10}$, and the barrier to entry $\pi = 10^{-10}$. Due to the insignificant nature of churn rates for each company and region, the utility region graph can be represented as a discrete map, as shown in Fig. 4.1. Furthermore, it is observed that the Pareto border remains unaffected by the specific values assigned to the budgets B_1 and B_2. Additionally, regardless of the values of B_1 and B_2, the Stackelberg equilibrium consistently lies on the Pareto border.

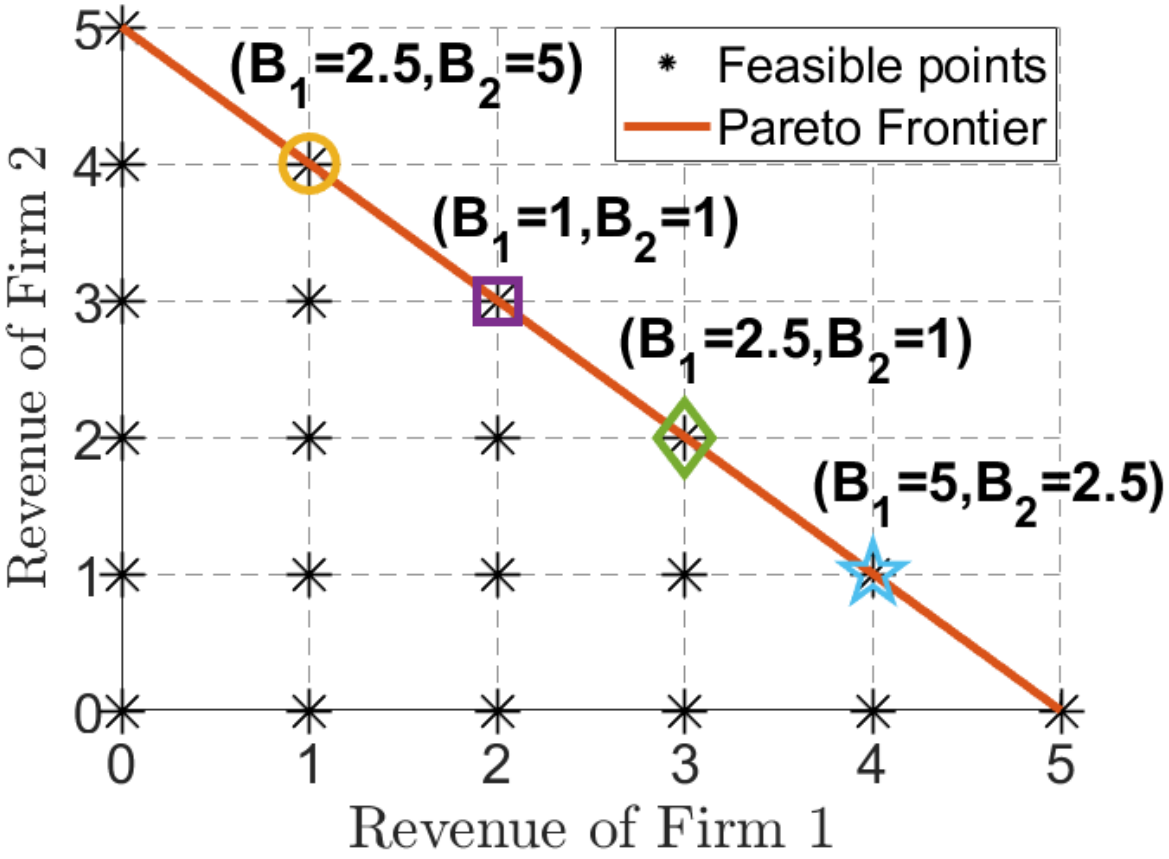

FIGURE 4.1 – Revenue of each firm at the Stackelberg equilbrium for values of $(\mathrm{B}_1, \mathrm{B}_2)$ in the utility region graph with the Pareto border and feasible points.

More general case : when the churn rates $\delta_{mk} > 0$.
In what follows, we illustrate the solutions of the Stackelberg game when both firms play pessimistically over a network of $K = 5$ regions. The parameters of the game are given by : $p_1 = (p_{11}, \ldots, p_{15}) = (1, 2, 3, 4, 5)$; $p_2 = (p_{11}, \ldots, p_{25}) = (2, 3, 1, 5, 4)$; $\delta_1 = (\delta_{11}, \ldots, \delta_{15}) = 10^{-1} \times (5, 4, 3, 2, 1)$; $\delta_2 = (\delta_{21}, \ldots, \delta_{25}) = 10^{-1} \times (1, 2, 3, 4, 5)$ and the entry price for the follower is fixed at $\pi = 10^{-6}$.

Budgets	$(\gamma^S_{11,\pi}, \gamma^S_{21,\pi})$	$(\gamma^S_{12,\pi}, \gamma^S_{22,\pi})$	$(\gamma^S_{13,\pi}, \gamma^S_{23,\pi})$
(0.6,0.6)	(0.2,0)	(0.4,0)	(0,0)
(0.6,0.6)	(0,0)	(0,0)	(0.6,0)
(0.6,5)	(0.6,0)	(0,1.298)	(0,1.377)
(5,0.6)	(0.5,0)	(1,0)	(1.5,0)
(5,5)	(0.833,0)	(1.666,0)	(2.5,0)

Budgets	$(\gamma^S_{14,\pi}, \gamma^S_{24,\pi})$	$(\gamma^S_{15,\pi}, \gamma^S_{25,\pi})$
(0.6,0.6)	(0,0.335)	(0,0.264)
(0.6,0.6)	(0,0.335)	(0,0.264)
(0.6,5)	(0,1.298)	(0,1.025)
(5,0.6)	(2,0)	(0,0.6)
(5,5)	(0,2.79)	(0,2.20)

TABLE 4.1 – Budget allocation at the Stackelberg Strategy for different value of $(\mathrm{B}_1, \mathrm{B}_2)$

Fig. 4.2 represents the revenues of the two firms in the utility region, when they both apply Stackelberg's pessimistic strategy and for different budget values. In the case of equal budgets $\mathrm{B}_1 = \mathrm{B}_2$ the follower has a higher revenue at the Stackelberg equilibrium due to the difference in the churn rate in regions 4 and 5. When one budget is much higher the corresponding Firm gets a larger revenue. We also observe that, at the Stackelberg equilibrium, there is no case where $\mathrm{B}_1 \leq \mathrm{B}_2$ such that $u^S_{1,\pi}(\gamma^S_\pi) \geq u^S_{2,\pi}(\gamma^S_\pi)$. The TABLE. 4.1 shows the Stackelberg strategy allocation for the couples $(\mathrm{B}_1, \mathrm{B}_2)$ highlighted in Fig. 4.2.

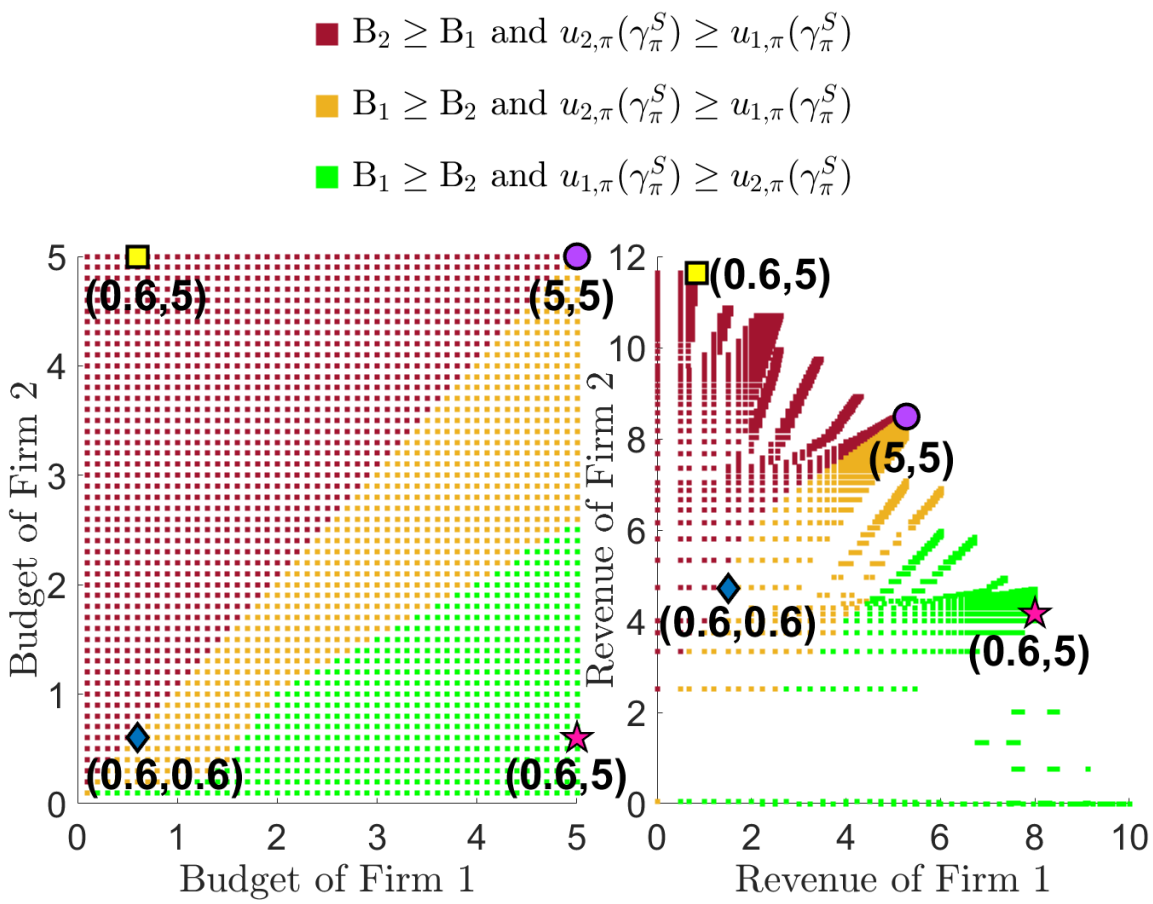

FIGURE 4.2 – Revenue of each firm (right) at the Stackelberg equilbrium for values of (B_1, B_2) shown on the left.

Another interesting aspect to explore is the impact of partial information on the decision-making process. For the purpose of addressing this question numerically, we assume a budget of $(B_1, B_2) = (5, 5)$ for both firms. We consider a scenario where each firm m makes a decision by estimating a noisy churn rate of the other competitor. Specifically, Firm m makes a decision based on $\widehat{\delta}{-m} = \delta{-m} + \omega$, where ω follows a normal distribution $\mathcal{N}(0, \sigma^2)$. To analyze the impact of partial information, we compute 1000 realizations of ω for each standard deviation value σ in the range $\{0, 0.1, 0.2, \ldots, 1\}$.

Fig. 4.3 presents the results of this numerical analysis, showing the probability of collision (the probability that both players invest in the same region) and the expectation of rate losses for each firm, denoted as (ρ_1, ρ_2) w.r.t. the standard deviation σ. Here, ρ_m represents the ratio of the expected utility achieved by firm m when using the estimated profile actions $\widehat{\gamma}^S$ to the expected utility achieved when using the true profile actions γ^S i.e., (i.e., $\forall m \in \{1, 2\}$, $\rho_m := \mathbb{E}[u_m^S(\widehat{\gamma}^S)/u_m^S(\gamma^S)]$). From the plot, we observe that the leader's revenue tends to increase as the uncertainty or noise level σ increases at the Stackelberg equilibrium, while the opposite

trend is observed for the follower. This suggests that increased uncertainty benefits the leader more than the follower in terms of revenue generation. Additionally, the probability of collision tends to increase with the standard deviation σ, indicating a higher likelihood of both players investing in the same region as the level of uncertainty grows.

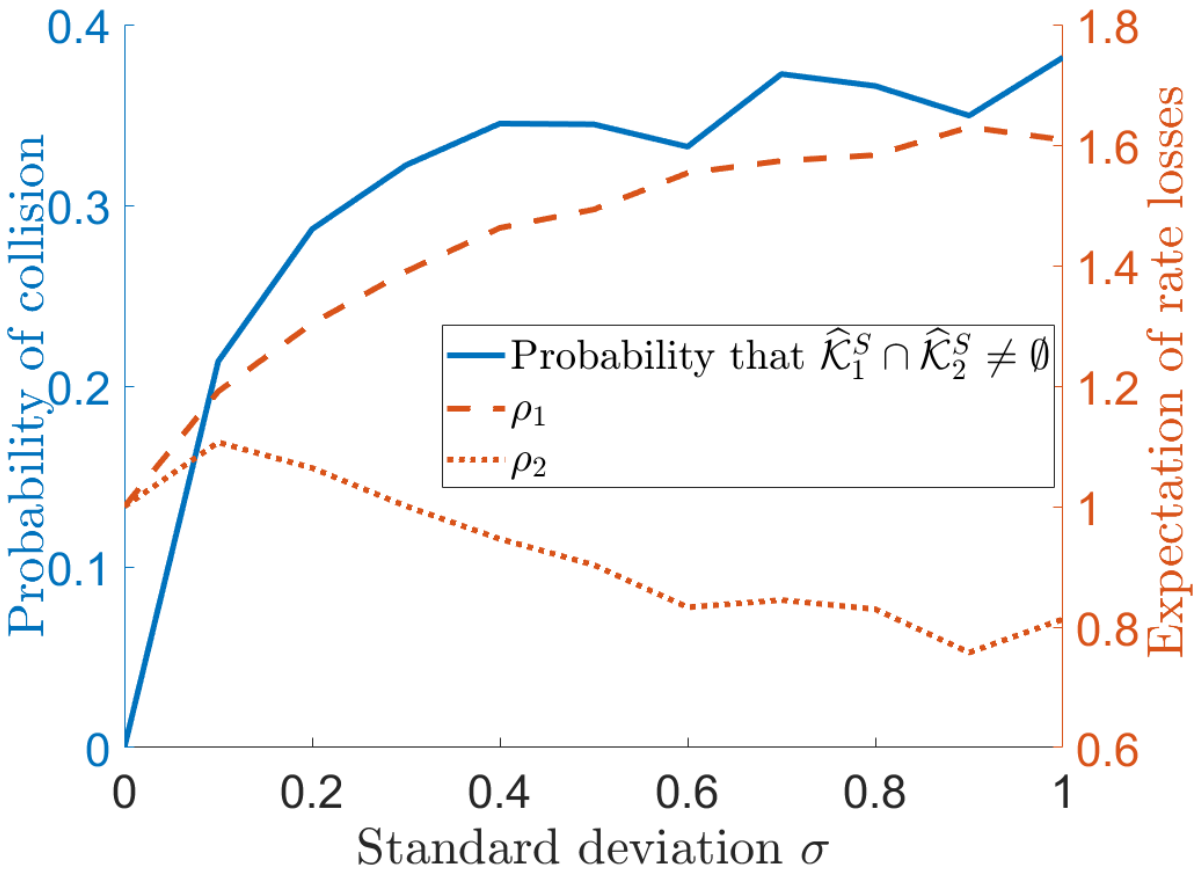

FIGURE 4.3 – Plot of the probability of collision and the expectation of rate losses for each firm (ρ_1, ρ_2) w.r.t. the standard deviation σ.

The presented numerical analysis demonstrates the potential for investigating the effects of partial information and uncertainty in the context of the Stackelberg duopoly game. Further exploration of these factors can provide valuable insights into the decision-making dynamics and strategic interactions between firms, contributing to the understanding and improvement of the proposed model.

4.4 Conclusion

In conclusion, the chapter presents a detailed analysis of a static Stackelberg duopoly game. We formulate a game model where two firms, a leader and a follower, compete to maximize

revenue under individual budget constraint. The utility functions of both firms are defined according to the so-called "winner takes all" model, and a weak Stackelberg equilibrium is considered (the analysis still holds for a strong Stackelberg equilibrium). The main result of the chapter, stated in Theorem 8, provides the characterization of the weak Stackelberg strategy. In this context, the leader acts as the first mover and sets its strategy to maximize its revenue under a budget constraint, taking into account the follower's potential response. On the other hand, the follower strategically responds to the leader's chosen strategy by maximizing its own revenue while minimizing the leader's revenue. The chapter presents a reformulation of the follower's optimization problem and provides a characterization of the follower's best response in Propositions 5 and 6, respectively. These results contribute to a better understanding of the game and provide insights into the Stackelberg strategy by proving that the best response map of the leader can be found by solving a convex OP. Numerical examples are provided to illustrate the application of the Stackelberg game model. The examples demonstrate the revenue outcomes for different budget allocations and parameter values, including scenarios with the Colonel Blotto Game and cases with non-zero churn rates. Furthermore, the numerical analysis conducted in this study emphasizes the importance of uncertainty and noise levels in influencing revenue and decision-making within the context of a Stackelberg duopoly game. The findings reveal that increased uncertainty tends to favor the leader firm in terms of revenue outcomes. Additionally, the study highlights that as uncertainty grows, there is a higher probability of both players investing in the same region, leading to collision.

4.5 Appendix

4.5.1 Proof of Proposition 5

In view of (4.3), the follower's OP can be rewritten in the following manner by considering both cases of Firm 2 winning or not in region k :

$$\max_{\gamma_2 \in \Gamma_2} \sum_{\mathcal{K}_2 \in 2^{\mathcal{K}}} \left[\sum_{k \in \mathcal{K}_2} p_{2k} \left(1 - \frac{\delta_{2k}}{\gamma_{2k}} \right) \right] \mathbb{1}_{\widetilde{\Gamma}_{2,\pi}(\mathcal{K}_2, \gamma_1)}(\gamma_2), \tag{P_1}$$

where $\widetilde{\Gamma}_{2,\pi}$ is introduced in (4.6) and $\mathbb{1}$ is the indicator function.

Let $\gamma_2, \widehat{\gamma}_2 \in \Gamma_2, \mathcal{K}_2, \widehat{\mathcal{K}}_2 \in 2^{\mathcal{K}}$ such that $\mathcal{K}_2 \neq \widehat{\mathcal{K}}_2$ and $\mathbb{1}_{\widetilde{\Gamma}_{2,\pi}(\mathcal{K}_2, \gamma_1)}(\gamma_2) = \mathbb{1}_{\widetilde{\Gamma}_{2,\pi}(\widehat{\mathcal{K}}_2, \gamma_1)}(\widehat{\gamma}_2) = 1$. Then, $\widetilde{\Gamma}_{2,\pi}(\mathcal{K}_2, \gamma_1) \cap \widetilde{\Gamma}_{2,\pi}(\widehat{\mathcal{K}}_2, \gamma_1) = \emptyset$ since $\mathcal{K}_2 \neq \widehat{\mathcal{K}}_2$ and (P_1) can be reformulated such as

$$\max_{\mathcal{K}_2 \in 2^{\mathcal{K}}} \left[\max_{\gamma_2 \in \Gamma_2} \Big[\sum_{k \in \mathcal{K}_2} p_{2k} \left(1 - \frac{\delta_{2k}}{\gamma_{2k}} \right) \Big] \mathbb{1}_{\widetilde{\Gamma}_{2,\pi}(\mathcal{K}_2, \gamma_1)}(\gamma_2) \right]. \tag{P_2}$$

Furthermore, for a given $\mathcal{K}_2$ there exits a strategy $\gamma_2 \in \widetilde{\Gamma}_m(\mathcal{K}_2, \gamma_1)$ that verifies the budget constraint if and only if the set $\mathcal{K}_2$ verifies $\sum_{k\in\mathcal{K}_2} \delta_{2k} \max\left(\frac{\gamma_{1k}}{\delta_{1k}} + \pi, 1\right) \leq \mathrm{B}_2$ i.e., the less restrictive action of $\widetilde{\Gamma}_{2,\pi}(\mathcal{K}_2, \gamma_1)$ verifies the budget constraint. Hence, by using the indicator function and by adding the new constraint on the feasibility sets of $\mathcal{K}_2$, the problem (P_2) is equivalent to $(P^\star)$.

4.5.2 Proof of Proposion 6

According to Proposition 5, the best response of Firm 2 is characterized by the best part $\mathcal{K}_2 \in 2^{\mathcal{K}}$ that maximises

$$\begin{aligned} &\max_{\gamma_2} \sum_{k\in\mathcal{K}_2} p_{2k}\left(1 - \frac{\delta_{2k}}{\gamma_{2k}}\right) \\ &\text{s.t.} \gamma_2 \in \widetilde{\Gamma}_{2,\pi}(\mathcal{K}_2, \gamma_1),\ \sum_{k=1}^{K} \gamma_{2k} \leq \mathrm{B}_2. \end{aligned} \tag{4.8}$$

Let us exploit the KKT conditions by defining first the Lagrangian :

$$\begin{aligned} \mathcal{L}(\gamma_2, \mu_2, \underline{\mu}_2, \lambda_2) := &\sum_{k\in\mathcal{K}\setminus\mathcal{K}_2} \underline{\mu}_{2k}\gamma_{2k} + \sum_{k\in\mathcal{K}_2} p_{2k}\left(1 - \frac{\delta_{2k}}{\gamma_{2k}}\right) - \lambda_2\left(\sum_{k=1}^{K}\gamma_{2k} - \mathrm{B}_2\right) \\ &+ \sum_{k\in\mathcal{K}_2} \mu_{2k}\left(\gamma_{2k} - \delta_{2k}\max\left(\frac{\gamma_{1k}}{\delta_{1k}} + \pi, 1\right)\right) - \sum_{k\in\mathcal{K}\setminus\mathcal{K}_2} \mu_{2k}\left(\gamma_{2k} - \delta_{2k}\max\left(\frac{\gamma_{1k}}{\delta_{1k}}, 1\right)\right). \end{aligned}$$

Let us denote by $\gamma^\star_{2k,\pi}$, $\mu^\star_{2k,\pi}$, $\lambda^\star_{2,\pi}$ and $\underline{\mu}^\star_{2k,\pi}$ the variables that verify the first-order optimality condition.

For all $k \in \mathcal{K}\setminus\mathcal{K}_2$, $\frac{\partial\mathcal{L}}{\partial\gamma_{2k}} = -\lambda^\star_{2,\pi} - \mu^\star_{2k,\pi} + \underline{\mu}^\star_{2k,\pi} = 0$, then $\mu^\star_{2k,\pi} = 0$, $\underline{\mu}^\star_{2k,\pi} = \lambda^\star_{2,\pi} > 0$ and $\gamma^\star_{2k,\pi} = 0$.

For all $k \in \mathcal{K}_2$, $\frac{\partial\mathcal{L}}{\partial\gamma_{2k}} = \frac{p_{2k}\delta_{2k}}{(\gamma^\star_{2k,\pi})^2} - \lambda^\star_{2,\pi} - \mu^\star_{2k,\pi} = 0$, then $\gamma^\star_{2k,\pi} = \sqrt{\frac{p_{2k}\delta_{2k}}{(\lambda^\star_{2,\pi} + \mu^\star_{2k,\pi})}}$.

Let $\widetilde{\mathcal{K}}_2 \in 2^{\mathcal{K}_2}$ (that may be empty) such that, $\widetilde{\mathcal{K}}_2 \in \{\widetilde{\mathcal{K}} \in 2^{\mathcal{K}_2} : \forall k \in \widetilde{\mathcal{K}},\ \mu^\star_{2k,\pi} = 0\}$. For all $k \in \widetilde{\mathcal{K}}_2$, the first-order optimality condition is verified when, $\gamma^\star_{2k,\pi} = \sqrt{\frac{p_{2k}\delta_{2k}}{\lambda^\star_{2,\pi}}} > \delta_{2k}\max\left(\frac{\gamma_{1k}}{\delta_{1k}} + \pi, 1\right)$ and $\gamma^\star_{2k,\pi} = \delta_{2k}\max\left(\frac{\gamma_{1k}}{\delta_{1k}} + \pi, 1\right)$, $\forall k \in \mathcal{K}_2 \setminus \widetilde{\mathcal{K}}_2$. Since $\lambda^\star_{2,\pi} > 0$, it follows that, $\sum_{k=1}^{K}\gamma^\star_{2k,\pi} = \mathrm{B}_2$. Hence, $\sum_{\ell\in\widetilde{\mathcal{K}}_2}\gamma^\star_{2\ell,\pi} = \mathrm{B}_2 - \sum_{\ell\in\mathcal{K}_2\setminus\widetilde{\mathcal{K}}_2}\gamma^\star_{2\ell,\pi} \Rightarrow \sqrt{\lambda^\star_{2,\pi}} =$

$\dfrac{\sum\limits_{\ell\in\widetilde{\mathcal{K}}_2}\sqrt{p_{2\ell}\delta_{2\ell}}}{\mathrm{B}_2-\sum\limits_{\ell\in\mathcal{K}_2\setminus\widetilde{\mathcal{K}}_2}\gamma^\star_{2\ell}}$. Thus, the solution of (4.8) is characterized by $\gamma^\star_{2k,\pi}=$

$$\begin{cases} 0 & \text{if } k\in\mathcal{K}\setminus\mathcal{K}_2,\\ \delta_{2k}\max\left(\dfrac{\gamma_{1k}}{\delta_{1k}}+\pi,1\right) & \text{if } k\in\mathcal{K}_2\setminus\widetilde{\mathcal{K}}_2,\\ \dfrac{\sqrt{p_{2k}\delta_{2k}}\left[\mathrm{B}_2-\sum\limits_{\ell\in\mathcal{K}_2\setminus\widetilde{\mathcal{K}}_2}\gamma^\star_{2\ell,\pi}\right]}{\sum\limits_{\ell\in\widetilde{\mathcal{K}}_2}\sqrt{p_{2\ell}\delta_{2\ell}}} & \text{if } k\in\widetilde{\mathcal{K}}_2. \end{cases}$$

Finally, the best response of the follower is obtained by a selection of $\mathcal{K}_2$ and $\widetilde{\mathcal{K}}_2$ solving the discrete OP as stated in Proposition 6.

4.5.3 Proof of Theorem 8

In view of (4.3) and Proposition 5, the utility of the leader can be reformulated such as $u^S_{1,\pi}(\gamma_1)=\sum\limits_{\mathcal{K}_1\in2^{\mathcal{K}}}\Big[\sum\limits_{k\in\mathcal{K}_1}p_{1k}(1-\dfrac{\delta_{1k}}{\gamma_{1k}})\mathbb{1}_{\widehat{\Gamma}_{1,\pi}(\mathcal{K}_1)}(\gamma_1)\Big]$, and we recall that $\widehat{\Gamma}_{1,\pi}(\mathcal{K}_1)$ is defined before Theorem 8. Thus, we identify the same utility structure as in the proof of Proposition 5 and at the Stackelberg equilibria, it can be written as

$$u^S_{1,\pi}(\gamma^S_{1,\pi})=\max_{\mathcal{K}_1\in2^{\mathcal{K}}}\max_{\gamma_1\in\Gamma_1}\widehat{S}_\pi(\mathcal{K}_1,\gamma_1) \tag{4.9}$$

where $\widehat{S}_\pi(\mathcal{K}_1,\gamma_1)$ is defined in (4.4). Concerning the existence of the Stackelberg strategy, the result is mainly based on the existence of a feasible solution in the set of constraints for the leader. Since $\mathcal{K}_1=\emptyset$ and $\gamma_1=(0,\dots,0)$ is in the set of constraints, we derive that the game $\mathcal{G}^S_\pi$ has at least one Stackelberg equilibrium.

In order to compute numerically (4.9) with well known solvers for convex optimization problems, let us prove that $\widehat{\Gamma}_{1,\pi}(\mathcal{K}_1)$ is a convex set. Let $\gamma^a_1\in\widehat{\Gamma}_{1,\pi}(\mathcal{K}_1)$ and $\gamma^b_1\in\widehat{\Gamma}_{1,\pi}(\mathcal{K}_1)$. Hence $\forall k\in\mathcal{K}_1$ and $i\in\{a,b\}$,

$$\frac{\gamma^i_{1k}}{\delta_{1k}}\geq\max\left(\frac{\mathrm{BR}^-_{2k,\pi}(\gamma^i_1)}{\delta_{2k}},1\right).$$

From the best response characterization of the follower in Proposition 6 one has that $\forall k\in\mathcal{K}_1$, $\mathrm{BR}^-_{2k,\pi}(\gamma^i_1)=0$. Hence $\forall k\in\mathcal{K}_1$, $\gamma^i_{1k}\geq\delta_{1k}$. Let $\tau\in(0,1)$ and $\gamma^b_{1k}\geq\tau\gamma^a_{1k}+(1-\tau)\gamma^b_{1k}\geq\gamma^a_{1k}$. From the monotony of the best response of the follower w.r.t the action of the leader it follows that, $\forall k\in\mathcal{K}_1$, $\mathrm{BR}^-_{2k,\pi}(\tau\gamma^a_{1k}+(1-\tau)\gamma^b_{1k})=0$.

Hence, $\tau\gamma^a_{1k}+(1-\tau)\gamma^b_{1k} \in \widehat{\Gamma}_{1,\pi}(\mathcal{K}_1)$. Finally, (4.9) is a strictly convex OP that can be solved with numerical solver for convex OP. Finally, at the Stackelberg equilibrium this analysis guarantees that $\forall k \in \mathcal{K}^S_{1,\pi}$ (region where the leader invest), $\mathrm{BR}^-_{2k,\pi}(\gamma^S_{1,\pi}) = 0$, and in view of Proposition 6 we derive that the follower's strategy is given by $\gamma^S_{2k,\pi} = \dfrac{\sqrt{p_{2k}\delta_{2k}}}{\sum\limits_{\ell\in\mathcal{K}^S_{2,\pi}}\sqrt{p_{2\ell}\delta_{2\ell}}}\mathrm{B}_2$ if $k \in \mathcal{K}^S_{2,\pi}$ and $\gamma^S_{2k,\pi} = 0$ otherwise, where $\mathcal{K}^S_{2,\pi}$ is defined in Theorem 8.

Chapter 5

Concluding remarks and perspectives

Overview

In this thesis, we have explored the effects of decentralization on various aspects of epidemic management and viral marketing through the lens of game theory. The analysis provides valuable insights into the trade-offs, efficiency considerations, and strategic decision-making processes involved in decentralized decision-making. The findings highlight the importance of considering factors such as graph connectivity, opinion dynamics, and competitive market dynamics in designing effective decentralized management strategies.

In Chapter 2, we developed a mathematical model to examine the effects of decentralization on epidemic management. By formulating the problem as a strategic-form game based on a networked Susceptible-Infected-Recovered (SIR) compartmental model, we assume a Weak Interconnection Regime (WIR) to investigate the Nash Equilibrium (NE) and to assess the efficiency of decentralized decision-making. We introduced the Price of Anarchy (PoA) and the Price of Connectedness (PoC) as metrics to evaluate the performance of the NE strategy, in order to compare the optimal centralized strategy or to highlight the importance of taking into account the graph structure in the decentralized decision making process. Through numerical simulations, we demonstrated the critical role of graph connectivity in decentralized decision-making. Additionally, we extended our analysis to consider healthcare resource constraints, shedding light on the implications of resource availability and adequacy and uncovered the existence of the Braess Paradox, which revealed counter intuitive effects of decentralized control.

In Chapter 3, we introduced a methodology to evaluate the impact of decentralization on epidemic management, incorporating time-varying opinion dynamics. We integrated the

networked SIR model with a time-varying opinion dynamics model, creating a generalized strategic-form game, where each player implements a trade-off between socio-economic losses, health losses, awareness campaigns, and opinions. To analyze the Generalized Nash Equilibrium (GNE) within the framework of our model, we made key assumptions regarding the epidemic graph and the time-varying social networks. These assumptions provided the necessary conditions for conducting the analysis. To address the complexity of the problem, we formulated an equivalent auxiliary game that allowed us to examine the GNE in a more tractable manner. We showcased the role of influence control in decentralized decision-making, highlighting scenarios where opinion control can significantly reduce the Price of Anarchy (PoA).

In Chapter 4, we delved into a static Stackelberg duopoly game to explore the effects of decentralization on revenue maximization in a competitive market. We developed a game model with a leader and a follower, with the leader acting as the first mover. By characterizing the weak Stackelberg strategy and analyzing the follower's best response, we provided insights into the decision-making dynamics of firms operating under budget constraints. Through numerical examples, including scenarios with the Colonel Blotto Game and non-zero churn rates, we illustrated the application of the Stackelberg game model and examined revenue outcomes for different budget allocations and parameter values.

Overall, this thesis provides a comprehensive understanding of the implications of decentralization on epidemic management and viral marketing competition. Through the lens of game theory, we have explored the efficiency of decentralized decision-making in the context of spreading phenomenon dynamics. Our findings highlight the critical role of graph connectivity, opinion dynamics, and competitive market dynamics in shaping the effectiveness of decentralized strategies. This research contributes theoretical insights and practical guidance that can inform decision-makers in the field of epidemic management, aiding in the development of effective strategies for disease control and mitigation.

Perspectives

Having examined the contributions of each chapter, we now turn our attention to potential perspectives for future work.

Problem of Decentralized Epidemic Management (Chapter 2 and Chapter 3) :

While the chapters provide valuable insights and analysis, there are several avenues for

future research that can enhance the models and their applicability. Some potential areas for improvement include :

Incorporating more realistic and complex dynamics : The models presented in the thesis provide a foundation for understanding epidemic management and decision-making. However, future work could explore more intricate dynamics, such as incorporating different stages of infection, heterogeneous populations, and varying transmission rates. One possibility is to investigate a dynamical game formulation, which would consider the evolution of strategies and dynamics of the epidemic and opinion dynamics over time. This would provide a more realistic and comprehensive analysis of the system dynamics and the strategic interactions between regions.

Addressing uncertainty, stochasticity and scalability : Real-world epidemic scenarios involve various sources of uncertainty and stochasticity. Future research could explore how to incorporate uncertainty in the models, such as incorporating probabilistic parameters or considering random variations in transmission rates. This would provide a more realistic representation of the inherent uncertainties in epidemic management. Scalability issues can also be addressed by considering the case of a large number of regions. The use of a mean-field game approach could be explored to approximate the behavior of the entire system based on the behavior of a representative region. This would allow for a more tractable analysis and facilitate the study of large-scale scenarios.

Real-time data integration and policy evaluation : The models presented in the thesis provide valuable insights into epidemic management strategies. However, the developed approaches can be combined with data-driven approaches. By incorporating real-world data on epidemic parameters, network structures, and opinion dynamics, the models can be calibrated and validated against empirical observations. This integration of data-driven techniques would enhance the accuracy and applicability of the models, enabling the assessment of different intervention strategies, such as vaccination campaigns or social distancing measures, and provide evidence-based recommendations for policy-makers.

In Chapter 3, new constraints could be considered in the game formulation. For example, constraints on the fractions of infected individuals in each region could be introduced to reflect the objective of limiting the spread of the virus. By incorporating such constraints, the model would capture additional public health considerations and provide more realistic guidelines for epidemic management strategies.

These potential extensions and improvements would further enhance the analysis and applicability of the proposed approaches, enabling a more comprehensive understanding of epidemic

management and decision-making in complex, real-world scenarios.

Problem of Viral Marketing (Chapter 4) :

Incorporating more realistic and complex dynamics : In Chapter 4, there is potential for further analysis and enhancement of the model by incorporating the network structure into the analysis. The current model focuses on the strategic behavior and outcomes in a Stackelberg duopoly game, where the influence between regions is decoupled. However, by explicitly considering the connections among regions, the model can be extended to better capture the interdependencies and interactions among the regions. One approach to incorporating the network structure is by formulating the model in a way that the fraction of individuals in each region who subscribe to the service of a particular firm becomes dependent on the profile actions of both firms. Specifically, for each region $k \in \mathcal{K}$, firm $m \in 1, 2$, and time period $t > 0$, the fraction of individuals $x_{km}(t)$ who subscribe to firm m can be made dependent on the profile actions γ_1 and γ_2. By introducing this network aspect, the model can better capture the influence and dynamics of interactions between regions and firms. It allows for a more realistic representation of how the strategic decisions of one firm can affect the decisions and outcomes in other regions. The network structure can introduce new strategic considerations and complexities into the Stackelberg duopoly game, leading to potentially different equilibrium strategies and outcomes. Incorporating the network structure into the analysis provides an opportunity to study the effects of different network topologies, dynamics, and interventions on the strategic behavior and performance of the firms. It allows for a more comprehensive understanding of how the connections among regions influence the decision-making process and the resulting outcomes.

Addressing uncertainty, stochasticity : Another interesting aspect to explore is the impact of partial information on the decision-making process. The analysis in Chapter 4 in Section 4.3 underscores the significance of uncertainty and noise levels in shaping revenue and decision-making for both the leader and follower firms. The study reveals that the leader firm tends to benefit more from increased uncertainty in terms of revenues. The study also indicates that the likelihood of both players investing in the same region, known as the probability of collision, increases with the increase of uncertainty. These results underline the need for further study of the factors contributing to this strategic advantage. Future research can delve into the implications of information asymmetry by considering various degrees of incomplete or imperfect information and evaluating different estimation methods. This deeper analysis would contribute to a more comprehensive understanding of how limited information influences strategic choices and outcomes for firms.

Bibliography

[1] R. Chaudhry, G. Dranitsaris, et al. A country level analysis measuring the impact of government actions, country preparedness and socioeconomic factors on Covid-19 mortality and related health outcomes. *EClinicalMedicine*, 25 :100464, 2020.

[2] C. Bambra, R. Riordan, J. Ford, and F. Matthews. The covid-19 pandemic and health inequalities. *J Epidemiol Community Health*, 74 :964–968, 2020.

[3] P.R. Martins-Filho, L.J. Quintans-Júnior, A.A. de Souza Araújo, K.B. Sposato, et al. Socio-economic inequalities and covid-19 incidence and mortality in brazilian children : a nationwide register-based study. *Public Health*, 190 :4–6, 2021.

[4] Daniel J Elazar. *Exploring federalism*. University of Alabama Press, 1987.

[5] S. Lasaulce, C. Zhang, V. Varma, and I.C. Morărescu. Analysis of the tradeoff between health and economic impacts of the Covid-19 epidemic. *Frontiers in Public Health*, 9 :173, 2021.

[6] N. Dagnall, K-G. Drinkwater, A. Denovan, et al. Bridging the gap between uk government strategic narratives and public opinion/behavior : Lessons from covid-19. *Frontiers in Communication*, 5 :71, 2020.

[7] I.C. Morărescu, V.S Varma, L. Buşoniu, and S. Lasaulce. Space-time budget allocation policy design for viral marketing. *Nonlinear Analysis : Hybrid Systems*, 37 :100899, 2020.

[8] O. Lindamulage de Silva, V.S Varma, I.C Morărescu, and S. Lasaulce. Optimal influence budget allocation for viral marketing using a multiple virus SIS model. working paper or preprint, March 2023.

[9] S. Jurvetson. What exactly is viral marketing. *Red Herring*, 78(110-112) :101, 2000.

[10] C. Nowzari, V.M. Preciado, and G.J. Pappas. Analysis and control of epidemics : A survey of spreading processes on complex networks. *IEEE Control Systems Magazine*, pages 26–46, 2016.

[11] S.F. Ruf, K. Paarporn, P-E. Paré, and M. Egerstedt. Dynamics of opinion-dependent product spread. In *2017 IEEE 56th Annual Conference on Decision and Control (CDC)*, pages 2935–2940, 2017.

[12] P. Magal, O. Seydi, and G. Webb. Final size of an epidemic for a two-group SIR model. *SIAM Journal on Applied Mathematics*, pages 2042–2059, 2016.

[13] W. Mei, S. Mohagheghi, S. Zampieri, and F. Bullo. On the dynamics of deterministic epidemic propagation over networks. *Annual Reviews in Control*, 44 :116–128, 2017.

[14] B. She, J. Liu, S. Sundaram, and P-E. Pare. On a networked sis epidemic model with cooperative and antagonistic opinion dynamics. *IEEE Transactions on Control of Network Systems*, pages 1–1, 2022.

[15] B. She, C. H. Leung, S. Sundaram, and P-E. Paré. Peak infection time for a networked sir epidemic with opinion dynamics. In *2021 60th IEEE Conference on Decision and Control (CDC)*, pages 2104–2109, 2021.

[16] S.F. Ruf, K. Paarporn, and P-E. Paré. Going viral : Stability of consensus-driven adoptive spread. *IEEE Transactions on Network Science and Engineering*, 7(3) :1764–1773, 2019.

[17] S.F. Ruf, P-E. Paré, J. Liu, et al. A viral model of product adoption with antagonistic interactions. In *2019 American Control Conference (ACC)*, pages 3382–3387, 2019.

[18] Y. Lin, W. Xuan, R. Ren, and J. Liu. On a discrete-time network sis model with opinion dynamics. In *2021 60th IEEE Conference on Decision and Control (CDC)*, pages 2098–2103. IEEE, 2021.

[19] V.M. Preciado, M. Zargham, C. Enyioha, A. Jadbabaie, and G-J. Pappas. Optimal resource allocation for network protection against spreading processes. *IEEE Transactions on Control of Network Systems*, 1(1) :99–108, 2014.

[20] F. Liu, Y. Chen, T. Liu, D. Xue, and M. Buss. Distributed link removal strategy for networked meta-population epidemics and its application to the control of the covid-19 pandemic. In *2021 60th IEEE Conference on Decision and Control (CDC)*, pages 2824–2829, 2021.

[21] R. Anzum and Md. Z. Islam. Mathematical modeling of coronavirus reproduction rate with policy and behavioral effects. *MedRXiv*, 2021.

[22] C. Gollier. Cost–benefit analysis of age-specific deconfinement strategies. *Journal of Public Economic Theory*, pages 1746–1771, 2020.

[23] R. Srinivasan. *Winner-Takes-All Dynamics*, pages 199–215. Springer Singapore, Singapore, 2021.

[24] B.A Prakash, A. Beutel, R. Rosenfeld, and C. Faloutsos. Winner takes all : competing viruses or ideas on fair-play networks. In *Proceedings of the 21st international conference on World Wide Web*, pages 1037–1046, 2012.

[25] G. Antonelli. Interconnected dynamic systems : An overview on distributed control. *IEEE Control Systems Magazine*, 33(1) :76–88, 2013.

[26] D. Bernoulli. Essai d'une nouvelle analyse de la mortalité causée par la petite vérole, et des avantages de l'inoculation pour la prévenir. *Histoire de l'Acad., Roy. Sci.(Paris) avec Mem*, pages 1–45, 1760.

[27] W.O. Kermack and A.G. McKendrick. A contribution to the mathematical theory of epidemics : II. *Proceedings of the royal society of london. Series A, Containing papers of a mathematical and physical character*, pages 55–83, 1932.

[28] R. Anderson and R. May. *Infectious diseases of humans : dynamics and control*. Oxford university press, 1992.

[29] A.J. Lotka and L.I. Dublin. On the true rate of natural increase. *Journal of the American Statistical Association*, 20(151) :305–339, 1925.

[30] J. A. P. Heesterbeek. A brief history of r 0 and a recipe for its calculation. *Acta biotheoretica*, 50 :189–204, 2002.

[31] R. Pastor-Satorras, C. Castellano, P. Van Mieghem, and A. Vespignani. Epidemic processes in complex networks. *Reviews of modern physics*, 2015.

[32] L. Stella, A.P Martínez, D. Bauso, and P. Colaneri. The role of asymptomatic individuals in the Covid-19 pandemic via complex networks. *arXiv preprint arXiv :2009.03649*, 2020.

[33] J. Kephart and S. White. Directed-graph epidemiological models of computer viruses. In *Computation : the micro and the macro view*, pages 71–102. World Scientific, 1992.

[34] M. Mesbahi and M. Egerstedt. *Graph theoretic methods in multiagent networks*, volume 33. Princeton University Press, 2010.

[35] R. Elie, E. Hubert, and G. Turinici. Contact rate epidemic control of COVID-19 : an equilibrium view. *arXiv 2004.08221*, 2020.

[36] A.R. Hota and S. Sundaram. Game-theoretic vaccination against networked SIS epidemics and impacts of human decision-making. *IEEE Transactions on Control of Network Systems*, pages 1461–1472, 2019.

[37] J. Omic, A. Orda, and P. Van Mieghem. Protecting against network infections : A game theoretic perspective. In *IEEE Conference on Computer Communications (INFOCOM)*, pages 1485–1493, 2009.

[38] Y. Hayel, S. Trajanovski, E. Altman, H. Wang, and P. Van Mieghem. Complete game-theoretic characterization of SIS epidemics protection strategies. pages 1179–1184. IEEE, 2014.

[39] S. Trajanovski and et al. Decentralized protection strategies against SIS epidemics in networks. *IEEE Transactions on Control of Network Systems*, 2(4) :406–419, 2015.

[40] O. Lindamulage De Silva, S. Lasaulce, and I.C. Morărescu. On the efficiency of decentralized epidemic management and application to Covid-19. *IEEE Control Systems Letters*, 6 :884–889, 2022.

[41] Y. Huang and Q. Zhu. A differential game approach to decentralized virus-resistant weight adaptation policy over complex networks. *IEEE Transactions on Control of Network Systems*, 7 :944–955, 2020.

[42] S. Tu and S. Neumann. A viral marketing-based model for opinion dynamics in online social networks. In *ACM Web Conference*, pages 1570–1578, 2022.

[43] J. Liu, P-E Paré, A. Nedić, C-Y Tang, C-L Beck, and T. Başar. On a continuous-time multi-group bi-virus model with human awareness. In *2017 IEEE 56th Annual Conference on Decision and Control (CDC)*, pages 4124–4129. IEEE, 2017.

[44] J. Liu, P-E Paré, A. Nedić, C-Y Tang, C-L Beck, and T. Başar. Analysis and control of a continuous-time bi-virus model. *IEEE Transactions on Automatic Control*, 64(12) :4891–4906, 2019.

[45] V.S Varma, I.C. Morărescu, S. Lasaulce, and S. Martin. Opinion dynamics aware marketing strategies in duopolies. In *2017 IEEE 56th annual conference on decision and control (CDC)*, pages 3859–3864. IEEE, 2017.

[46] S. Gracy, I.C. Morărescu, V.S Varma, and P.E Pare. Analysis and on/off lockdown control for time-varying sis epidemics with a shared resource. In *2022 European Control Conference (ECC)*, pages 1660–1665, 2022.

[47] V. Taynitskiy, E. Gubar, D. Fedyanin, I. Petrov, and Q. Zhu. Optimal control of joint multi-virus infection and information spreading. *IFAC-PapersOnLine*, 53(2) :6650–6655, 2020.

[48] K. Kandhway and J. Kuri. How to run a campaign : Optimal control of SIS and SIR information epidemics. *Applied Mathematics and Computation*, 231 :79–92, 2014.

[49] C. Nowzari, V.M Preciado, and G.J Pappas. Optimal resource allocation for control of networked epidemic models. *IEEE Transactions on Control of Network Systems*, 4(2) :159–169, 2015.

[50] G.S Zaric and M.L Brandeau. Dynamic resource allocation for epidemic control in multiple populations. *Mathematical Medicine and Biology*, 19(4) :235–255, 2002.

[51] V.M Preciado, M. Zargham, C. Enyioha, A. Jadbabaie, and G. Pappas. Optimal vaccine allocation to control epidemic outbreaks in arbitrary networks. In *52nd IEEE conference on decision and control*, pages 7486–7491. IEEE, 2013.

[52] V.S Varma, Y. Hayel, and I.C Morărescu. A non-cooperative resource utilization game between two competing malware. *IEEE Control Systems Letters*, 7 :67–72, 2022.

[53] L. Euler. Solutio problematis ad geometriam situs pertinentis. *Commentarii academiae scientiarum Petropolitanae*, pages 128–140, 1741.

[54] C.H. Papadimitriou and K. Steiglitz. *Combinatorial optimization : algorithms and complexity*. Courier Corporation, 1998.

[55] F. Riaz and K.M. Ali. Applications of graph theory in computer science. In *2011 Third International Conference on Computational Intelligence, Communication Systems and Networks*, pages 142–145. IEEE, 2011.

[56] E.W. Dijkstra. *A short introduction to the art of programming*, volume 4. Technische Hogeschool Eindhoven Eindhoven, 1971.

[57] A.L. Barabasi and Z.N. Oltvai. Network biology : understanding the cell's functional organization. *Nature reviews genetics*, 5(2) :101–113, 2004.

[58] C. Godsil and G.F. Royle. *Algebraic graph theory*, volume 207. Springer Science & Business Media, 2001.

[59] C-D. Meyer. *Matrix analysis and applied linear algebra*, volume 71. Siam, 2000.

[60] J.V. Neumann and O. Morgenstern. Theory of games and economic behavior, 2nd rev. 1947.

[61] J.F. Nash. Equilibrium points in n-person games. *Proceedings of the national academy of sciences*, 36 :48–49, 1950.

[62] D. Monderer and L.S. Shapley. Potential games. *Games and economic behavior*, 14 :124–143, 1996.

[63] S. Lasaulce and H. Tembine. *Game theory and learning for wireless networks : fundamentals and applications*. Academic Press, 2011.

[64] T. Alpcan and T. Başar. *Network security : A decision and game-theoretic approach*. Cambridge University Press, 2010.

[65] O. Gross and R. Wagner. A continuous colonel blotto game. Technical report, Rand Project Air Force Santa Monica Ca, 1950.

[66] D. Braess. Über ein paradoxon aus der verkehrsplanung. *Unternehmensforschung*, 12 :258–268, 1968.

[67] W. Knödel. *Graphentheoretische methoden und ihre anwendungen*, volume 13. Springer-Verlag, 2013.

[68] K Gina. What if they closed 42d street and nobody noticed ? *New York Times*, 1990.

[69] J Vidal. Heart and soul of the city. london. *The Guardian*, 1, 2006.

[70] D. Fudenberg and J. Tirole. *Game theory*. MIT press, 1991.

[71] G. Debreu. A social equilibrium existence theorem. *Proceedings of the National Academy of Sciences*, 38 :886–893, 1952.

[72] K. Fan. Fixed-point and minimax theorems in locally convex topological linear spaces. *Proceedings of the National Academy of Sciences*, 38 :121–126, 1952.

[73] I.L. Glicksberg. A further generalization of the kakutani fixed theorem, with application to nash equilibrium points. *Proceedings of the American Mathematical Society*, 3 :170–174, 1952.

[74] J. B. Rosen. Existence and uniqueness of equilibrium points for concave n-person games. *Econometrica : Journal of the Econometric Society*, pages 520–534, 1965.

[75] K.J. Arrow. *Social Choice and Individual Values*. Yale University Press, 1963.

[76] J. Arora. *Introduction to optimum design*. Elsevier, 2004.

[77] T. Athan and P. Papalambros. A note on weighted criteria methods for compromise solutions in multi-objective optimization. *Engineering optimization*, 27 :155–176, 1996.

[78] C. Papadimitriou. Algorithms, games, and the internet. In *Proceedings of the thirty-third annual ACM symposium on Theory of computing*, pages 749–753, 2001.

[79] C. Dutang. Existence theorems for generalized nash equilibrium problems : An analysis of assumptions. *Journal of Nonlinear Analysis and Optimization*, pages 115–126, 2013.

[80] F. Di Lauro and et al. COVID-19 and flattening the curve : A feedback control perspective. *IEEE Control Systems Letters*, pages 1435–1440, 2020.

[81] A. Charpentier, E. Romuald and et al. COVID-19 pandemic control : balancing detection policy and lockdown intervention under ICU sustainability. *Mathematical Modelling of Natural Phenomena*, 2020.

[82] F. Casella. Can the COVID-19 epidemic be controlled on the basis of daily test reports ? *IEEE Control Systems Letters*, pages 1079–1084, 2020.

[83] H. Salje, C.T. Kiem, and et al. Estimating the burden of SARS-CoV-2 in France. *Science*, pages 208–211, 2020.

[84] Open stats coronavirus Covid-19 statistiques/France. *Technical report*, 2020. https://www.coronavirus-statistiques.com.

[85] S. Cauchemez, F. Chauvin, and et al. Sortie progressive de confinement prerequis et mesures phares. *Conseil scientifique Covid-19*, 2020.

[86] Santé publique France. www.santepubliquefrance.fr.

[87] L. Guan and et al. Transport effect of COVID-19 pandemic in France. *Annual reviews in control*, 2020.

[88] X. Vives. *Oligopoly pricing : old ideas and new tools*. MIT press, 1999.

[89] K.J. Arrow and G. Debreu. Existence of an equilibrium for a competitive economy. *Econometrica*, 22 :265–290, 1954.

[90] H.K. Khalil. *Nonlinear systems*. Prentice-Hall, Englewood Cliffs, New Jersey, U.S.A., 3rd edition, 2002.

[91] H.S. Rodrigues and M.J. Fonseca. Can information be spread as a virus ? Viral marketing as epidemiological model. *Mathematical methods in the applied sciences*, 39 :4780–4786, 2016.

[92] K. Kandhway and J. Kuri. How to run a campaign : Optimal control of SIS and SIR information epidemics. *Applied Mathematics and Computation*, 231 :79–92, 2014.

[93] H.S. Rodrigues and M.J. Fonseca. Viral marketing as epidemiological model. *arXiv preprint arXiv :1507.06986*, 2015.

[94] H. Demsetz. Barriers to entry. *The American Economic Review*, 72 :47–57, 1982.

[95] K. Basu and N. Singh. Entry-deterrence in stackelberg perfect equilibria. *International Economic Review*, 31 :61–71, 1990.

[96] V. Doshi, S. Mallick, et al. Competing epidemics on graphs-global convergence and coexistence. In *IEEE INFOCOM 2021-IEEE Conference on Computer Communications*, pages 1–10. IEEE, 2021.

[97] N. Niknami and J. Wu. Competitive influence maximisation model with monetary incentive. *International Journal of Parallel, Emergent and Distributed Systems*, 37(6) :680–695, 2022.

[98] Z. Xu, A. Khanafer, and T. Başar. Competition over epidemic networks : Nash and stackelberg games. In *2015 American Control Conference (ACC)*, pages 2063–2068. IEEE, 2015.

[99] G. Leitmann. On generalized stackelberg strategies. *Journal of optimization theory and applications*, 26 :637–643, 1978.